ANL-6710
Engineering and
Equipment
(TID-4500, 21st Ed.)
AEC Research and
Development Report

ARGONNE NATIONAL LABORATORY
9700 South Cass Avenue
Argonne, Illinois 60440

TRANSIENT BEHAVIOR OF A NATURAL-CIRCULATION LOOP OPERATING NEAR THE THERMODYNAMIC CRITICAL POINT

by

Darrel G. Harden
Oklahoma State University

Reactor Engineering Division, ANL
and
Associated Midwest Universities

May 1963

This report is one of a series that describes heat transfer and fluid-flow studies performed at Argonne under a program sponsored jointly by the Associated Midwest Universities and the Argonne National Laboratory.

The earlier reports in this series are ANL-6625, ANL-6667, and ANL-6674.

Operated by The University of Chicago
under
Contract W-31-109-eng-38
with the
U. S. Atomic Energy Commission

DISCLAIMER

TABLE OF CONTENTS

Page

CHAPTER

I. INTRODUCTION 5

II. SURVEY OF LITERATURE 7

III. THEORETICAL ANALYSIS OF LOOP TRANSIENTS 13

Qualitative Analysis 17

Programming Analysis for Solution with a Digital Computer 22

IV. EXPERIMENTAL APPARATUS 26

V. EXPERIMENTAL PROCEDURE 38

VI. EXPERIMENTAL RESULTS AND DISCUSSION 43

VII. COMPUTER RESULTS AND DISCUSSION 60

VIII. DISCUSSION OF RESULTS AND CONCLUSIONS 66

SELECTED BIBLIOGRAPHY 69

APPENDICES

A. Mass Flow Rate Calculations 73

B. Properties of Freon-114 74

C. Digital Computer Program 77

D. Alternate Derivation and Analysis 89

E. Selected Data 92

NOMENCLATURE 93

ACKNOWLEDGMENT 95

LIST OF FIGURES

No.	Title	Page
1.	Schematic of the Loop for Analytical Representation.	14
2.	Response of Natural-circulation Loop to Step Increase in Heat Input	18
3.	Fluid Control Volume Position Versus Local Acceleration in a Closed, Natural-circulation Loop.	21
4.	Front View of Test Loop	27
5.	Schematic Diagram of Test Apparatus	28
6.	Instrumentation Block Diagram.	29
7.	Control Panel Board	30
8.	Instrument Racks and Visicorder	31
9.	Assembly Drawing of Test Section.	32
10.	Heat Exchanger Detail.	33
11.	Bulk Thermocouple and Static Pressure Tap Installation Details	33
12.	Venturi Detail	36
13.	Density-Enthalpy Product for Freon-114 along an Isobar as a Function of Temperature.	43
14.	Isobars of Density-Enthalpy for Freon-114	44
15.	Effect of Inlet Temperature on Flow Rate	46
16.	Mass Flow Rate as a Function of Power Input at a Constant Inlet Temperature	47
17.	Power Instability, Loop No. 1, 14 kw, 480 psia, Oct. 3, 1962 .	48
18.	Effect of Pressurization, Loop No. 2, 16 kw, Nov. 9, 1962 . . .	49
19.	Initial Oscillation Accompanying "Percolator Effect," Loop No. 2, 14 kw, Nov. 9, 1962	50
20.	Flow and Pressure Oscillation Approaching Burnout at Subcritical Pressures, Loop No. 2, 9 kw, Oct. 23, 1962.	51
21.	Rapid Heating through the (ρh) Maximum and Subsequent Cooling, Loop No. 2, Nov. 9, 1962	53
22.	Initial Transient Encountered in Heating, Loop No. 1, 5 kw, Oct. 2, 1962.	54

LIST OF FIGURES

No.	Title	Page
23.	Operation in the Two-Phase Region, Loop No. 1, 6 kw, Oct. 3, 1962	55
24.	Shutdown from Supercritical Conditions, Loop No. 2, 14 kw, Nov. 9, 1962	56
25.	Effect of Pressure Increase on Magnitude and Frequency, Loop No. 2, 14 kw, Nov. 9, 1962	58
26.	Heating through Critical Temperature at Constant Pressure, Loop No. 1	58
27.	Comparison of Experimental and Calculated Flow Rates	60
28.	Transients Encountered with Loop No. 2 for the Least Stable Case	61
29.	Transient Behavior of Loop No. 2 Approaching the Maximum in the Density-Enthalpy Product from the Low-temperature Side	62
30.	Predicted Response of Loop No. 1 in a Stable Operating Region	63
31.	Response of Loop No. 2 in a Stable Operating Region	63
32.	Transient Behavior of Loop No. 2 Operating at 600 psia	64
33.	Enthalpy-Temperature Relationship for Freon-114 in the Critical Region	74
34.	Density-Temperature Relationship for Freon-114 in the Critical Region	74
35.	Definition of State Regions Given by Various Sources Shown on the Pressure-Volume Diagram	75
36.	Simplified Computer Flow Chart for the Steady-state Analysis	77
37.	Simplified Computer Flow Chart for the Transient Analysis	77
38.	Dimensions of Experimental Loops Used in Computer Program	78
39.	Density-Enthalpy Product for Freon-114 along an Isobar as a Function of Density	90
40.	The Variation of the Density-Enthalpy Product with Density along Isobars for Water	91

TRANSIENT BEHAVIOR OF A NATURAL-CIRCULATION LOOP OPERATING NEAR THE THERMODYNAMIC CRITICAL POINT

by

Darrel G. Harden

CHAPTER I

INTRODUCTION

Interest in utilizing natural-circulation loops to obtain results that aid in the design of some boiler and nuclear reactor coolant systems has focused attention on the dynamic behavior of such loops. Much analytical and experimental work has been done so as to permit predictions of the transient behavior of both single-phase and two-phase natural-circulation systems. One region in which transient behavior has been noted experimentally, but which has not been investigated, is that region near the thermodynamic critical point of the fluid.

Two very desirable characteristics of a natural-circulation system fluid are that the fluid possess a large heat capacity, and the density variation with temperature be large. Both requirements are met when the fluid is in the near-critical region. The specific heat capacity in the critical region becomes large, but only over small temperature differences. Since an actual system will operate with a finite temperature difference, ΔT, between the inlet and exit of the heater section, the heat capacity of the fluid will have a finite value. At constant pressure, the density of a supercritical fluid decreases rapidly with increasing temperature near the critical point. The magnitude of the density change, although smaller, is analogous to the change in density of water and its vapor as the water is vaporized.

The changes in the transport properties viscosity and thermal conductivity are also of interest. The viscosity decreases to a minimum value at the critical point which means that the viscous damping characteristic of the fluid is at its minimum value. The thermal conductivity decreases by approximately 100 per cent.

Two possible applications in which a natural-circulation loop might operate near the thermodynamic critical point of the fluid are when (1) the loop is designed for operation in this region to utilize a single-phase heat-transfer medium and take advantage of the expected high heat-transfer coefficients, and (2) the fluid passes through the critical region as it is heated in a supercritical pressure power cycle. In either of the cases, the limitations associated with the physical and hydrodynamic instability in the

operation of a nuclear reactor are eliminated or considerably smoothed, since the heat-transfer agent is a supercritical single-phase fluid. In both applications, knowledge of the expected dynamic behavior is desired.

Qualitatively, a natural-circulation loop can be considered as a physical system having inertia, resistance to flow, a pressure differential due to density head, and energy storage in the system fluid. Disturbances in heat input or heat removal, with the resultant changes in density head and fluid flow rate, upset the equilibrium balance, and an adjustment must occur to satisfy the new conditions. At certain combinations of power level and system pressure for a given loop configuration, the gravitational driving force within the system will increase while the damping within the system may decrease until sustained oscillations in flow and pressure may occur. It may be that, under certain operating conditions, dynamic equilibrium will never be attained as long as the fluid is in the region of the critical point unless a system geometry can be devised which would minimize the unstable effects.

One analysis of hydraulic stability consists of solving the continuity, momentum, energy, and phenomenological equations describing the system. When such equations are written to include all the minute details of the system, they often become too complex and no longer amenable to solution.

The principal objective of this study was to study experimentally and analytically the transients encountered in the critical region. The experimental portion consisted of constructing a closed natural-circulation loop containing Freon-114 and instrumentating to measure the flow and pressure transients. Freon-114 was chosen as the system fluid because of its low critical temperature and pressure (294.2°F and 474.8 psia), and availability of thermodynamic data. The choice of fluid is otherwise unimportant because the basic mechanism of the flow instability near the thermodynamic critical point should be the same for all fluids.

The analytical portion of the study consisted of simulating the loop by utilizing a digital computer to predict the measured transients. The one-dimensional conservation equations were written for a control volume, and then the control volumes were cascaded to obtain the simulated loop. The system of linear equations thus obtained was solved with an IBM 704 electronic computer.

CHAPTER II

SURVEY OF LITERATURE

A survey of the literature reveals that the first information on heat transfer in the critical region was published in 1939 by Schmidt, Eckert, and Grigull.[37] Since then, several experimental and analytical investigations have aimed at the development of predictive methods for, and the understanding of, heat transfer in this region. In the process of obtaining heat-transfer data in this region, several experimenters have reported pressure and flow oscillations of such severity that it was impossible to make heat-transfer measurements in this area.

Schmidt, Eckert, and Grigull[37] investigated the heat-transfer characteristics of ammonia in a thermal syphon-type apparatus. The experimental procedure was to charge the constant-volume system with an arbitrary amount of fluid and heat to the critical region. The change of state from the onset of heating could be followed on a p-v or T-S diagram as a line of constant volume. Near the critical pressure, both pressure and temperature fluctuated widely with time, so that measurement in this region was made difficult and, in part, impossible. These fluctuations appeared not only during heating but persisted for hours afterwards. In passing through the critical state during heating, the pressure and temperature increase was retarded greatly because of the increases of the volume coefficient of expansion and of heat capacity C_p.

Holman and Boggs[19] studied the heat-transfer characteristics of Freon-12 in its critical region in a closed natural-circulation loop. They observed in the regions close to the critical state fluctuations in pressure of the order of 20 to 30 psi, accompanied by an intense vibration of the test apparatus. When the rate of flow of cooling water was increased so that the pressure in the apparatus was reduced, the fluctuations subsided; however, if the flow rate was decreased or the power increased, the fluctuations became more severe and did not subside until the pressure had risen well above the critical value. In many instances the pressure fluctuations did not subside until a pressure of 150 to 200 psi above the critical pressure was attained. The instability of operation in the vicinity of the critical point was attributed to the rapid change of properties in this region.

Pressure and flow oscillations similar to those reported by Holman and Boggs[19] were found by VanPutte and Grosh,[38] who studied heat transfer to water in the critical region. Fluctuations in pressure and flow observed in the near-critical region tended to destroy steady-state conditions. These fluctuations seemed to be a function of the system pressure and the test-section power input when the conditions in the test section were supercritical. With a constant power input, the frequency and magnitude of the fluctuations increased as the pressure approached the critical pressure.

The fluctuations also increased in frequency and magnitude as the power input was increased. When the fluctuations were encountered at a pressure near the critical pressure (3250 to 3700 psi), the fluctuations could be stopped by raising the pressure about 200 psi.

In a series of experiments with carbon dioxide in the critical region by Smith and coworkers,[4,20,21] no flow or pressure instabilities were noted.

The occurrence of pressure fluctuations severe enough to induce mechanical vibration of the tube and subsequent rupture has been reported in several papers. Hines and Wolf[18] in a recent study of the pressure fluctuations encountered in a diabatic flow of RP-1 and diethylcyclohexane (DECH) at supercritical pressures reported fluctuations in pressure of 380 psi, peak to peak, with frequencies in the range from 1000 to 10,000 cps. The vibration was very destructive to thin-walled tubing. In tests with thick-walled tubing, similar pressure fluctuations were measured, but the tubes were able to resist the effect of the mechanical stresses. They give a comprehensive survey of the literature of similar occurrences.

In a documentation of "boiling songs" and associated mechanical vibrations, Firstenberg[10] reported the results of informal interviews with various researchers in which "boiling songs," mechanical vibrations, and pressure fluctuations were discussed. Several of the conclusions reached were:

1. Under certain conditions of local boiling, which includes a boiling-like mechanism at supercritical pressures, intense sounds (boiling songs) and mechanical vibrations can be generated.

2. The occurrence of these intense sounds and mechanical vibrations are intimately related to the operating conditions in the heated portion of the loop.

3. The boiling songs and associated vibrations are accompanied by large-amplitude pressure and flow fluctuations, although such fluctuations may occur without the generation of sounds or vibrations.

4. When these unusual phenomena occur in a system, the condition is reproducible and reversible.

5. These unusual phenomena exhibit a threshold condition, generally occurring at about 70-80 per cent of the burnout heat flux.

6. In the case of intense sound generation, increasing the heat flux while maintaining a constant inlet subcooling and flow rate results in an increased intensity which maximizes and then decays as burnout is approached.

7. The intensity of the associated vibrations may show the same pattern as sound-generation phenomena, or may persist until the burnout condition.

8. During vibration, and probably during sound generation, the heated surface exhibits a periodicity in bubble formation, that is, all bubbles are synchronized and grow and collapse simultaneously.

9. The occurrence of boiling songs and associated vibrations appears to be confined to local (subcooled) boiling systems. There has not been a recorded occurrence of these phenomena in bulk boiling (net vapor generation) systems.

10. The unusual phenomena result from pressure waves and/or flow fluctuations which induce variable heat transfer in the system. The variability in the heat-transfer rate and energy dissipation of the pressure wave results in the intense sounds and vibrations.

Firstenberg concluded that the severity of the vibrations and intensity of the sounds indicate a possible limiting condition for some boiling systems. Because of other, more immediate needs in cases where these phenomena were observed, they were considered to constitute a nuisance condition and thus were not investigated systematically. It was recommended that some systematic investigation of these phenomena be initiated, directed at obtaining an understanding of the cause-and-effect relations, and discovering methods for eliminating the occurrences.

Goldman[14] in a report of heat-transfer experiments involving supercritical water at 5000 psia distinguished between heat transfer without "whistle" or a "normal" mode and heat transfer with "whistle." The frequency of the whistle sound varied from about 1400 to 2200 cps. Inlet temperature appeared to have the greatest effect on frequency, whereas pressure had little, if any, effect. A pressure increase in the system of about 50 psi occurred at the onset of the whistle sound.

Griffith and Sabersky[16] studied fluid motion photographically in the neighborhood of a heating surface in a container filled with fluid at its thermodynamic critical point to determine if any bubble-like motion could be detected, and if so, to relate this motion to any sharp increases in the heat-transfer rate. The visual results gave some indication that bubble-like aggregates may form; but, under the conditions of this test, the bubble-like motion did not lead to any abrupt increase in the heat-transfer rate as is observed in nucleate boiling.

The fluctuation of the natural-circulation flow rate in systems at subcritical pressure, particularly those in which boiling takes place, has been widely encountered in boilers and nuclear reactors. As yet, there

is no single theory that describes two-phase hydraulic characteristics over the entire range from atmospheric pressure to 2000 psia, [see Ref. (45)].

The goal of analytical work concerning a test-loop stability analysis is to predict the dependence of the inception point, frequency, and amplitude of oscillations on system parameters. Two approaches are used. In the first, the general equations of the system, such as the energy, continuity, and momentum equations, are solved, the resultant solution indicating the influence of system parameters on stability. In the second approach, some controlling phenomenon, such as an extremum in the pressure drop versus flow rate curve, is assumed to be the only phenomenon of importance, and system stability is evaluated by investigation of factors affecting this phenomenon.

The analytical and experimental work associated with reactor and test-loop stability has been reviewed by Anderson and Lottes.[2] The conclusions reached as a result of this survey are: (1) the experimental information in the field of reactor and test-loop stability is sparse, (2) analytical procedures are still in a preliminary state, and (3) because of over-design of reactors due to lack of information, a more precise method of prediction of stability is important to the future development of boiling water reactors.

A more recent review by Beckjord[45] discusses hydrodynamic stability in reactors. References to recent reactor stability work are given. Hydrodynamic instabilities fall into two classes from the reactor point of view. The first class includes power-to-reactivity feedback instabilities in which hydrodynamic phenomena predominate. The second class are those in the form of varying coolant flow rates or density waves traveling in the fuel channel, which would affect the reactor in a way similar to external disturbances. The reactor power would fluctuate with hydrodynamic variations.

Foltz and Murray[11] in a study of two-phase Freon-114 flow rates and pressure drops in long and short parallel tubes reported periodic fluctuations in the flow in the long tubes at high heat flux. Under the condition of high heat input the flow in the two longer pipes would begin to fluctuate, slightly at first, then with increasing amplitude, until the flowmeter bobs were going from top to bottom. The slamming of flowmeter bobs against the bottom stop indicated a flow reversal. The two pipes would be out of phase, with one tube having a flow rate of about 700 lb_m/hr when the other pipe had no flow. The fluctuations were cyclic with a period of about 10 sec. The two short pipes remained relatively steady with some fluctuations of about ± 4 percent of average flow. The fluctuations could be damped out, without decreasing the heat load, by restricting the flow through the short pipes. The same fluctuating flow could be obtained at a lower heat flux by restricting the flow to the inlet manifold. In each case the fluctuations occurred when the heat input was sufficient to vaporize about 70 per cent of the liquid flowing in that pipe.

Lee et al.[22] in a design study of thermosiphon reboilers (natural-circulation vertical-tube evaporators) described a pulsating flow they encountered. In an effort to understand better the cause of the high velocities which they observed at the outlet of the 5- and 10-ft reboiler tubes, a small laboratory, single-tube glass thermosiphon reboiler was built and operated. Heat was supplied by means of an electrical heating element wrapped around the tube. Slow-motion pictures of the unit showed very plainly a rapid pulsating flow in the tube with each slug of liquid and vapor leaving the tube at high velocity. Each pulse of mixed liquid and vapor leaving the top of the tubes was accompanied by a "kickback" of the liquid in the bottom of the tube. It was concluded that anything that could be done to increase the resistance to "kickback" would permit higher fluxes before vapor lock, which was defined as the onset of a surging type of flow, occurred.

Anderson et al.,[47] by solving the time- and space-dependent conservation equations with an analog computer, were able to predict the behavior of a two-phase natural-circulation system during transients. Their model was useful for investigating the point at which their system would exhibit oscillatory behavior.

Quandt[32] developed an analysis for predicting the onset of stable parallel channel flow oscillations (or "chugging") which occur under certain operating conditions. The analysis is based on a linearized treatment of the conservation equations and equation of state for small perturbations about some steady-state value.

Wallis and Heasly[41] presented mathematical models for three modes of oscillation of a simple two-phase flow, natural-circulation system, together with qualitative results of experiments with a small-scale loop model. Their basic approach was to consider the loop as a dynamic system of nonlinear time delays, storage, elements, and resistances. Standard methods of control-theory analysis were then applied to predict the onset of instabilities.

Alstad et al.[1] solved the conservation and state equations by finite-difference methods for temperatures and rates of flow in the transient operation of a natural-circulation loop with a single-phase fluid as the circulating fluid. Comparisons for two experimental water loops of predicted with actual performances employing water were found satisfactory.

Wissler,[42] utilizing an analog computer, studied the oscillatory behavior of a two-phase natural-circulation loop at atmospheric pressure. The general conclusion of the stability analysis was that a natural-circulation loop could be made unstable in the sense that a small displacement from the equilibrium state could lead to undamped oscillations.

Garlid[12] developed a model for a two-phase natural-circulation loop based on a concept of cascaded control volumes and lumped parameterization. The model was applied to a general system and, hence, gave only general results.

Myer,[28,29] and Myer and Rose[46] discussed the derivation of the transient equations as applied to the parallel flow configuration (constant pressure difference across the heated section) and presented the results of the simultaneous solution of the system of equations utilizing a digital computer. They gave details of the method, comparison with experiment, and features which distinguished their model from other analytical models.

The conclusion can be made, based on this survey of the literature, that flow and pressure oscillations in diabatic flow have been encountered over a wide range of operating conditions with many different systems. A single unifying theory is needed to relate these seemingly unrelated phenomena.

CHAPTER III

THEORETICAL ANALYSIS OF LOOP TRANSIENTS

The fluid in a natural-circulation loop can be considered as a thermodynamic system which (a) possesses the characteristic of inertia, (b) exchanges momentum with the walls of the surrounding tubing to produce a resistance to flow, (c) contains a pressure differential due to density head for the acceleration of the system fluid, and (d) has a capability for energy storage in the system fluid. Sustained oscillations of the fluid mass can be obtained by the effect of certain combinations of the system variables.

A somewhat analogous mechanical model is the free piston in a gravity field: the mass of the piston corresponds to the mass of the fluid in the loop; the pressure differential due to the density head corresponds to a driving force acting on the piston mass; friction and momentum pressure losses are represented by viscous damping. To accelerate the free piston uniformly up the bore of the containing cylinder, it is necessary to supply a driving force in the direction of motion in excess of the restraining forces acting in the opposite direction. By periodically increasing and decreasing the driving force, the piston can be made to oscillate about some equilibrium point.

Assume that steady-state conditions exist for the flow in a natural-circulation loop. Disturbances in heat input or heat removal from the system fluid with the resultant changes in density head and fluid flow rate upset the equilibrium balance, and an adjustment must occur to satisfy the new conditions. Under some operating conditions, the adjustment to the new mass-velocity level is reached by a damped transient with some initial oscillation about the new steady-state condition. The operating conditions of interest in this investigation were those in which the adjustment resulted in sustained flow oscillations about the "new" steady-state mass-velocity value.

One analysis of the dynamic stability of a fluid-flow system consists of solving the continuity, momentum, energy, and state equations describing the system. Time-dependent conservation equations with special reference to natural-circulation loops have been derived by several authors.[1,12,28,41,42] The equations are nonlinear partial differential equations in space and time. A direct analytical solution is impossible with present mathematical knowledge. Several alternatives which have been considered are:

(1) reduction of the nonlinear system to a linear one by making simplifying assumptions enabling one to obtain an analytical solution.

(2) use of perturbations about an initial steady-state and then investigation of the resulting time-dependent behavior to determine whether the result indicates unstable, stable, or oscillatory behavior.

(3) solution of the set of equations by finite-difference methods with a high-speed electronic computer or an electric analog computer.

In this work a one-dimensional model was used, for which a system of equations was written and solved by finite-difference methods with a digital computer.

Figure 1 depicts a schematic of the loop. The closed loop consists of two legs of vertical round tube of constant cross-sectional area. At $z = 0$ the fluid enters the hot leg and flows in a one-dimensional (counterclockwise) manner in the positive z direction around the loop. Variations in fluid properties, velocity, and heat flux in the radial direction were taken to be negligible. Heat conduction in the axial direction was neglected. The portions of the hot and cold legs not occupied by the test section or cooler were adiabatic.

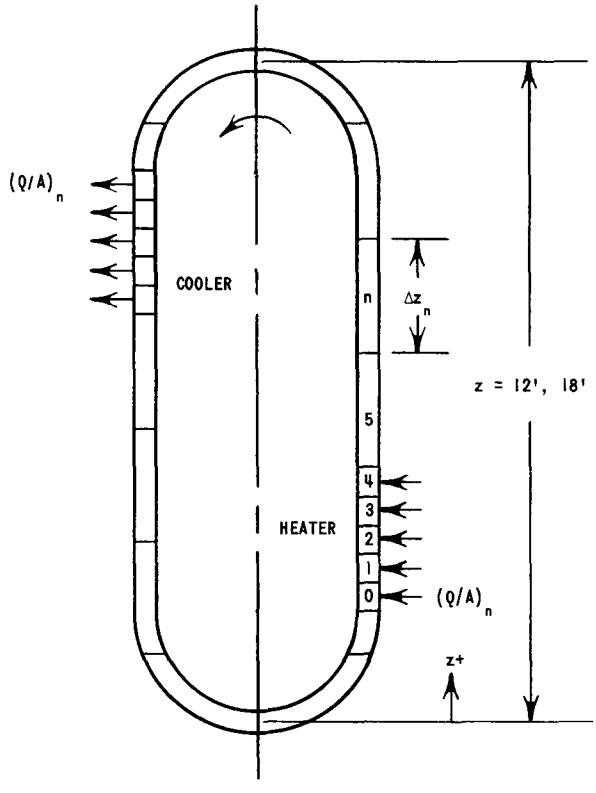

Fig. 1. Schematic of the Loop for Analytical Representation

In a thermodynamic analysis, the loop can be considered as having diabatic and adiabatic sections. In analyzing diabatic flow, two approximations are generally made. The first is that no external work is involved in the process. The second is that the flow is incompressible in the sense that the density is independent of pressure and a function of temperature or enthalpy only. These approximations are dependent on the major effect of heat transfer being a change in temperature with only a secondary change in pressure. This is ordinarily the case; but, when heat is added at a sufficiently high rate or the fluid is in a region where large changes in density occur with even small quantities of heat added, the induced pressure change may require a consideration of the pressure effect on the compressibility in the flow. The assumption of a constant reference pressure p^* can, in some

cases, be fulfilled in practice by installing a surge tank in the system to damp pressure fluctuations. As a first approximation, then, the assumption will be made that density ρ may be evaluated as a function of enthalpy h only:

$$\rho = \rho(h, p^*) \quad . \tag{III-1}$$

The major difficulty encountered in a compressible model in which the density is evaluated as a function of enthalpy and pressure is one of numerical stability in the solution of the equations describing the system. The required time-step size, Δt, is of the order of the time for a sonic wave of speed c to pass through one space step:

$$\Delta t \leq (\Delta z/c) + |u| \quad ,$$

[see Ref. (34), p. 197]. Therefore, in a problem in which the fluid has a high sonic velocity, the time step becomes prohibitively short from a computer-time cost standpoint.

A natural-circulation loop can be operated near the critical point in either the single-phase or two-phase region. Experimental results in the two-phase region showed transient traces of mass flow rate similar to the "coffee percolator" or slug-flow effect which is encountered in many industrial applications, for example, in reboilers. Therefore, attention was focused on the single-phase compressed-liquid region where severe transients were reported in the literature and which were encountered during this experimental program.

Considering the fluid in the n^{th} element as the thermodynamic system, the equation for conservation of mass can be written as

$$(\partial \rho/\partial t) + (\partial G/\partial z) = 0 \quad , \tag{III-2}$$

where G is the mass velocity and z the elevation.

Assuming (1) the work done on the system by frictional forces is negligibly small, (2) the kinetic and potential energy terms can be neglected, and (3) the effect of pressure changes with time on the enthalpy rise rate is small, the equation for conservation of energy can be written [see Ref. (28)] as

$$\rho\, \partial h/\partial t + G\, \partial h/\partial z = Q/A \quad , \tag{III-3}$$

where Q is the linear rate of heat input to the fluid and A the cross-sectional area.

The equation of motion determined by making a momentum balance in the nth volume element is

$$\frac{A\,\Delta z}{g_c}\,\frac{\partial G}{\partial t} = -\,A\,dp - \frac{f\,|\bar{G}|\,G}{2\rho g_c d}\,A\,dL - \frac{\rho g}{g_c}\,A\,dz - dD_i \quad . \tag{III-4}$$

where g_c is a constant of proportionality, L the length, D_i the lumped sectional drag force, and f the single-phase friction factor. Because of the assumption that the density is not a function of pressure, local compression is not allowed; hence, a local decrease in density results in disturbances in the local pressure and velocity which are propagated at the speed of sound throughout the loop. This effect is the same as that which would result if one of the beads on a string of closely spaced beads were moved: all the beads would move the same distance with the same velocity. Therefore, because of this assumption, the momentum equation must be integrated over the entire loop circuit and is used to represent the behavior of the average mass velocity, $\bar{G}$, only:

$$\frac{L}{g_c}\,(d\bar{G}/dt) = -\Delta p - F \quad , \tag{III-5}$$

where

$$\bar{G} = \frac{1}{L}\int_0^L G_n\,dL \quad , \tag{III-6}$$

$$\Delta p = (g/g_c)\int_0^z \rho_n\,dz \quad , \tag{III-7}$$

and the total resistance to fluid flow, F, is

$$F = \int_0^L \frac{f\,|\bar{G}|\,\bar{G}}{2g_c\rho_n d}\,dL \quad . \tag{III-8}$$

The assumption was made that the momentum losses due to internal drag forces in the loop were negligible. Since the loop is a closed circuit,

$$\int dp = 0 \quad .$$

For a given reference pressure, the frictional resistance to flow due to the momentum exchange with the wall of the conduit was calculated as a function of the actual mass velocity by means of a relation of the form

$$F = N\,\frac{|\bar{G}|\,\bar{G}}{\bar{\rho}} + N_1 \quad , \tag{III-9}$$

where N was a constant whose value depended on the mean mass velocity and mean density of the fluid.

An expression for the local change in the mass velocity in terms of the local heating can be obtained by elimination of the time rate of density and enthalpy change in the continuity and energy equations by means of the equation of state. Applying the chain rule of differentiation to the equation of state, Eq. (III-1), the result is

$$\partial\rho/\partial t = (d\rho/dh)(\partial h/\partial t) \quad . \tag{III-10}$$

If this result is substituted into the equation of continuity, Eq. (III-2), then the expression becomes

$$-(\partial G/\partial z) = (d\rho/dh)(\partial h/\partial t) \quad . \tag{III-11}$$

If this is solved for $(\partial h/\partial t)$ and the result substituted into the energy equation, Eq. (III-3), the expression for the local change in the mass velocity is obtained:

$$(\partial G/\partial z) = (1/\rho)(d\rho/dh)\,[G(\partial h/\partial z) - (Q/A)] \quad . \tag{III-12}$$

This equation and the momentum equation, Eq. (III-5), describe the energy-hydrodynamic relationships of the flow system. A complete picture of the mass-velocity behavior in the steady and transient state can be obtained by the simultaneous solution of these equations. The techniques and methods used are discussed in the last section of this chapter.

Qualitative Analysis

A qualitative picture of the transient loop behavior can be obtained by examining these equations. In the steady-state condition, the momentum equation states that $(d\overline{G}/dt) = 0$ and, therefore, $\Delta p = F$. In the energy equation $G(\partial h/\partial z) = Q/A$; therefore, $(\partial G/\partial z) = 0$. Now, if an increase in heating power is applied to the flowing system, $Q/A > G(\partial h/\partial z)$ and, hence, the difference $[G(\partial h/\partial z) - (Q/A)]$ takes on some negative value. Since the term $[(1/\rho)(d\rho/dh)]$ is always negative, there is a positive increase in $(\partial G/\partial z)$. The change in $(\partial G/\partial z)$ results in an increase of $(\partial\overline{G}/\partial t)$ because of the increased Δp which, in turn, must be balanced out by an increase in the resistance to fluid flow, F, to return $d\overline{G}/dt$ to zero.

The result of this sequence of events is shown in Fig. 2. In this figure, it can be seen that the inertia of the stream resulted in the initial overshoot and the subsequent undershoot. The system damping caused the mass velocity to decay to the new steady-state value after a few cycles. It should be noted that the same sequence of events could have been initiated by changing either the Δp or F term in the momentum equation. However, in diabatic flow, the change in heat addition is usually the forcing function for a flow change.

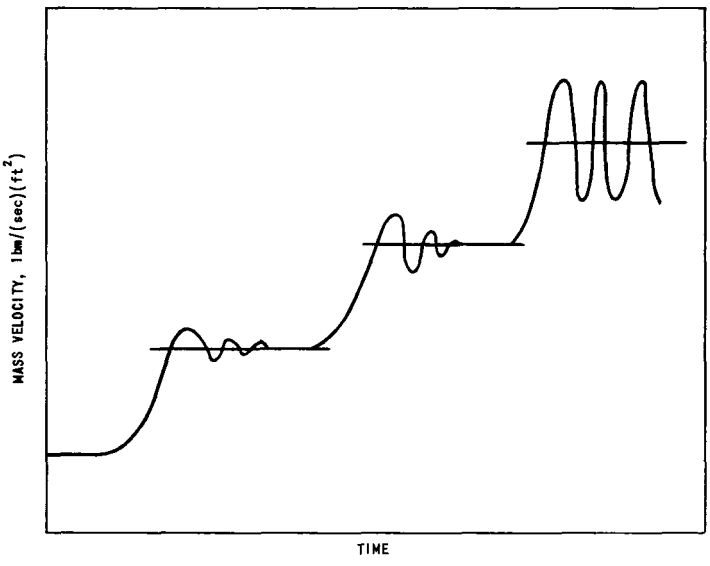

Fig. 2

Response of Natural-circulation Loop to Step Increase in Heat Input

A possible explanation of the sustained flow oscillation is deduced by further analysis of Eq. (III-5) and (III-12). There are four terms in Eq. (III-12) which would force a change in $(\partial G/\partial z)$: $[(1/\rho)(d\rho/dh)]$, G, $(\partial h/\partial z)$, and Q/A. The latter is the only variable which can be controlled independently. The quantities G, $[(1/\rho)(d\rho/dh)]$, and $(\partial h/\partial z)$ can be manipulated primarily by changing the thermodynamic state of the fluid. The most favorable condition for large changes in $(\partial G/\partial z)$ is that the multiplier term $[(1/\rho)(d\rho/dh)]$ and the term $[G(\partial h/\partial z) - (Q/A)]$ be large.

Let us consider again the sequence of events leading to the damped oscillation in the Fig. 2, and this time assume that the multiplier is several times larger. An increase in the heat input results in $[G(\partial h/\partial z) - (Q/A)]$ being again negative. This difference is multiplied by a large number and, therefore, a large positive $(\partial G/\partial z)$ results. When the overshoot occurs, $[G(\partial h/\partial z) - (Q/A)]$ becomes positive and again is multiplied by the same large number. This process continues as long as the large changes in $(\partial G/\partial z)$ result in Δp's which cannot be damped rapidly enough by the friction and momentum losses in the system.

Thus far the analysis has been primarily on the basis of a single control volume of fluid. When a series of these are cascaded to simulate a heater or cooler section, further deductions can be made concerning the dynamic behavior of the loop. In Eq. (III-12), three terms will be affected because of the change in thermodynamic state and position z as the fluid moves from one control volume to the next. The local mass velocity G will be changing because of the fluid expansion, $[1/\rho\,(d\rho/dh)]$, and $(\partial h/\partial z)$ will be changing because of the heat addition. The value of Q/A may be changing because of the variation in heat-transfer coefficient with the thermodynamic state of the fluid. Hence, there are several possible mechanisms for changes in $(\partial G/\partial z)$ to occur, considering only the equation describing the local change of mass velocity.

To obtain a better physical picture of what is happening, let us assume there is a control volume of fluid at the upper end of the heater section which is about to undergo a large expansion due to the heat which will be added during a time interval. When the heat is added and the expansion takes place, there will be simultaneous increases in specific volume of the fluid and in the pressure of the system. The pressure increase occurs because of the increase of specific volume, since for the first few time intervals we can consider the loop as having a constant total volume. The local pressure increase is transmitted at the speed of sound throughout the loop. Since we assumed that the control volume of fluid was at the top of the heater, only a small amount of fluid is involved in the large volume increase. Hence, it would be reasonable to assume that if the heating were to be decreased and the cooling increased at this time, the effect of the pressure and flow increase could be quickly cancelled. This is the effect that is achieved by the loop dynamics. The increase in the fluid flow at the top of the heater caused the fluid at the cooler to flow faster and be cooled more quickly, and at the same time the fluid is heated less in the heater section.

The fluid is heated less in the heater because of two factors. The initial increase in specific volume would tend to propagate a mass-velocity disturbance in both directions, with the result that the incoming fluid is slowed and the outgoing fluid accelerated. The initial slowing of the incoming fluid and the increase of cooling rate in the cooler results in a return of the pressure and flow to normal, and, indeed, an undershoot of the steady-state values. The cycle resumes as soon as the next control volume of fluid is heated sufficiently to the point that further heat addition will result in large increases in specific volume.

If the thermodynamic state of the system fluid is such that the control volume of fluid which is about to undergo a large expansion because of the heat to be added during a time interval is at the lower end of the heater, then it would be expected that, as the mass of fluid in the initial control volume passes through successive control volumes, it would continue to expand. The progress of this mass of fluid through the heater is marked by an increase in flow rate as the fluid ahead of this particular mass of fluid is being accelerated upward through the heater by the heat addition. In this case a transient of lower frequency would be expected because of the larger amount of fluid involved before the driving force, as discussed above, for the transient is reduced.

To summarize the qualitative analysis, it has been conjectured that the initiation of a sustained transient is caused by a change in the rate of acceleration of the fluid in the heater or cooler. This conjecture was based on reasoning from a physical model and from examination of the one-dimensional equations describing this model.

The hypothesis is advanced that sustained flow oscillations will not exist in any system as long as the driving force remains constant. If it does vary in a flow system, then the change must be damped by increased damping which takes effect automatically. This increased damping may occur as a result of factors inherently in the system fluid or due to external damping devices built into the system, which act only when required to reduce the magnitude of the transient condition.

This condition has long been recognized as applicable to an adiabatic forced-circulation system. In this case the driving force is some external mechanical device, and it is easy to see that variation of the driving force will result in flow and pressure oscillations. Also, in a natural-circulation system, it is easy to visualize the variation in flow rate when the heat added to the system is varied in some manner. What is not so apparent in a diabatic system is that the driving force for pressure and flow oscillations is generated internally in the fluid as a result of the interaction of the heat addition and thermodynamic state of the fluid, and is essentially independent of any external driving force.

In the steady-state operation of a diabatic system under most conditions, the addition of heat results in a uniform acceleration of the fluid through the heater section. When the thermodynamic condition of the fluid is such that the heat addition will result in a change of the thermodynamic state of the fluid to a condition in which the slope of the density-enthalpy curve changes, variations in the thermal accelerating force will occur because of the local variation in the mass velocity. When the conditions are such that large changes in local mass velocity occur, then sustained pressure and flow fluctuations will occur.

The oscillation mechanism will, in general, depend on (1) the time needed to expel from the heater the low-density fluid which has been formed, and (2) the time necessary for the thermodynamic state of the fluid to become such that a nonuniform rate of acceleration of the fluid is again significant. The first term will depend on where in the test section the low-density fluid is formed. The latter term will depend largely on the time required to heat the element of fluid to the same thermodynamic state as existed previously. To calculate the transient time in the adiabatic section of the hot leg adequately, it is necessary to know the point at which the nonuniform acceleration begins to occur; hence, in a finite-difference solution of the conservation equations, the length of the increments should be as small as possible, consistent with the economics of purchasing computer time. An order-of-magnitude approximation is that the length of the increment be equal to its diameter.

Another way to visualize the operation of a natural-circulation loop and the conditions during a transient is to use a plot of position versus local acceleration, such as in Fig. 3. If an observer moved with a control

volume of fluid around the loop, then Fig. 3(a) shows a history of the spatial accelerations experienced by this control volume in steady-state operation. The fluid enters the heater at point 1 and is uniformly accelerated because of the heat addition to point 2, which is the exit of the heater. The fluid control volume then continues at a constant velocity up the hot leg and over to the cooler at point 3. In the cooler, the fluid is uniformly decelerated from point 3 to 4 to the initial velocity at which it entered the heater. The fluid then travels at a constant velocity back to point 1. The slope of the curve in the heater, that is, from point 1 to 2, will depend primarily on the heat input and the thermodynamic state of the fluid at the entrance to the heater. In a constant-area, single-phase or high-pressure, two-phase system, the density in the riser portion of the loop will not vary much with time; hence, the velocity in this portion of the loop will be constant and equal to the velocity at the outlet of the heater. Thus, the transient time of the control volume through the adiabatic section is represented by a vertical line on the position-acceleration diagram.

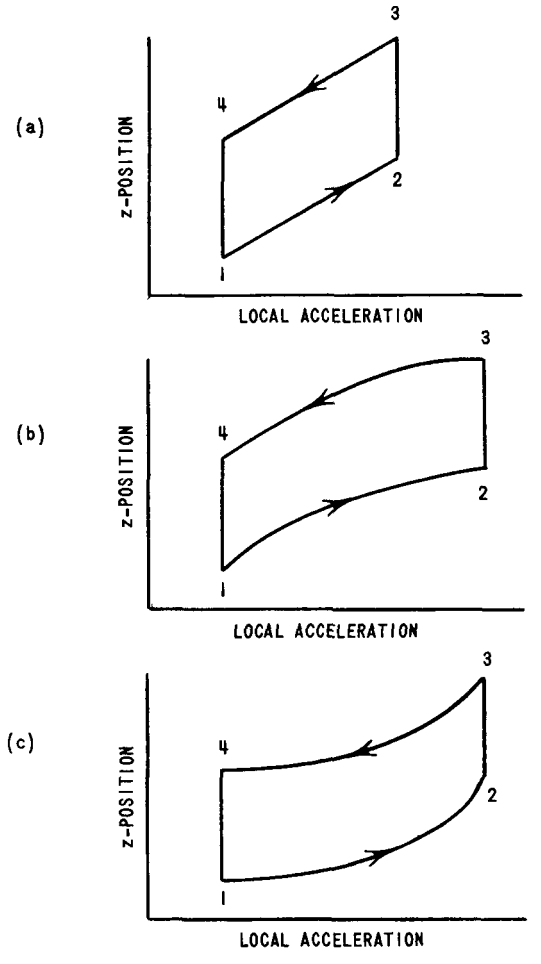

Fig. 3. Fluid Control Volume Position Versus Local Acceleration in a Closed, Natural-circulation Loop

The sequence of events which occurs when the control volume of fluid begins to experience a greater rate of acceleration at the upper end of the heater section, such as is encountered when the slope of the density-enthalpy curve increases, is shown in Fig. 3(b). If the loop flow is initially as shown in (a), then during the time for the loop to adjust to the new flow pattern shown in (b) there will be a transient condition. On the other hand, if the loop is initially in the state shown in (b), there will be a transient introduced in going to the condition in (a). The question can be posed as to which transition would be easier for the thermodynamic system to undergo.

A diagram which would result when the initial acceleration in the heater is large is shown in (c).

The results of experiments to confirm these conjectures will be presented in Chapter VI. The analysis of the system equations for

simultaneous solution by finite-difference methods is next described. If the simultaneous solution of the system equations yields stable flow conditions when the acceleration of a fluid control volume in the heater or cooler is constant, and oscillations when the acceleration is nonuniform, then the hypothesis will have been confirmed for this single-phase system. If the computer model predicts the two ranges of frequencies corresponding to where in the heater or cooler the nonuniform acceleration occurs, the hypothesis can be extended to two-phase systems because of the similarity of the accelerating forces, thus providing a unifying theory for the oscillations encountered in subcooled and two-phase systems.

Programming Analysis

A difference approximation to Eq. (III-12) written for each increment in the heater tube would supply a description of the variation of local mass velocity about the average. A single integrated momentum equation yields the behavior of the average mass velocity with time. The simultaneous solution of these equations will give a complete description of the mass velocity of the fluid in the system as a function of time and space.

However, if only the behavior of the average mass velocity with time is desired, then for ease of programming for a digital-computer solution, another procedure is followed. A difference approximation to the energy equation, Eq. (III-3), is used to obtain local changes in enthalpy. Local values of density are evaluated from the local values of enthalpy. The elevation driving pressure can then be calculated from the density distribution. The mass velocity which results from the elevation head is then computed and, if this checks the initial mass velocity, the computation ends.

The general approach to the solution of these equations is to assume that the loop operates under some power input and steady-state conditions prevail. The problem is of the "initial value" type with time as an independent variable. The steady-state conditions at $t = 0$ define the initial state of the system. The damping in the system serves as the "boundary condition" to the problem. The energy, continuity, momentum, and state equations for the loop, as developed in finite-difference form, are solved for the values of mass velocity, enthalpy, and pressure at time $t + \Delta t$ in terms of the quantities at time t.

A digital-computer program for an IBM-704 was developed to solve the finite-difference equations by an iterative method to determine the dynamic behavior of the system during the transient. The independent variable of the problem is time t referred to by an integer j in the finite-difference equations. The main unknown dependent variables are coolant enthalpy h(j), mass velocity G(j), and pressure p(j). The auxiliary unknown dependent variables are coolant density and temperature, which can be determined in terms of the main dependent variables from the tabulated values.

Two simplifying assumptions made with reference to the digital computer are as follows:

(a) Quasi-steady-state conditions are assumed to prevail during the transient, i.e., it is supposed that at each instant during the transient there exists an instantaneous steady state and, as a consequence, the steady-state friction factor can be applied instantaneously.

(b) To allow for the spatial variation of the fluid properties, the loop is divided into n increments. "Lumped parameter" representation is used for every increment, and the fundamental equations describing the behavior of each segment are generally expressed in terms of the inlet, outlet, and average properties of the fluid in that increment.

The loop is sectionalized in the z-direction by division into n intervals, not necessarily evenly spaced. The mesh increment is given by

$$\Delta z_n = z_n - z_{n-1} \quad .$$

Conditions are evaluated at a number of times during the transient: $t(0) = 0$, $t(1),\ldots t(j),\ldots t(j+1)$. The time steps $\Delta t(j)$ are not necessarily evenly spaced:

$$\Delta t(j) = t(j) - t(j-1) \quad .$$

The analysis is divided into two main parts - steady state and transient. In the steady-state analysis, the thermodynamic properties in each control volume and the mass velocity prevailing throughout the system because of the steady-state heat input are calculated by the computer and stored. These quantities will be used as initial conditions in the transient analysis which calculates the main independent variables (h, $\bar{G}$, and p) at time $t + \Delta t$ in terms of the quantities at time t after the step increase in heat input.

The steady-state quantities are evaluated from the transient equations by starting from given inlet coolant properties and an assumed mass velocity and maintaining constant heat input and heat-extraction levels during the successive time steps until all the calculated quantities converge to within a prescribed error. It should be noted that here time is used as a dummy variable - only as a means to determine the steady-state quantities.

The transient analysis consists of three main parts: (1) enthalpy calculations, (2) mass-velocity calculations, and (3) pressure calculations. The state properties (h, p, and ρ) are calculated at time $t + \Delta t$ from the initial spatial distribution of these properties, calculated for the steady state, and the value of mass velocity $\bar{G}$ at time t. These properties are

then held constant during the calculation of mass velocity. If the system density distribution is known at time $t + \Delta t$, the mass velocity is calculated at time $t + \Delta t$. After this calculation, the mass velocity is examined for convergence. If the mass velocity has converged, another step increase in heat input is made and the calculations repeated. This procedure is continued until the mass velocity fails to converge or a specified heat input has been reached.

Following the procedure outlined by Nahavandi,[51] the energy and transport equations are used to calculate the average and exit coolant enthalpies for each segment, respectively, at time $t + \Delta t$ as a function of quantities at time t. The energy equation, Eq. (III-3), when expressed in finite-difference form and solved for the average enthalpy of the fluid in the increment at time $t + \Delta t$, is as follows:

$$\bar{h}_n(j+1) = \bar{h}_n(j) + \frac{\Delta t}{\bar{\rho}_n(j)} \left\{ (Q/A)_n(j) + \frac{\bar{G}(j)}{\Delta z_n} \left[h_{n,i}(j) - h_{n,e}(j) \right] \right\} \quad . \text{(III-13)}$$

The energy equation for the adiabatic sections of the loop, in finite-difference form, can be simply derived from Eq. (III-13) by neglecting the heat addition term:

$$\bar{h}_n(j+1) = \bar{h}_n(j) + \frac{\Delta t}{\bar{\rho}_n(j)} \left\{ \frac{\bar{G}(j)}{\Delta z_n} \left[h_{n,i}(j) - h_{n,e}(j) \right] \right\} \quad . \text{(III-14)}$$

For the purpose of developing the transport equations, it is assumed that the enthalpy distribution along the flow path in each segment is linear. For any increment, one may write

$$\bar{h}_n(t) = \frac{1}{2} \left[h_{n,i} \left(t - \frac{1}{2} T \right) + h_{n,e} \left(t + \frac{1}{2} T \right) \right] \quad , \text{(III-15)}$$

where

$$T = \bar{\rho}_n \Delta z_n / \bar{G} \quad . \text{(III-16)}$$

Expansion of the above equation in Taylor Series, neglect of the second-order terms, and putting the result in finite-difference form yields

$$h_{n,e}(j+1) = h_{n,e}(j) + \frac{\Delta t}{T} \left[2\bar{h}_n(j) - h_{n,e}(j) - h_{n,i}(j) \right] + \bar{h}_n(j+1) - \bar{h}_n(j) \quad ;$$

$$h_{n,e}(j+1) = h_{n+1,i}(j+1) \quad . \text{(III-17)}$$

To obtain the mass velocity at time $t + \Delta t$, the momentum equation, Eq. (III-5), is written in finite-difference form as follows:

$$\bar{G}(j+1) = \bar{G}(j) + \frac{g_c \Delta t}{L} [\Delta p(j+1) - F(j)] \quad . \tag{III-18}$$

Functions describing wall-friction observations in steady-state pressure-drop experiments are supplied by means of empirical equations:

$$F(j) = N(j) \frac{|\bar{G}(j)| \bar{G}(j)}{\bar{\rho}(j)} + N_1 \quad . \tag{III-19}$$

The pressure at time $t + \Delta t$ is obtained by assuming a constant volume and mass system exists. The increase in specific volume of the fluid at time $(j + 1)$ is used to compute the pressure at $(j + 1)$. An approximate modulus of elasticity is used to calculate the pressure change.

CHAPTER IV

EXPERIMENTAL APPARATUS

A test apparatus was constructed to investigate the instability characteristics of a natural-circulation loop operating near the thermodynamic critical point of the system fluid. The loop geometry was patterned after that of Schmidt, Eckert, and Grigull[37] and of Holman and Boggs.[19] The main criterion of the design was that the flow passage be as smooth and free of obstructions as possible.

Two loops were constructed with the major difference between the two being 5.33 ft of vertical height to provide a higher flow rate and to provide increased volume to reduce the severity of the pressure surges.

The experimental data required were time histories of mass velocity and of density variations around the loop. To this end, instrumentation was provided to obtain data from which the mass velocity and density could be calculated. In addition, the wall temperatures of the test section were measured to furnish data for calculations of the heat-transfer coefficient.

The test apparatus (see Figs. 4-8) consisted of a closed, constant-area circulatory system made of stainless steel type 304, commercially drawn tubing, with an inside diameter of 0.93 in. and a 0.035-in. wall thickness. The oval shape was chosen to avoid sharp bends which would increase the momentum pressure head loss and thus reduce the mass flow rate. The flow path length, measured along the pipe axis, was 28 ft for the small loop, designated as Loop No. 1, and 38 ft for Loop No. 2. The two volumes, exclusive of associated tubing, were 0.129 and 0.180 ft^3. The heating power was supplied by a 70-kva Sciaky Ignitron Contactor whose output voltage could be varied from zero to 45 v continuously. The electric power was dissipated in the test section, which acted as a resistance element and which was cooled by the flow of the test liquid in natural circulation. Heat removal was provided for by a concentric-tube cooler through which tap water flowed.

Component Description

An assembly drawing of the heating section is shown in Fig. 9. Copper blocks were silver soldered to the ends and connected to the output of the Sciaky power supply. Electrical insulation from the rest of the loop was provided by Durabla gaskets and washers.

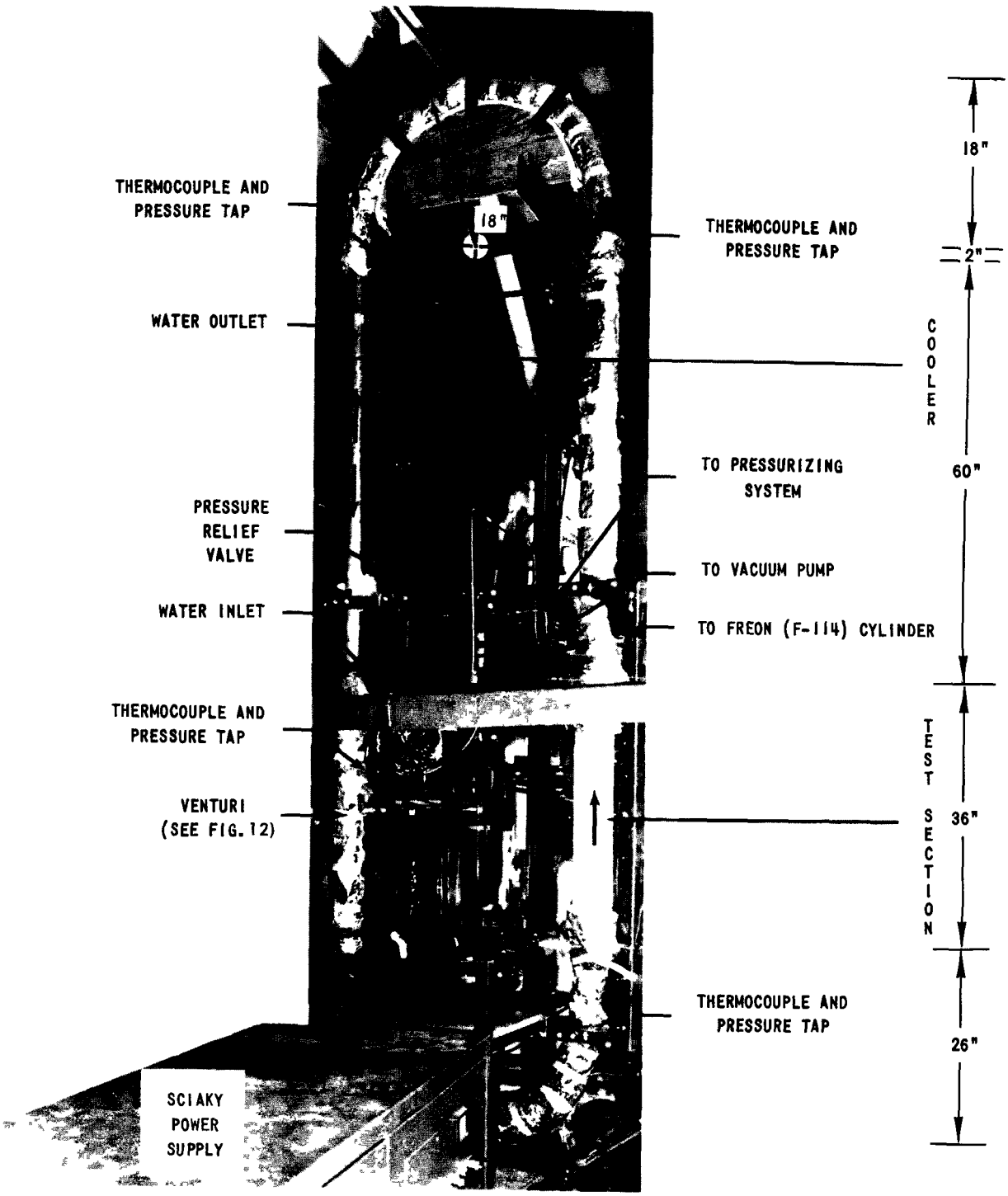

112-2330

Fig. 4. Front View of Test Loop

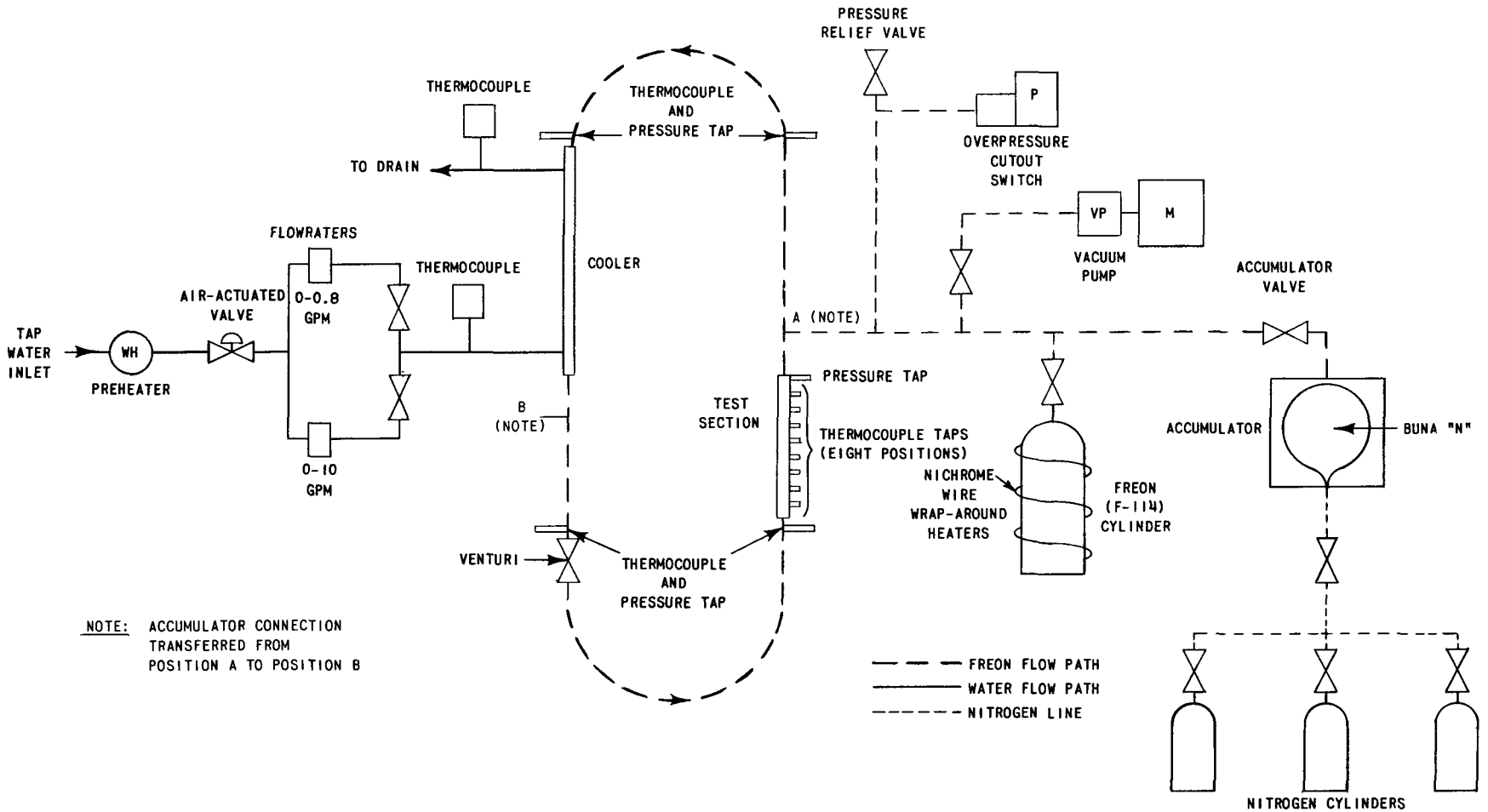

Fig. 5. Schematic Diagram of Test Apparatus

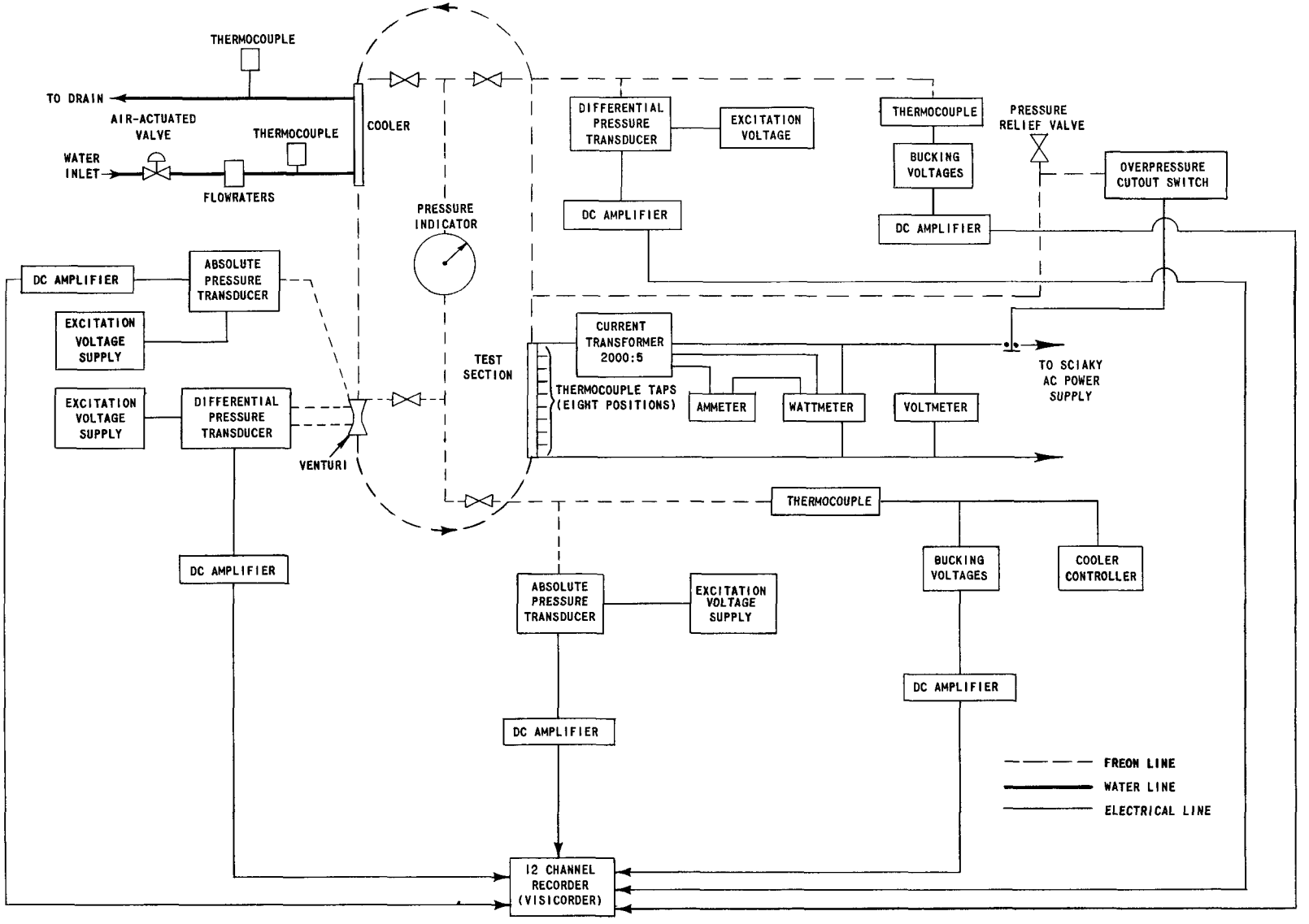

Fig. 6. Instrumentation Block Diagram

1. TEST SECTION TEMPERATURE INDICATOR
2. FLOWRATERS
3. HEISE PRESSURE GAUGE
4. THERMOCOUPLE JUNCTION BOX
5. REMOTE POWER CONTROL
6. AMMETER
7. VOLTMETER
8. WATTMETER
9. POTENTIOMETER
10. DIFFERENTIAL PRESSURE TRANSDUCER

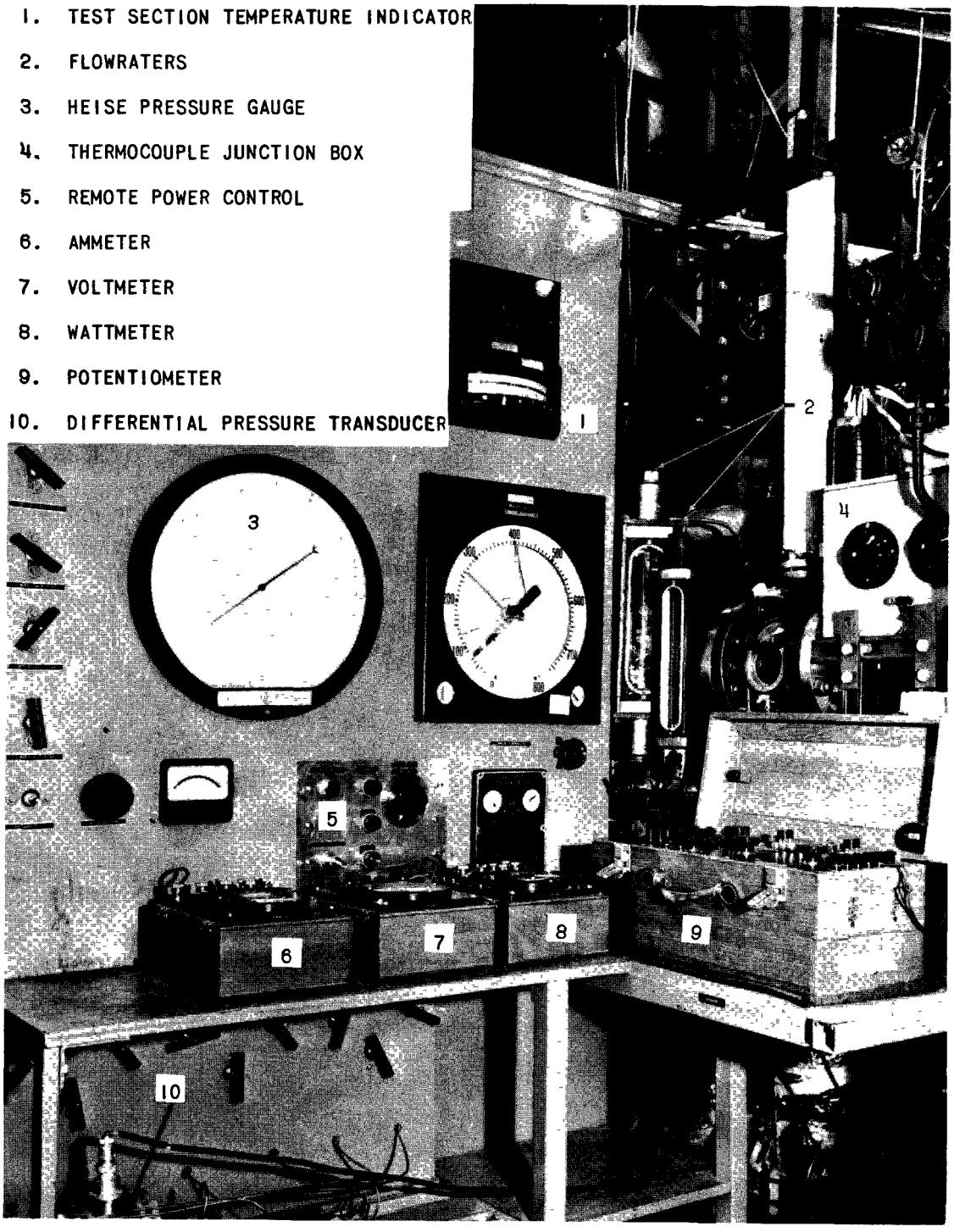

112-2329

Fig. 7. Control Panel Board

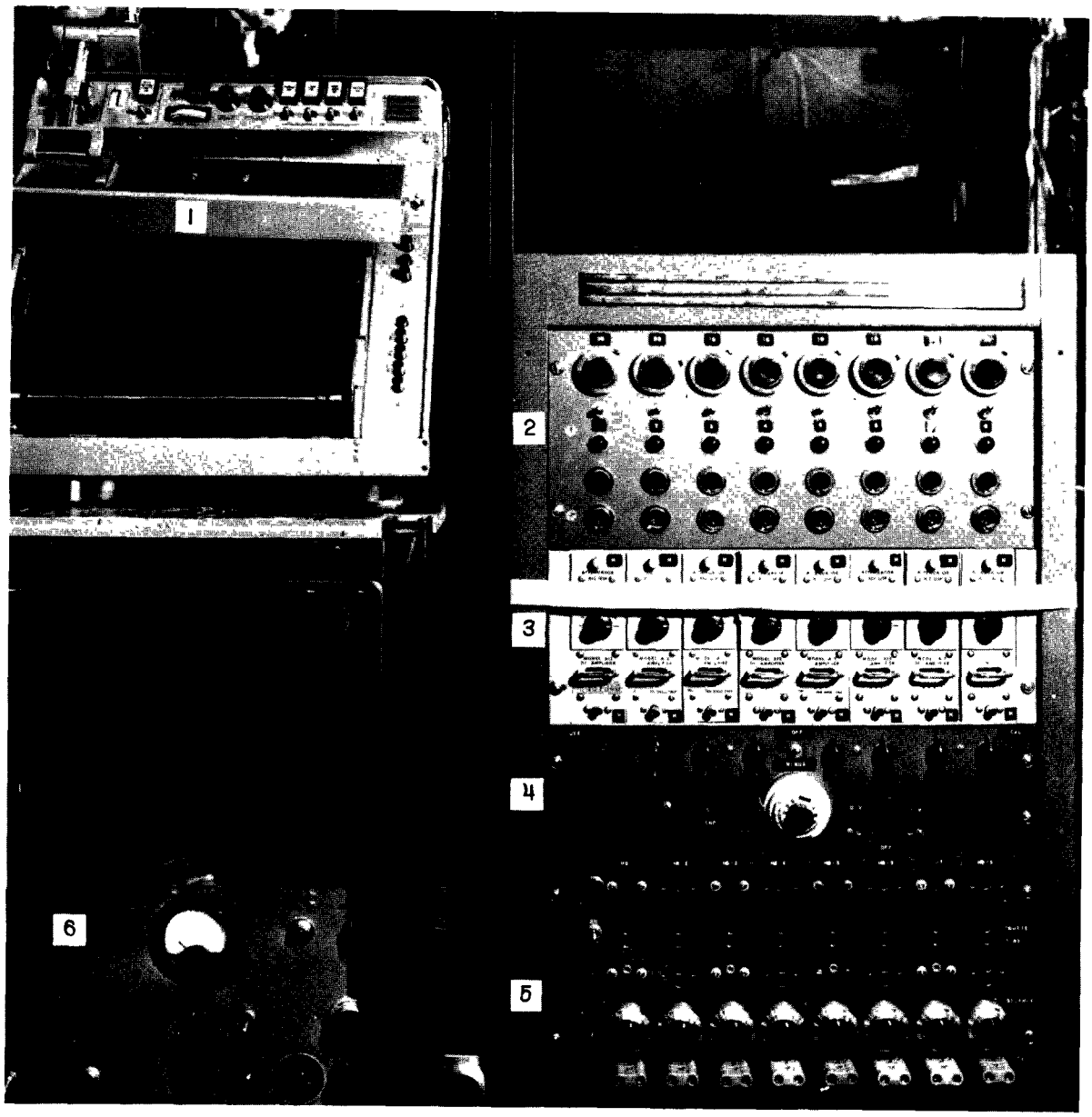

1. VISICORDER
2. BUCKING VOLTAGES
3. DC AMPLIFIERS
4. CALIBRATION POTENTIOMETER
5. POWER SUPPLIES
6. BURNOUT CONTROL PANEL

112-2328

Fig. 8. Instrument Racks and Visicorder

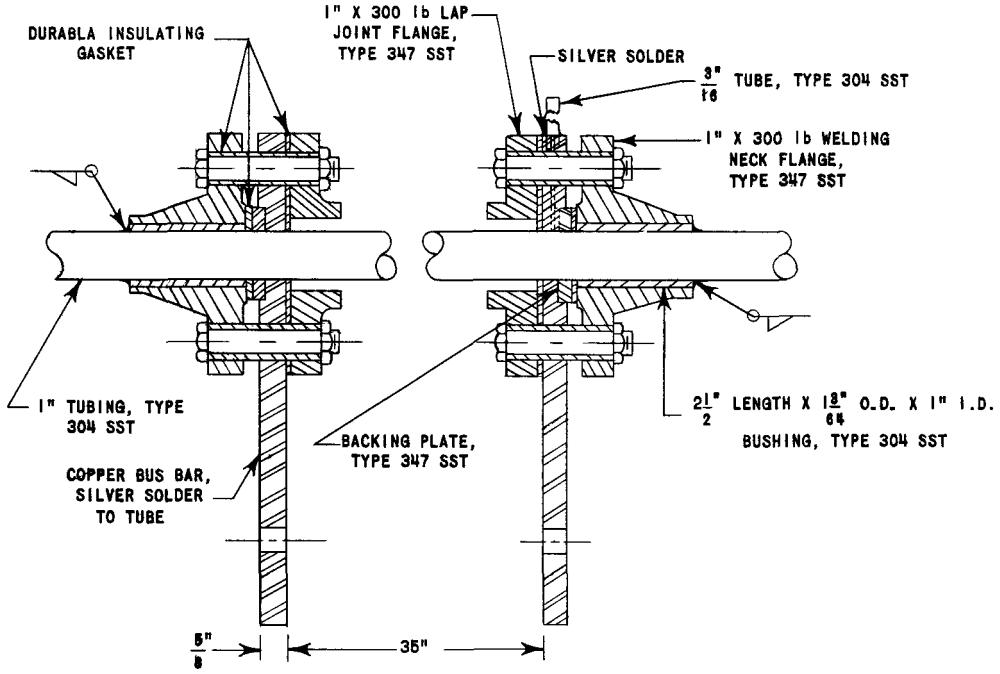

Fig. 9. Assembly Drawing of Test Section

To protect personnel and the test section, several automatic safety features were included in the apparatus:

(1) overpressure protection by means of a rupture disc;

(2) shutdown of electrical power if the system pressure exceeds a preset pressure;

(3) burnout detector.

Rupture-disc breaks and electrical-power shutdown by the pressure cutout switch were encountered several times in the experimental program. Burnout detection was based on visual observation of the test-section temperatures on two potentiometric-type temperature indicators. Although the response time of the indicators was slow, the heat fluxes were low enough that manual reduction of power was sufficiently fast to prevent overheating the heater tube when burnout conditions were encountered.

The 5-ft-long cooling jacket was welded to the tube (see Fig. 10). No allowance was made for the uneven thermal expansion between the jacket and the tube. Cooling was with tap water. The inlet and outlet temperatures and the volumetric rate of flow of the cooling water flowing through the heat exchanger was measured to provide data for a heat-balance check on the energy input to the system. The temperatures were measured with chromel-alumel thermocouple probes placed in the water lines. The volumetric flow rate was measured with a calibrated Flowrator.

Two Flowrators with ranges of 0 to 0.6 and of 0 to 10.0 gpm were connected in parallel on the water-inlet line to measure the volume rate of water flow. Inlet water flow was to have been controlled by an air-actuated valve slaved to a thermocouple signal originating at the inlet to the test section, but operating experience led to manual control. The cooling capacity of the cooler was found to be excessive under some operating conditions and insufficient for others. This effect will be explained in more detail in Chapter V.

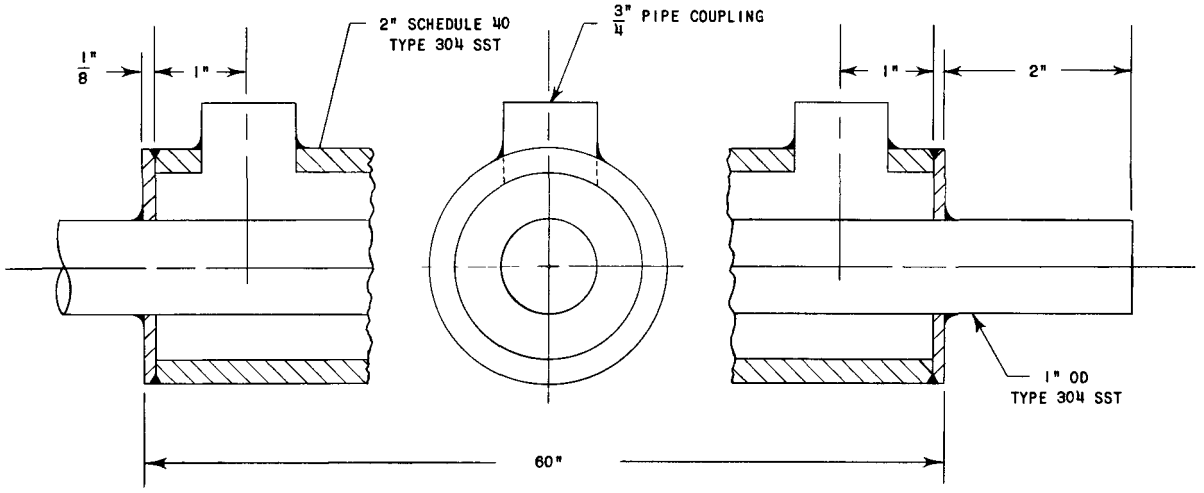

Fig. 10. Heat Exchanger Detail

All Freon-114 bulk temperatures were measured with bare 30-gauge chromel-alumel thermocouple probes in the fluid stream. The probes were positioned perpendicularly to the tube axis, with the tip at the tube centerline. This positioning was accomplished by using a Swagelock union in which a 1/8 NPT x 3/16 Swagelock male connector had been arc-welded on one of the flats of the hex body (see Fig. 11). The inlet thermocouples for the test section and cooler were placed immediately

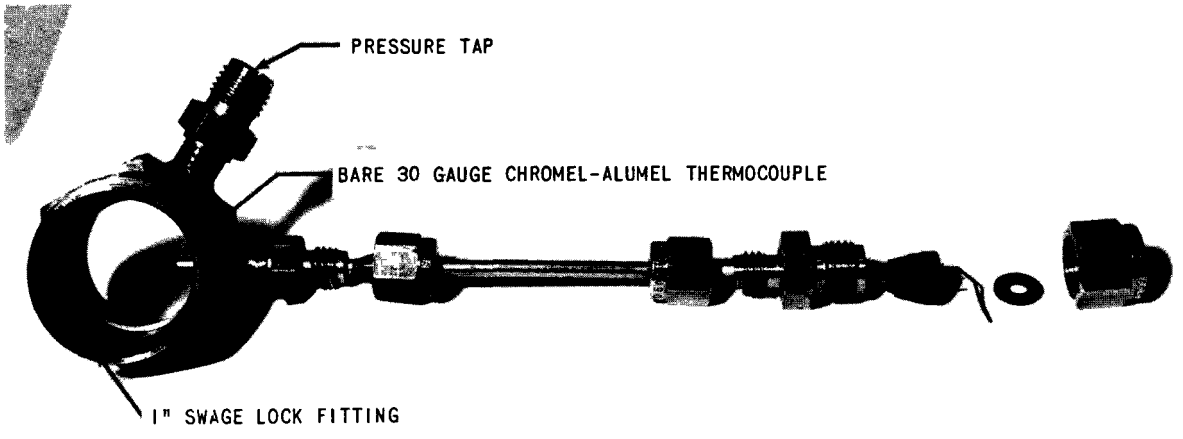

112-2327

Fig. 11. Bulk Thermocouple and Static Pressure Tap Installation Details

upstream of these components. The outlet thermocouples were placed approximately 20 diameters from the exit. This placement assured that the temperatures were measured at points where the velocity and temperature profiles were constant, or nearly so, across the tube.

All bulk temperature thermocouples were calibrated in a hypsometer-type apparatus. In this apparatus, the pressure could be varied from 0 to 2500 psig, giving a continuous range of calibration temperatures to 660°F. The thermocouples used in this experiment were calibrated in the range from 200 to 500°F. No significant deviation of the thermocouple emf from the tables of the manufacturer were noted; hence, the tabulated values of emf versus temperature were used.

A Minneapolis-Honeywell "Visicorder" continuously recorded the thermocouple emf's. The dc signal from the thermocouple was amplified one thousand times by a transistor amplifier before recording. It was not possible to detect temperature fluctuations of less than about 1°F because for small signal fluctuations the pickup noise level was comparable to the signal. The thermocouples had good frequency response, the time constant being about 8 to 20 ms. The time constant was deduced by comparing the 30-gauge bare-wire thermocouples with 28-gauge bare-wire thermocouples which had been tested for response and which were found to be in this range (see Ref. 15).

Outside surface temperatures of the heater section were measured with chromel-alumel thermocouples discharge welded to the outside of the section. All wall thermocouples were wrapped two turns around the tube, to minimize any conduction errors, and secured in place by wrapping with glass tape.

Several thermocouples were inserted in the insulation surrounding the loop to check the heat loss to the environment. This knowledge about the test section was of particular importance in order to correct energy input to the system fluid.

Energy Input

The energy input to the test section was measured with a precision Weston portable wattmeter with a range of 0-500 w and an accuracy of 0.25 per cent of full scale. As a check of the values obtained, the heat generation was also determined by the product of the voltage E across the test section and the current through it. The current was reduced with a current transformer with ratios of 5:2000 and 5:4000 and read on a calibrated ammeter. Voltage drop along the test section was measured with a Weston portable voltmeter with a range of 0-30/75 v and an accuracy of 0.25 per cent of full scale.

The heat flux density of the test section is only a function of the total resistance and the heat-transfer area A_H, and is shown by the following equations:

$$Q/A_H = \frac{1}{A_H} \frac{E^2}{R^1} \frac{1 \text{ Btu}}{1.054 \text{ kw-sec}} \quad ;$$

$$R^1 = \rho L/A \quad . \qquad \text{(IV-1)}$$

Flow Measurement

To obtain indication of transient flow, a Pottermeter was originally installed in the loop. The Pottermeter is a volumetric flow-measuring transducer with a digital electrical signal output whose frequency (cps) is directly proportional to flow rate. Each pulse represents a discrete volume for flow totalization. This method of flow measurement was found to be unsatisfactory because the Pottermeter rotor would become stuck after a few hours of operation. Inspection of the Pottermeter upon removal from the loop revealed no significant deposits or corrosion. Two Pottermeters were tried before abandoning this method of flow measurement.

Since a venturi can be used to measure flows with a high degree of accuracy and its accuracy is not affected to as large a degree by corrosion or deposits as some of the other meters, this type of equipment was used as the flow-measuring device. The venturi was chosen over the mechanically simpler thin-plate orifice because of its higher pressure recovery. The flow rate in the loop could vary over wide limits, and, hence, the venturi was sized to obtain pressure drops of reasonable magnitudes at the expected high and low flow rates. The venturi was designed according to the principles set forth in Ref. (48). The details of the design are shown in Fig. 12.

The flow pressure drop in the venturi was measured by two methods: (1) a manometer containing a fluid of 2.95 specific gravity was used for steady-state runs, and (2) a differential pressure transducer Stathan Model PM 80 TC, 0-5 psig was used for the transient runs. The signal from the transducer, connected by short lines to the pressure taps, was recorded by the Visicorder. This arrangement gave rapid response to a change in the flow rate as made evident by the change in the pressure drop. The accuracy of the differential pressure transducer was 0.25 per cent full scale. Nonlinearity and hysteresis were less than 0.1 per cent.

System pressures at four points (see Fig. 4) in the system could be measured by means of pressure transducers or by a Heise bourdon tube pressure gauge. Connection to the system was by means of a 1/8 NPT x 1/4-in. Swagelock male connector arc-welded to the Swagelock union (see Fig. 11). The pressure transducers were used for the transient

measurements while the gauges were used for steady-state operation. The Heise gauges had a calibrated accuracy of 0.1 per cent of the full-scale reading. All pressure tap lines were cooled in a counterflow water cooler to insure that the instrument lines were always full of liquid and that the temperature limit of 250°F of the fluid in contact with the transducers was not exceeded. The accuracy of the absolute pressure transducer was 0.25 per cent full scale. Nonlinearity and hysteresis were less than 0.1 per cent.

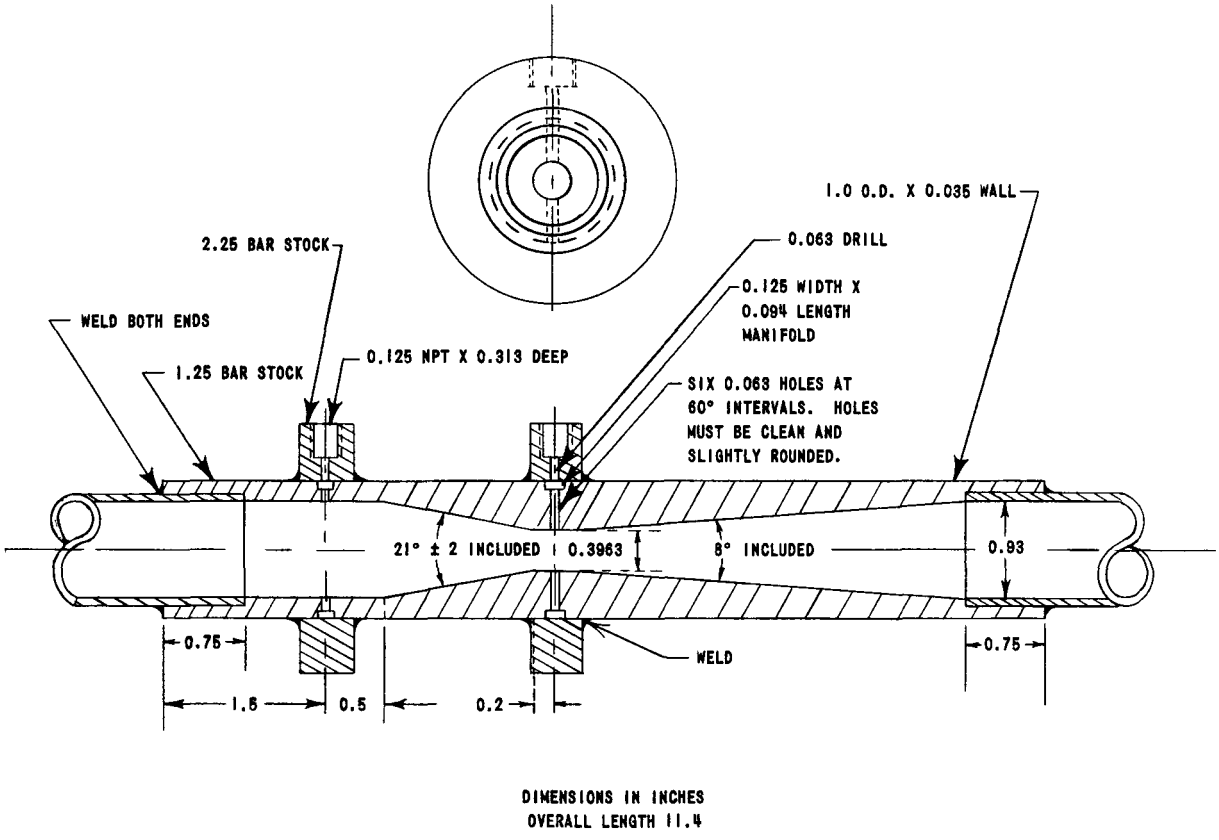

Fig. 12. Venturi Detail

The accuracy of the amplifying and recording instrument was sufficient to introduce no appreciable error in the recorded quantities.

Before beginning a series of runs, the bucking voltage-amplifier recorder combination was checked by introducing a calibrated signal in place of the usual signal. Any variation of the recorded signal with respect to the input signal was corrected by adjusting the gain in the amplifier. In this manner the performance of the recording unit could be checked and adjusted.

It was possible to raise the system pressure by two methods: (1) heating the constant-volume system, or (2) use of a nitrogen bag accumulator. The method of raising the pressure during warmup is discussed

in Chapter V. A pressurizing system was included to insure that the loop was always filled completely with liquid before the start of heating and to make control of the system pressure easier.

The accumulator was also intended to damp fluctuations in the system pressure and absorb the volumetric expansion of the Freon as the temperature was raised. Without the automatic pressure control effected with the hydraulic accumulator, continual bleeding of the system charge was necessary to keep a given pressure in the system. Also, the heat input and removal rates had to be controlled much more closely. The hydraulic accumulator was a Greer $2\frac{1}{2}$-gal balloon type with nitrogen on the gas side. The test fluid entered the steel tank and collapsed the gas bag when the pressure increased, while the gas bag expanded and pushed the test fluid into the system when the system pressure decreased.

Three nitrogen bottles were connected in parallel with the gas-side volume to reduce the pressure rise in the gas side because of the liquid expansion on the liquid side. To minimize the liquid expansion, the system was filled with just enough liquid to allow pressurization. This was accomplished by filling the system with some arbitrary amount of fluid and then checking to see if the system would pressurize. If it would, then fluid was bled from the system until the pressure began to fall. At this point, the system contained the minimum amount of liquid which would allow pressurization. To insure that the temperature of the liquid in the accumulator did not exceed the operating temperature of 250°F, the line from the loop to the accumulator was run through a water cooler.

CHAPTER V

EXPERIMENTAL PROCEDURE

Before beginning the experimental work, the loop was hydrostatically tested at 1000 psi and checked for leaks. When all leaks were stopped, the system, which had been cleaned with trichloroethane solvent during assembly, was evacuated to remove the air.

The loop and associated tubing was then filled by boiling the Freon-114 into the loop. This was accomplished by adding heat to the Freon-114 container with wrap-around resistance heaters and infrared heating lamps, thus raising the temperature and pressure of the combined loop and Freon-114-supply cylinder system (see Fig. 5). Heat was added until the temperature of the Freon-114 in the container was at the saturation temperature corresponding to the pressure in the cylinder and loop. At the same time, cooling water was passed through the cooler in the loop, so that the Freon-114 distilled into the loop condensed to the liquid state. After the loop was filled, the system pressure was raised with the accumulator, and all manometer and transducers lines were bled to remove any air which might still be in the system.

To determine the charge of the system (pounds mass of Freon-114 in the constant-volume system) use was made of the thermodynamic tables for Freon-114. After a partial filling or bleeding of the system, it was necessary to measure the pressure and temperature of the system in a phase region in which the pressure and temperature are independent thermodynamic coordinates. With these two coordinates, the specific volume could be obtained from the tables. Then, since the total volume of the system was known, the charge could be calculated from the equation

$$\text{Charge} = \frac{\text{Volume of system, ft}^3}{\text{Specific Volume, ft}^3/\text{lb}_m} \quad .$$

In an experimental loop, such as Schmidt's,[37] in which all the heating was in the two-phase region where pressure and temperature are dependent coordinates, it was necessary to weigh the fluid as the loop was filled to obtain the system charge.

Three procedures could be used to start the loop in operation from normal room temperatures. The choice of startup procedure depended on the circumstances of a particular test. These procedures were:

(1) Charge the system with a mass of fluid which upon heating would expand to the critical volume at the critical pressure and temperature. Since the critical volume is approximately one-third the liquid saturation volume for most fluids at ordinary room temperatures and pressures, it would be necessary to fill the system about one-third full in

order to reach the critical point. The heating process can be followed on the T-S diagram as a constant-volume line. This was the procedure used by Schmidt, Eckert, and Grigull.[37] In this case, mild heating rates only can be applied until the system reaches the operating temperature and pressure range. In this method of heating, the fluid is entirely in the two-phase or superheated regions. The first and only attempt in this experimental program at starting operation of the loop by this method resulted in a rupture of the test section due to overheating.

(2) Fill the system completely with fluid. To obtain a desired pressure, bleed part of the fluid back into the supply tank as the fluid expands upon heating. This method allows heating to the critical temperature along the saturated liquid line. Above the critical temperature, the heating continues in the supercritical region. An alternative to partially bleeding off the system charge would be to adjust heat input or heat removal in order to bring the system to the desired operating point. This was the procedure used by Holman and Boggs.[19]

(3) Fill the system completely with fluid by pressurizing with an accumulator to the desired operating pressure. As the fluid is heated, it expands into the accumulator, which holds the system pressure constant. This was the main procedure used in this investigation. A variation of this procedure is to pressurize by means of an external pump or accumulator, then close the connecting valve. The initial pressure setting is maintained by balancing the heating and cooling rates, and by partial bleeding of the system charge. This was the procedure used by Van Putte and Grosh.[38]

It is known from experimental work that, as the critical region is approached, a large decrease in density at a constant pressure is encountered. A large density decrease (specific volume increase) in a constant-volume system will result in a large pressure increase. To prevent the pressure increase, it is necessary to reduce the mass of the system or to provide additional volume for the expansion. From preliminary operating experience it was found that in the critical region it was difficult to manipulate the controls fast enough to prevent the development of a large pressure surge. It was then decided to use an accumulator pressurizing system with a large surge chamber on the nitrogen side of the accumulator. It was assumed that the addition of the accumulator would not affect the loop operation except to reduce the pressure changes encountered in the critical region.

The pressurizer system was connected to the loop through $\frac{1}{8}$-in. tubing for Loop No. 1. This was found to be unsatisfactory because of the time delay due to the restricted fluid flow in the small line during a pressure transient; this prevented the accumulator from functioning effectively except for very slow transients. In the second loop, the pressurizer was connected to the loop through $\frac{1}{2}$-in. tubing, which allowed a much faster

response of the accumulator. Even this arrangement proved ineffective in damping the high-frequency pressure oscillations, although it functioned much more effectively than the first arrangement for pressure surges of lower frequency.

Addition of the pressurizer system made three methods available to maintain the system at a constant pressure. (1) Freon-114 could be bled from the system back to the supply reservoir (but not added); (2) it was possible to inject or remove fluid from the circulating system with the pressurizer system by raising or lowering the nitrogen pressure in the accumulator bag; and (3) heat input exactly balanced against heat removal. Changes in system pressure could be effected by any of the three methods; however, the second method was primarily used.

Operation of the loop was begun by pressurizing the system to the desired operating pressure. A low rate of heating power was applied to the test section to start the fluid flowing. Cooling water flow was not turned on until the fluid in the loop had been heated to near the operating temperature. After approximately 5 min of heating at 1 - 2 kw, the power would be increased by 2-kw increments to the desired operating power.

With the accumulator in the system to absorb the volume increase due to heating, the system essentially operated at a constant pressure except for small fluctuations about the mean. This left only two variables to vary in running the test program: the system pressure, and the heat added or removed. Therefore, a series of runs could be made at a constant pressure with variable heat input, or a constant heat input could be maintained and the pressure varied. The third controlling variable was the regulation of the inlet temperature by controlling the cooling water flow rate. This was the primary method of controlling the inlet temperature once the pressure and heat input were set.

Visual observation of the recorded fluid temperature, pressure drop across the venturi, and system pressure was maintained. This capability was a very important factor in this test program. Since the compressed-liquid region was the main thermodynamic region of interest in this investigation, a knowledge of temperature and pressure gave the thermodynamic state of the system at all times. This knowledge of the thermodynamic state of the fluid at various points in the loop made much easier the manipulation of the system pressure and heating rate to obtain a given thermodynamic state.

Since the purposes of the experimental program were to define the region in which the pressure and flow fluctuations occurred and to find the cause, the test program was of an exploratory nature. Considerable latitude was possible in running the test program since the variables which defined the thermodynamic state of the system and the flow measurements were being continuously recorded and thus could be rechecked at any time.

Initial exploratory runs revealed the unstable condition to be strongly dependent upon the inlet and outlet temperatures of the fluid in the heater section at a constant power input; that is, the fluctuations could be associated with the thermodynamic state of the system fluid. The test program was then concentrated on finding a functional relationship.

As the fluid was heated to the critical region, a rapid fluctuation in flow and pressure would be encountered. The frequency of these fluctuations, in the range from 10 to 20 cps, were essentially independent of the heating rate. The magnitude of the fluctuations depended to some extent on the heating rate: a higher heating rate resulted in larger fluctuations. At pressures from the critical to about 40 psi above critical, the fluctuations were encountered when the exit temperature of the fluid in the test section ranged from 280 to 285°F, temperatures 10-15°F below the critical temperature, 294.26°F. Hence, the phenomena could not be attributed to the critical point but rather to a critical region.

Fluctuations encountered when heating from below critical temperatures at a constant system pressure could be decreased or eliminated by lowering the system pressure. Thus, the fluctuations depended on the system pressure as well as the temperature of the fluid.

The fact that fluctuations were encountered at temperatures below the critical temperature presented a problem in getting to the critical temperature. In one procedure, heat was added at low power inputs (to provide smaller magnitude of fluctuations) while the cooling water was off to bring the system temperature to near the critical temperature; this method would take as long as one hour to reach the critical condition. In the second method, heat was added rapidly during transition through this region of instability, by leaving the cooling water off and using high power inputs to raise the system temperature rapidly. Once the fluid was heated to the point that the critical temperature was reached somewhere along the heated section, the loop operated stably. The mass velocity would be considerably higher.

It was thus determined that two regions of stable operation could be defined. One region was defined when the outlet temperature of the heater section was below a certain temperature range, which will be called the transition temperature range; the transition temperature range depended on the system pressure. The other region was defined when the inlet temperature to the test section was above the transition temperature range.

Once the fluid temperature had been heated past the transition temperature region and the loop was operating stably, flow of cooling water could be increased to reduce the inlet temperature and precipitate another mode of unstable operation. This time the fluctuations would be in the frequency range of 0.1 to 0.5 cps, and were analogous to the "coffee percolator

effect" observed in two-phase systems. Further lowering of the inlet temperature would result in the transition back to fluctuations of higher frequency.

When operating in the near-critical region at low power inputs, it was found that under certain conditions the wall temperature of the test section would decrease by about 50°F, indicating some improvement in the heat-transfer coefficient. This condition usually occurred when the inlet temperature of the system fluid was such that further increase in the inlet temperature resulted in an increased flow rate. Likewise, a decrease in the inlet temperature with the resultant decrease in flow rate resulted in a rise of the test-section wall temperature.

A few exploratory runs were made at subcritical pressures in which the fluid entered the test section as a compressed liquid and left in a superheated state. With the smaller loop, Loop No. 1, this mode of operation resulted in large pressure and flow fluctuations of the percolator type. By decreasing the flow of cooling water, the fluid could be made to pass to the superheated region entirely. Runs in this region were quite stable, but much higher wall temperatures were encountered as would be expected, since in this region the vapor heat-transfer coefficient is much lower.

The problem of cooling the test fluid mentioned in Chapter IV will now be explained in detail. When the fluid temperature was below the critical temperature, high power inputs (say 14 kw) would not permit the cooler to remove the heat input at the highest possible flow rate (10 gpm) of cooling water. As a consequence, the fluid temperature at the inlet to the test section would continue to rise. In the critical region a flow rate of less than 0.5 gpm was sufficient to maintain a constant inlet temperature at the same 14-kw power input. This wide variation in cooling requirements limited the steady-state test program in the regions of lower temperature to low power inputs (say 8 kw).

The possibility of the spring effect of the accumulator exciting the system fluctuations was investigated by closing the valve connecting the accumulator and the loop completely. This closing had no effect on the inception of the oscillations. If the system were oscillating, closing the valve had no effect. Hence, it was concluded that the presence of the accumulator in the system did not contribute to the oscillation mechanism.

CHAPTER VI

EXPERIMENTAL RESULTS AND DISCUSSION

The experimental program was devised to investigate the operation of a natural-circulation loop in the near-critical region to determine where and why pressure and flow fluctuations had been encountered in similar loops as reported in the literature. To this end, measurements of transient temperature, pressure, and flow were made. A summary and discussion of the results are presented in this chapter.

It was discussed in the preceding chapter that the occurrence and severity of the fluctuations noted seemed to be strongly dependent upon the thermodynamic state of the fluid in the loop. In order to define this thermodynamic state, the products of density and enthalpy along various isobars were plotted versus temperature (see Fig. 13). The stimulus for this plot came from the fact that when the energy equation is written for a control volume and the approximation that the enthalpy is equal to the internal energy is made, the density and enthalpy appear as a product, i.e.,

$$(Gh)_{inlet} - (Gh)_{exit} - Q/A = (\Delta z)\,\frac{d}{dt}\,(\rho h) \quad .$$

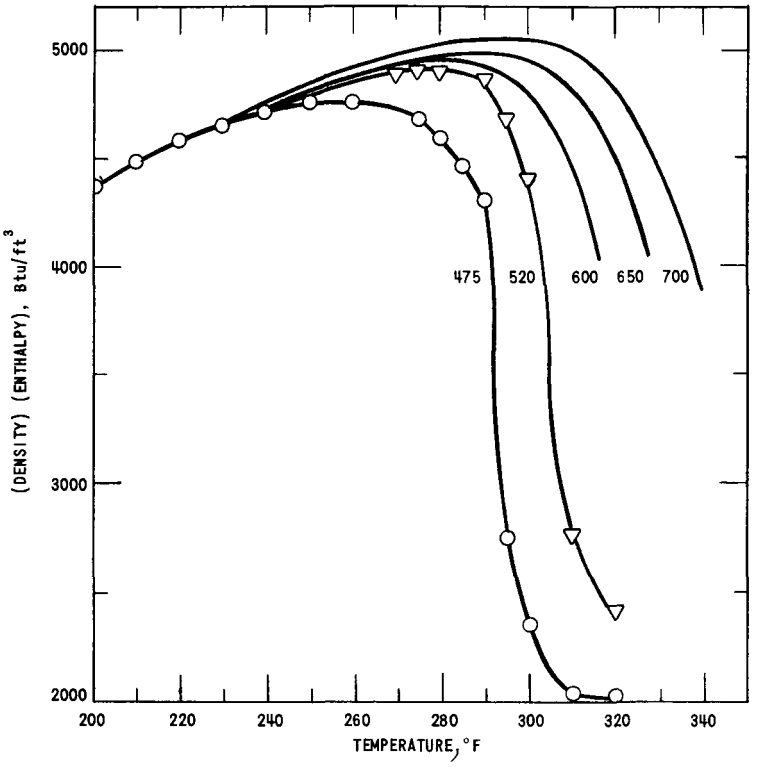

Fig. 13. Density-Enthalpy Product for Freon-114 along an Isobar as a Function of Temperature. (Pressures in lb_f/in^2).

It is seen from Fig. 13 that the product of density and enthalpy has maximum values that shift with higher pressures to higher temperatures. It was noticed from the experimental results that the flow oscillations were most severe in the thermodynamic region in which the density-enthalpy product passed through its maximum value. In this region, as little as $1\frac{1}{4}$ kw was necessary to maintain a sustained flow oscillation. Approach of the maximum value from the left or low-temperature side resulted in flow and pressure oscillations in the 10-20 cps range; approach from the right or high-temperature side resulted in flow and pressure oscillations in the range from 0.1 to 0.2 cps. Since experimental results indicated that the oscillations were dependent on system temperature and pressure, the occurrence of sustained flow oscillations in the region of the maximum in the (ρh) product was another indication that the cause of the sustained flow oscillation was strongly dependent upon these thermodynamic variables.

The significance of the ρh product as a function of T or h is that it is a measure of the volume expansion of the fluid with heat addition. A change in the slope of the product signifies a different rate of volume expansion with heat addition, which, when introduced into the momentum equation, requires increased or decreased flows.

A steady-state flow requires that the driving head remain constant with time. As the ρh slope changes a condition is introduced in which the driving head must change with time. Hence, a sustained flow oscillation results if the condition which forces the change in driving head can be reproduced with time.

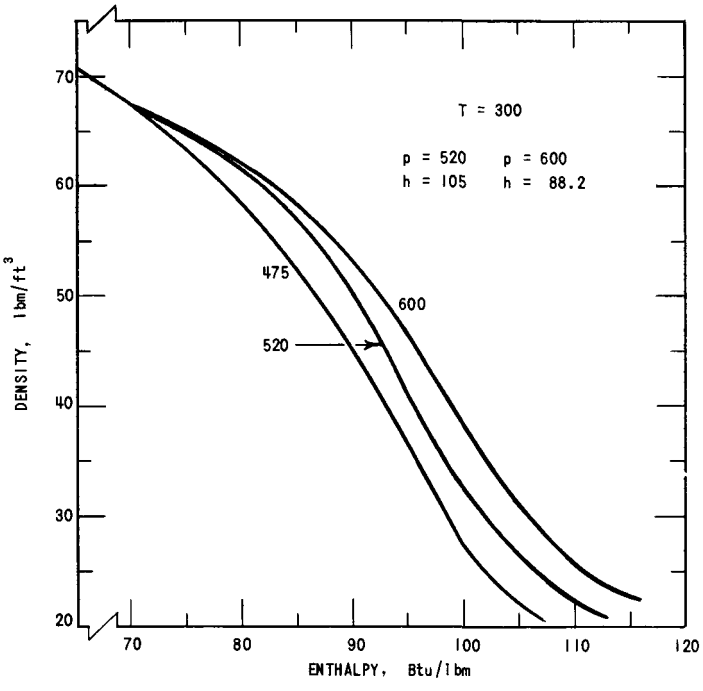

Fig. 14. Isobars of Density-Enthalpy for Freon-114.

The density-enthalpy product is a thermodynamic function of the fluid that can be determined if two independent thermodynamic properties are known. In this case, temperature and pressure are known. A change in the slope of the ρh product versus T or h indicates a change in the rate of change of one of the quantities with respect to the other; that is, if ρ is plotted against h, there is a change in the slope of this curve at the point where the change in slope of ρh occurred (see Fig. 14).

The occurrence of the maximum in ρh versus

T corresponds to a change in slope of ρ versus h and hence to a change in $d\rho/dh$. It is seen from Eq. (III-12) that an increase in $d\rho/dh$ would result in a greater change in the local mass velocity during a transient. This will cause a change in the average mass velocity in the loop, followed by further changes in the local densities throughout the system, since the time rate of change of density depends on the mass velocity in addition to the heat input.

The physical manifestation of the fluid under operating conditions in which the ρh product changes slope is as follows. A positive value for $d(\rho h)/dT$ means that the enthalpy increase is greater than the density decrease; hence, the fluid will be accelerated smoothly through the heater section. A negative value for this slope means that the density increase is greater than the enthalpy increase; hence, the fluid will be accelerated more rapidly in the heater section than in the previous case.

However, there is a point at which the negative slope decreases to a small value. This introduces another change in the rate of acceleration of the fluid with the heat addition.

The problem appears to be one of different rates of acceleration of the fluid with heat addition. In the nth cell, the fluid accelerates more rapidly than in cell n-1. This tends to decrease the flow of fluid into cell n-1. At the same time, the fluid that left the nth cell will try to travel at its exit velocity. In a closed circulatory system with an almost incompressible fluid, a transient is certain to develop. This is the sequence of events shown in Fig. 3(b).

The oscillatory behavior in the near-critical region can be analyzed in terms of the variation of ρ with h. Under operating conditions in which the slope of ρ versus h is constant or nearly so, the loop operates with no variation in flow rate other than random fluctuations. Adjustments of the operating parameters such as heat input (heat removal), system pressure, and inlet temperature, which bring the fluid in the loop to a point where further adjustment will result in a change in slope of ρ versus h, introduces the possibility of an unstable condition. Further adjustment of the system parameters, which results in a change of the slope of the ρ versus h curve, will result in sustained flow oscillations.

The oscillations become more severe as the heat input is increased and will not subside until the fluid state is changed from the region in which the change in slope of the ρ versus h curve occurs; that is, to prevent oscillations, the slope of the curve of ρ versus h should be as nearly constant as possible in the heater section, or in the heater and riser in the case of two-phase systems.

The problem encountered in trying to operate with the system fluid at a condition such that a change in the density versus enthalpy slope occurs is the same as that encountered when the heat flux along the length of a channel is increased from its steady-state value to some higher value in a stepwise manner. The pressure immediately begins to rise along the heater tube. This increase can be relieved by velocity changes, however, only around the entire loop. Fluid is expelled from the heater section more rapidly than at the steady state and is introduced at the inlet at a lower rate. These disturbances are propagated in their respective directions to the cold leg of the loop, and tend to reinforce and cancel each other at different times during the subsequent transient.

From examination of Eq. (III-12) and the physical experimental model, an explanation can be obtained for the two different frequencies of oscillation. It has been seen that changes in the value of $1/\rho\ (d\rho/dh)$ lead to sustained flow oscillation. Comparison of theory and experiment leads to the conjecture that the portion of the tube in which the magnitude of the $1/\rho\ (d\rho/dh)$ multiplier changes value is important. If this multiplier becomes large in the upper portion of the tube, then the mass of fluid to be expelled from the heater section is small and can be accelerated rapidly by the buoyant force created by the heat addition. If this term becomes large in the lower portion of the heater tube, then the mass of fluid to be expelled from the heater section is large and cannot be accelerated as rapidly. In addition, the element of fluid is undergoing further expansion as it passes through the heater tube. Thus, it seems likely that the first case, in which small amounts of fluid are involved, could be corrected quickly, while the second case would take longer.

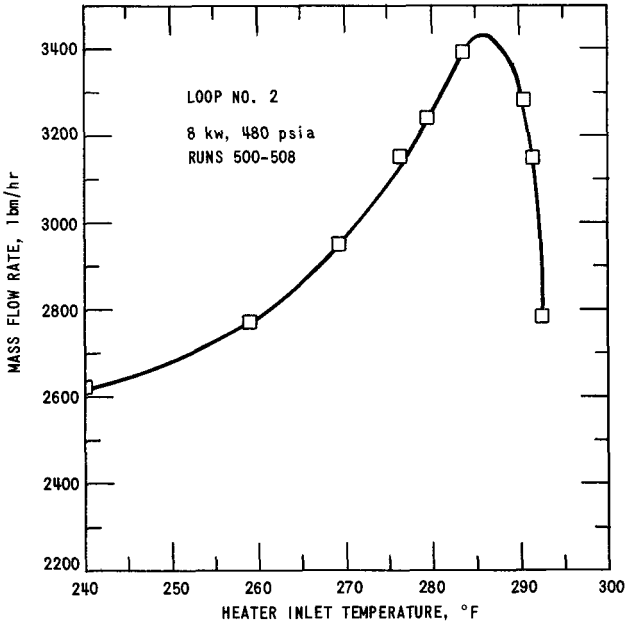

Fig. 15. Effect of Inlet Temperature on Flow Rate

The density and enthalpy changes of a fluid in the near-critical region are larger with temperature and pressure than the changes encountered at lower pressures and temperatures (see Appendix B). In a natural-circulation loop in which the flow rate is dependent on the heat input and the consequent density change, the density change with temperature assumes a significant role in determining the flow rate. Figure 15 shows a typical increase in flow rate at a constant heat input and pressure as the fluid temperature is increased. The data points were obtained in steady-state runs at a particular inlet temperature. The maximum in the curve occurs

at an inlet temperature below the critical temperature. The inlet temperature to the test section at the maximum corresponds to the temperature at the maximum in the density-enthalpy product. As the inlet temperature is increased past the temperature corresponding to the maximum in the ρh curve, the flow rate drops sharply as a result of the decrease in the density driving head.

In Fig. 16 is shown the relationship between mass flow rate and the input power to the heater at a constant inlet temperature. The rate of increase of the mass flow rate decreases as the input power is increased. The explanation for this can be determined from examination of the density-temperature curve (see Appendix B). At 515 psia and inlet bulk temperatures in the 285-290°F range, the average inlet density to the test section can be approximated by 57 lb_m/ft^3 to within 1 lb_m/ft^3. The outlet density from the test section will range from 54 to 28 lb_m/ft^3 as the power is increased from 4 to 17 kw. The rate of change of outlet density decreases sharply at the higher power inputs (higher outlet temperatures). This means that the driving head for flow circulation does not increase proportionately with the power input; hence, the mass flow curve tends to approach an asymptotic value which is determined by the slope of the density-temperature curve, i.e.,

$$\frac{\partial \dot{m}}{\partial Q} \rightarrow \text{Constant as } \left(\frac{\partial \rho}{\partial T}\right)_p \rightarrow \text{Constant value}$$

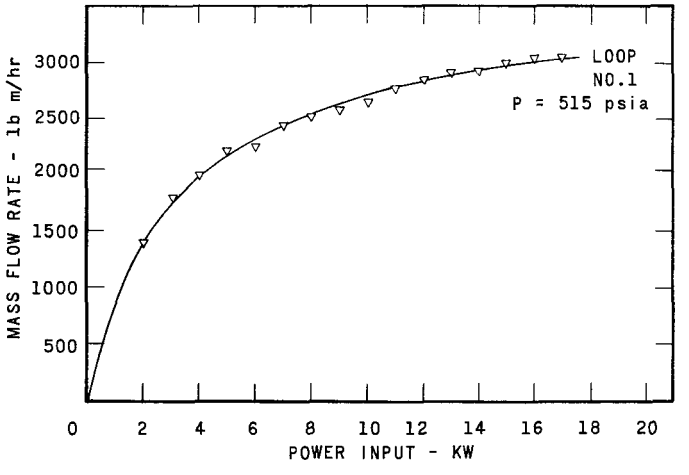

112-2209

Fig. 16. Mass Flow Rate as a Function of Power Input at a Constant Inlet Temperature

As stated above, the inlet bulk temperature to the heater section corresponded to the temperature at the maximum of the ρh curve at this pressure. This curve then represents the upper limiting value of the flow rate which could be obtained in this loop.

Under some conditions, the wall temperature of the test section increased or decreased by 50°F, a condition generally occurring in the region in which the maximum flow occurred. The wall temperature of the test section would decrease as the flow began to increase. After the maximum flow occurred, the wall temperature would again increase as the flow decreased. This latter condition would have resulted in a burnout had the heating been continued. However, in order to continue the experimental work, the power would be reduced when the maximum in flow had occurred.

In Fig. 17 is shown what will be termed a power instability. The power input to the test section was normally very steady. In the run to which Fig. 17 refers, the power was varying by about one kw because of the large change in tube wall temperature that was occurring, resulting in changing the electrical resistance of the tube sufficiently to cause a variation of power output from the power supply. This back-and-forth interplay of electrical resistance and power resulted in the sustained flow and temperature oscillations shown.

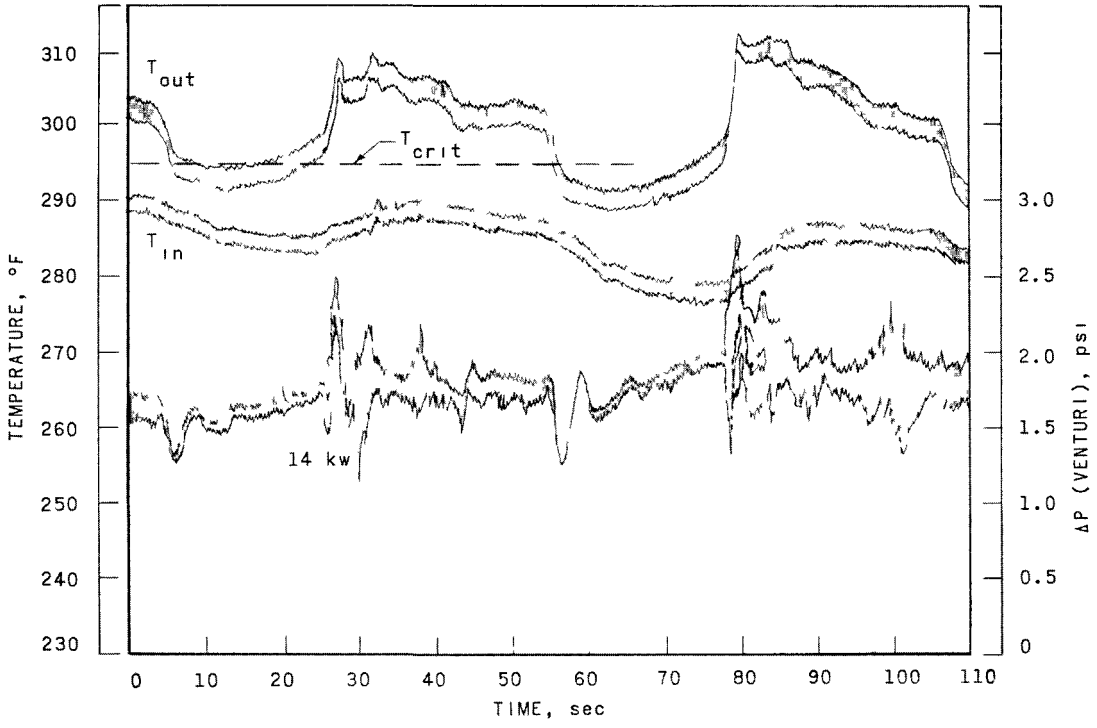

112-2200

Fig. 17. Power Instability, Loop No. 1, 14 kw, 480 psia, Oct. 3, 1962

The initial effect of a pressurization is shown in Fig. 18. The initial state of the fluid corresponded to the major part of the fluid in the heater tube being to the right of the maximum in the ρh curve. The purpose of the pressurization was to shift the thermodynamic state of the fluid

so that the major part of the fluid in the heater section bracketed the maximum in the ρh value and, hence, the system would tend to be unstable. Further pressurization would shift the state of the fluid to the left of the maximum in the ρh curve, and the system would become stable again. As can be seen, the loop was operating fairly stably before the beginning of pressurization. The spread of the venturi pressure differential at this time reflects the fact that the inlet temperature was a little to the left of the maximum in the ρh curve. As pressurization was begun, the venturi pressure differential showed an increase, because the pressurizer accumulator was located upstream of the venturi; thus, the fluid injected because of the pressurization shows at this point. Next, the inlet temperature to the heater began to fall rather rapidly as soon as the mass of injected fluid reached that point. Note, though, that the outlet temperature had begun to increase with pressurization; this is because of the decrease in the heat capacity of the fluid as the pressure was increased. The decrease in the heat capacity can be seen in the thermodynamic plot of enthalpy versus temperature (see Appendix B). The slope of the enthalpy with temperature

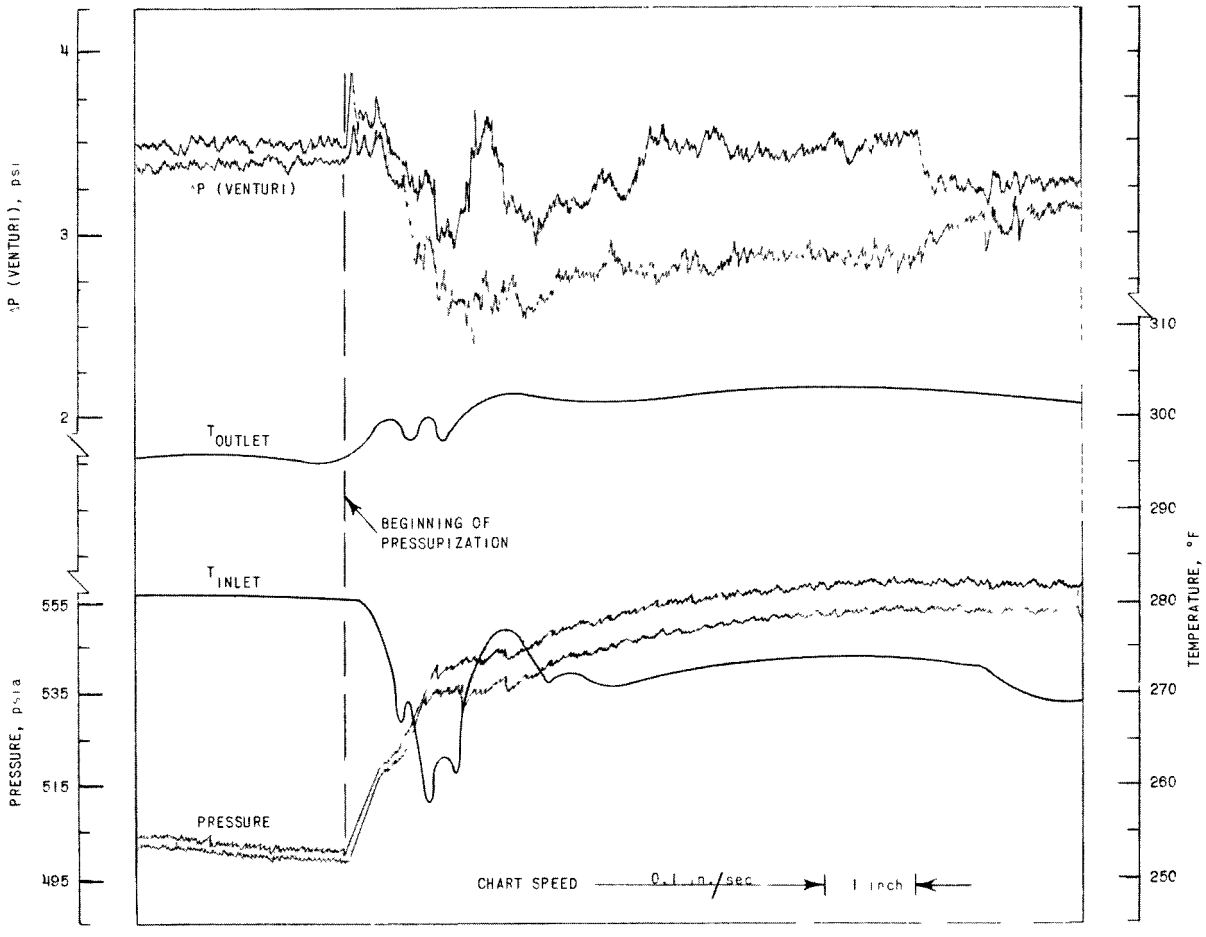

Fig. 18. Effect of Pressurization, Loop No. 2, 16 kw, Nov. 9, 1962

along an isobar is the specific heat. Increasing the pressure decreases the slope of the enthalpy isobaric line. The decrease in mass velocity following the initial upsurge is due to the change in the volume coefficient of expansion as shown by the change in slope with pressure of the density-temperature curve. After a few seconds, the loop settled down to steady and sustained flow and pressure oscillations which were in the range from 10 to 20 cps.

Further increase of pressure resulted in the loop beginning to settle down to smaller oscillations. This state corresponded to the major part of the fluid being on the low-temperature side of the (ρh) maximum. This transient record shows the sequence of events which was expected.

It was noticed that when the fluid was in the thermodynamic region in which the "coffee percolator effect" would be found, the perking was preceded by small-amplitude, high-frequency fluctuations prior to the large flow excursion. Such an event is shown in Fig. 19. The frequency of the initial oscillation is 10 cps, roughly 100 times that of the percolator frequency.

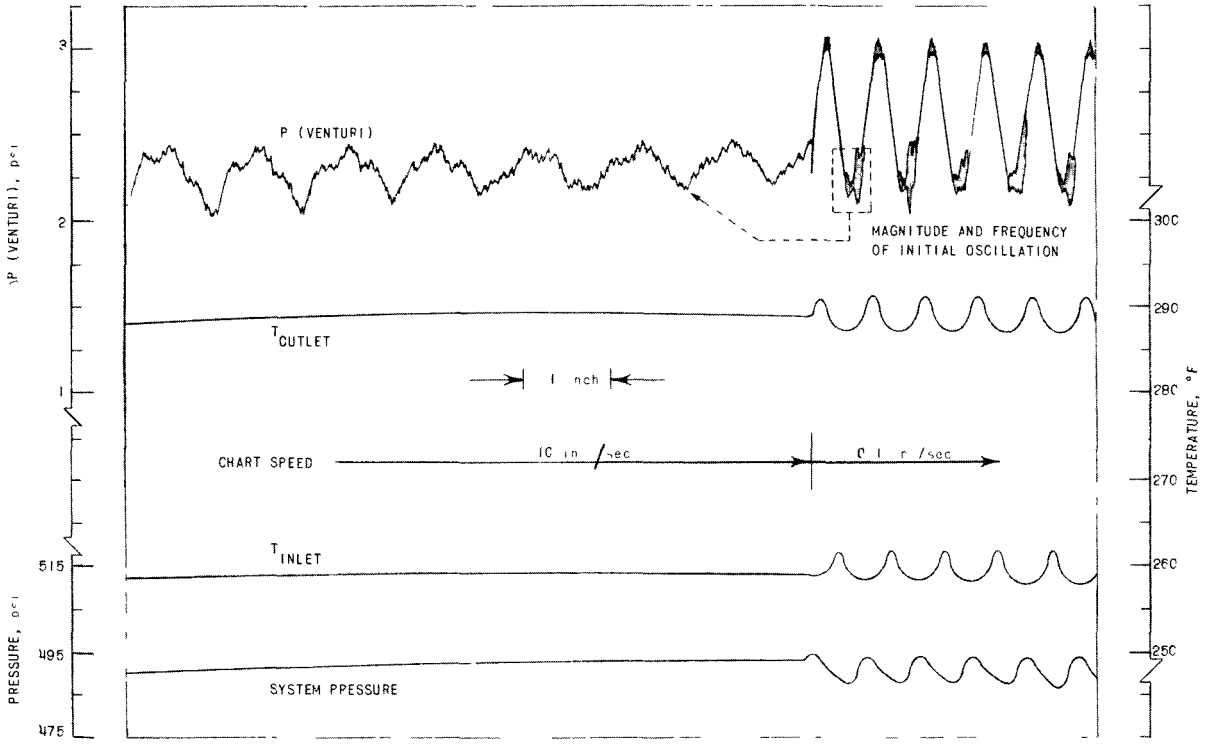

Fig. 19. Initial Oscillation Accompanying "Percolator Effect," Loop No. 2, 14 kw, Nov. 9, 1962

The loop could be operated at subcritical pressures in the subcooled or two-phase region. In the subcooled regions the operation of the loop was

very stable. When the fluid began to enter the two-phase region, the percolator effect would occur, provided the heat input was low. This oscillation could be controlled by increasing the system pressure to force the liquid back into the subcooled region.

The transition from the subcooled region to the two-phase region at moderate to high heat fluxes was accompanied by pressure and flow oscillations. Near the saturation point, burnout was observed; this would have destroyed the heater section had the power input been higher. This subcooled burnout was detected by observing the wall temperature of the test section on a potentiometric-type recorder. The sequence of events is shown in Fig. 20. This effect has been noted in several subcooled burnout studies [see Ref. (10)].

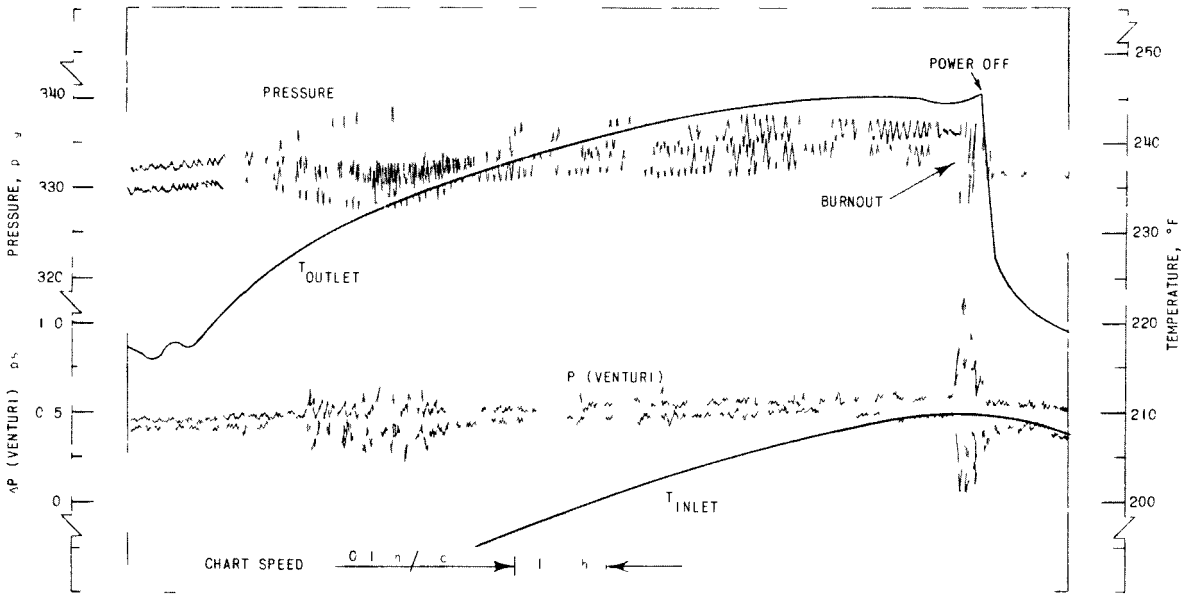

Fig. 20. Flow and Pressure Oscillation Approaching Burnout at Subcritical Pressures, Loop No. 2, 9 kw, Oct. 23, 1962

Early in the test program it was noticed that sustained flow oscillations would begin when all test variables were being held constant. Generally, these oscillations would begin as the thermodynamic state of the maximum in ρh was being approached in a series of steady-state steps from the low-temperature region. It is conjectured that these oscillations were triggered by a change in the heat-transfer coefficient or by the changes in $\overline{G}$ and $\partial h/\partial z$. In most instances, indicators of the test-section wall temperature did not show a change in temperature which would mean an improvement in the heat-transfer coefficient; therefore, the changes in $\overline{G}$ and $\partial h/\partial z$ were considered at the triggering mechanism.

It can be seen from the equation which describes the local change in G that for $\partial G/\partial z$ to change, $G\,\partial h/\partial z \lessgtr Q/A$. Approaching the maximum value of ρh from the low-temperature side results in an increase in G and decrease in $\partial h/\partial z$. It is conjectured that the increase in G, which is dependent on the decrease in ρ, is greater than the increase in $\partial h/\partial z$. The basis for this conjecture is that the maximum in the curve occurs because the decrease in density becomes larger than the increase in enthalpy. If the conjecture is true, then G increases faster than $\partial h/\partial z$ decreases, and the product will become greater than Q/A. This introduces the initial transient. If the $(1/\rho)\,(d\rho/dh)$ multiplier is large, the inertia of the stream is not damped by the resistance to flow in the loop and sustained flow oscillation result.

The record of a complete sequence of events showing the initial heating through the ρh maximum and the subsequent cooling back through the same maximum is shown in Fig. 21. As was deduced from the equation expressing $\partial G/\partial z$ as a function of the other variables, a rapid heating through the ρh maximum should produce a minimum of sustained flow oscillations; that is, in Eq. III-12, as long as $Q/A > G\,\partial h/\partial z$, then $\partial G/\partial z$ remains positive, and the fluid continues to accelerate with less chance for a sign change for $\partial G/\partial z$ which will occur if $G\,\partial h/\partial z$ momentarily becomes larger than Q/A. This is shown in the left half of the figure. Once the thermodynamic condition was reached that $(1/\rho)\,(d\rho/dh)$ had reached a nearly uniform value (this corresponds to being predominantly on one side or the other of the maximum in the ρh curve) throughout the heater length, the flow oscillations ceased. The flow of cooling water was then increased to reduce the inlet temperature and hence to traverse the maximum in the ρh curve from right to left. This action shifts the occurrence of the large $(1/\rho)\,(d\rho/dh)$ product to the bottom of the heater section, and the "coffee percolator" effect is obtained.

Isolated transients were encountered under some operating conditions, usually during the initial heating of the system. Figure 22 is a record of one such occurrence. An increase in system pressure of approximately 20 psi occurred, followed by an increase in flow and outlet temperatures. Note that the inlet temperature continued to increase at the same rate until some time after the initiation of the transient. This transient occurred while the system pressure and heat addition were being held constant; hence, an explanation for the transient is not readily available. It is conjectured that a momentary improvement in the heat-transfer coefficient changed the heat input to the system. From the equation describing the local increase in mass velocity, it can be seen that a momentary increase in the heat-transfer coefficient has the same effect as a step increase in heat input and the consequent transient. Shortly after this transient, the system reached a condition of sustained flow oscillations in the frequency range from 10 to 20 cps.

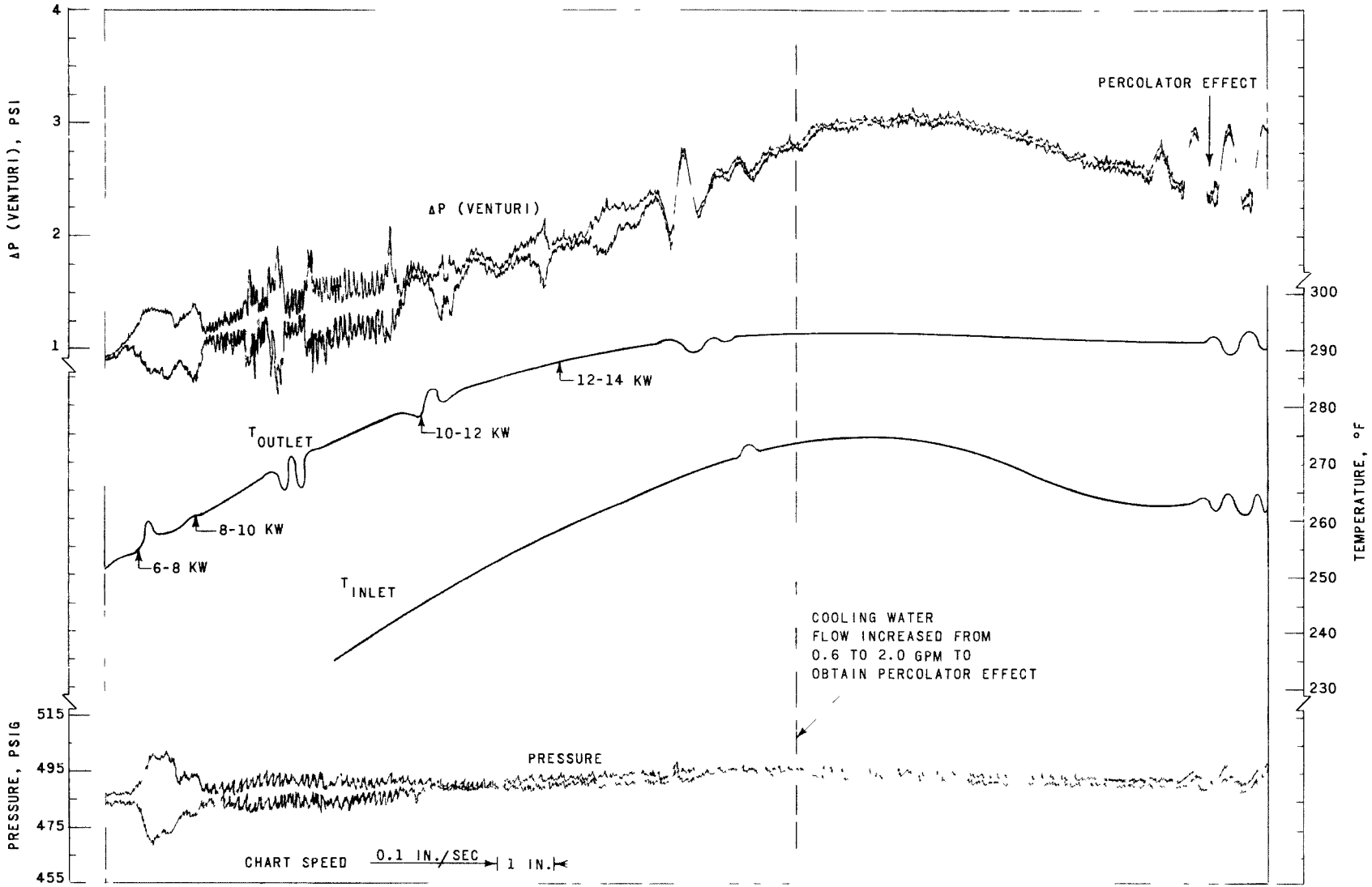

Fig. 21. Rapid Heating through the (ρh) Maximum and Subsequent Cooling, Loop No. 2, Nov. 9, 1962

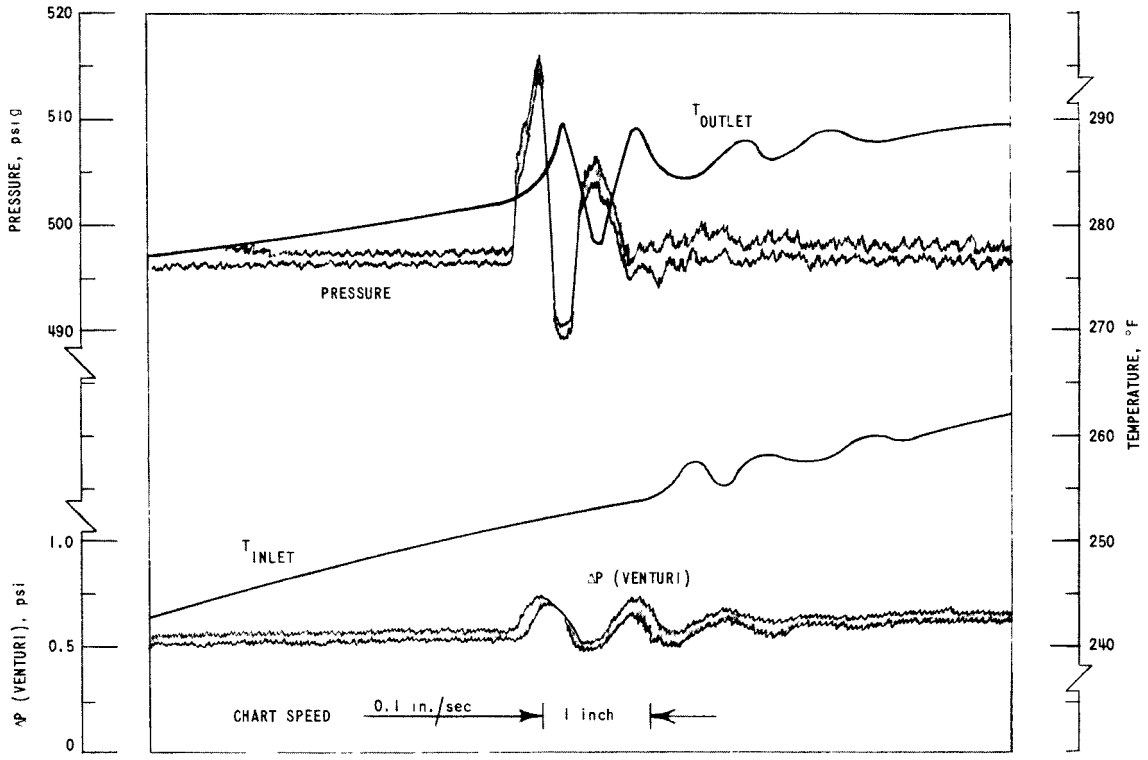

Fig. 22. Initial Transient Encountered in Heating, Loop No. 1, 5 kw, Oct. 2, 1962

When operating in the thermodynamic region in which the liquid was entering the test section in the subcooled state and leaving the test section in the two-phase or superheated region, severe pressure changes were noted with the small loop, Loop No. 1. Several transients are shown in Fig. 23. The decrease in local density is reflected in the pressure rise. Then follows the change in outlet temperature because of the change in specific heat capacity because of the pressurization. The pressure drop across the venturi, which measures the mass velocity, shows a periodic maximum value and then an oscillation about the mean, which decays exponentially. Note that the variation of inlet temperature was much smaller than that of the outlet.

This type of transient was not nearly as severe with Loop No. 2, which had the elevation for the driving head increased by 5.33 ft and a 50 per cent increase in volume. The increase in volume helped reduce the magnitude of the pressure fluctuations.

Once the fluid had been heated to the condition such that the minimum temperature difference across the test section was attained, attempts to reduce the inlet temperature to the test section resulted in severe and erratic transients in flow and temperature. One procedure to reduce the inlet temperature was to increase the flow of cooling water by a small

amount and then wait for the inlet temperature to decrease. The increased flow of cooling water would seemingly have no effect until suddenly the inlet temperature would drop sharply, by as much as 30°F. No recording of this event is shown because of the erratic nature of the transient. Figure 18 shows a transient of somewhat analogous type.

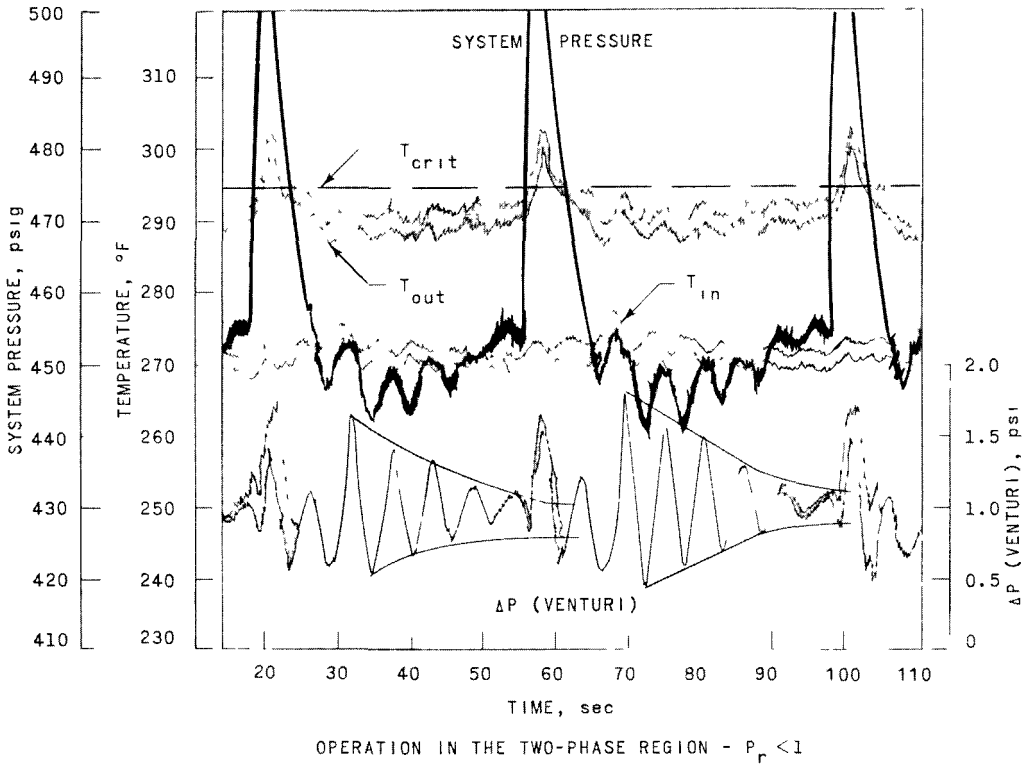

112-2198

Fig. 23. Operation in the Two-Phase Region, Loop No. 1, 6 kw, Oct. 3, 1962

Another procedure to shut the loop down was to reduce the power to zero. The same type of transient as noted above would be encountered.

The explanation for the severe transient encountered in a shutdown from the critical region can be determined from examination of the term $[G/\partial h/\partial z) - (Q/A)]$. If Q/A is reduced, then for the first few seconds the $G(\partial h/\partial z)$ term is larger, because of the fluid inertia, than Q/A which makes the bracketed term positive and, hence, $\partial G/\partial z$ negative. This effect, combined with the reduced value of $\partial G/\partial t$ because of the reduced value of $\partial \rho/\partial t$ with the resultant decrease in the driving head term, Δp, results in a somewhat severe and erratic transient when trying to back out of the critical region.

The most successful procedure in coming out of the critical region in terms of the transient encountered was to pressurize the system and then reduce power. This effect is shown in Fig. 24. The possibility of

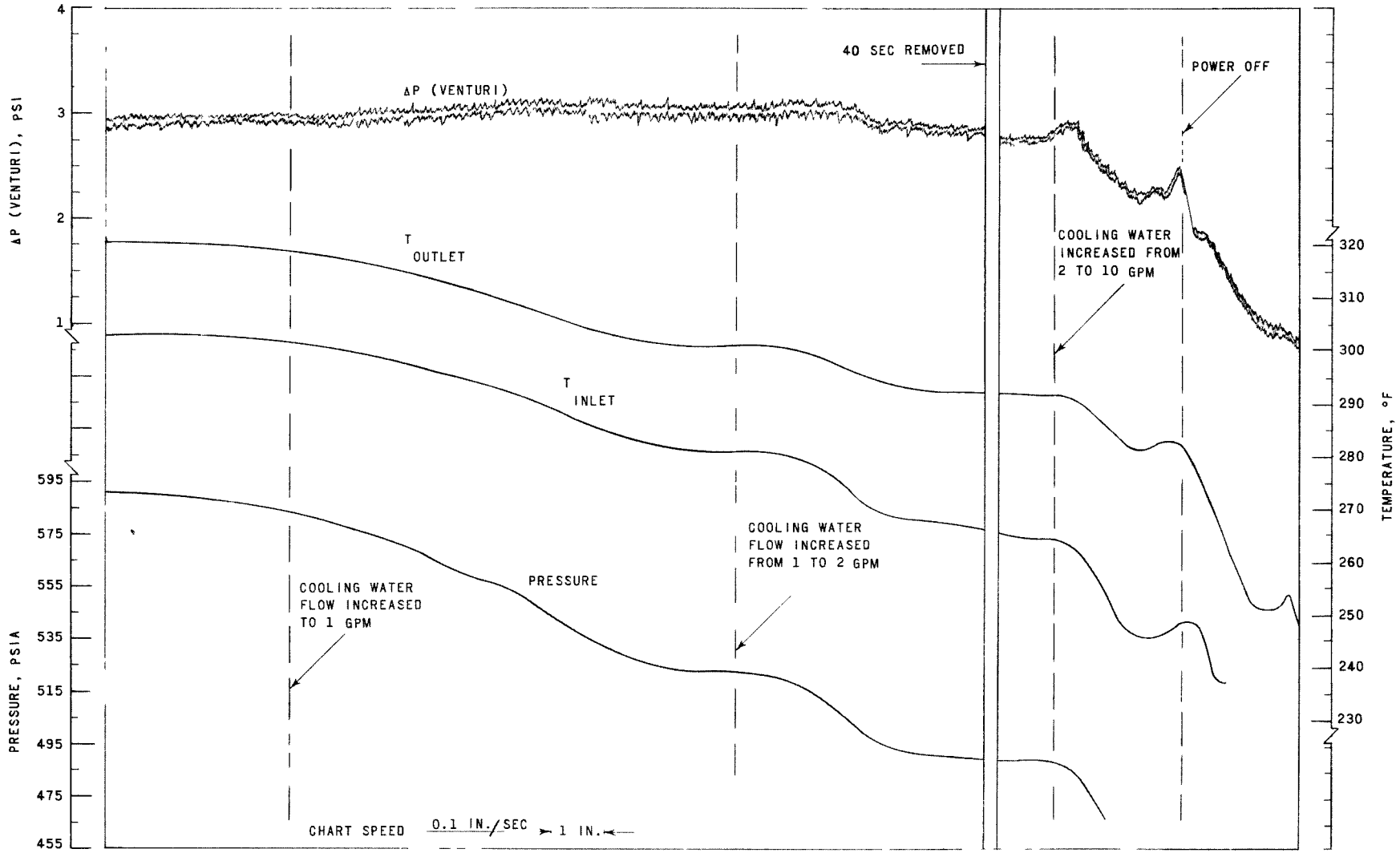

Fig. 24. Shutdown from Supercritical Conditions, Loop No. 2, 14 kw, Nov. 9, 1962

encountering a transient due to pressurization, such as is shown in Fig. 18, existed, but this was preferred to the procedure of cooling the inlet temperature or reducing power promptly. By pressurizing, the heat input could be maintained. Without pressurizing the flow of cooling water had to be increased quickly enough so that the tube did not overheat due to the loss of natural-circulation flow, or the power had to be decreased promptly. In Fig. 24 it can be seen that the inlet temperature could be lowered in an orderly fashion by increasing the flow rate of cooling water. Once the temperature level of the fluid was below the critical region, the power could be reduced to zero without introducing any unusual transients.

The percolator effect could be obtained at supercritical pressures by adjusting the thermodynamic state of the fluid so that the maximum in the ρh product occurred in the lower portion of the tube. If the system pressure were raised while maintaining the same inlet temperature, the thermodynamic state of the fluid would shift so that now the maximum in the ρh product occurred in the upper portion of the tube. Thus, it would be expected that the frequency of the vibration would increase, since smaller amounts of fluid were undergoing the change in rate of acceleration which is the condition for the flow oscillation.

A record of the test to verify this conjecture is shown in Fig. 25. Initially, the loop was perking at a frequency of 0.2 cps, with 10- to 20-cps oscillations occurring at the beginning and end of the large flow fluctuation. Increase of the system pressure resulted in increase of the magnitude and frequency of the flow fluctuations. The magnitude of the flow oscillation increased by approximately 100 per cent, and the dominant frequency increased from 0.2 to 10 cps.

The increase in the temperature difference due to the decrease in specific heat capacity is illustrated in Fig. 26. In the enthalpy-temperature plot (see Appendix B), it can be seen that, with a constant heat input and system pressure and assuming a constant flow rate, as the inlet temperature to the test section is increased the enthalpy change across the test section will be large, then decrease, and then become large again as the slope of the enthalpy-temperature curve changes along an isobar. In Fig. 26 is shown a trace of this occurrence. The initial condition was such that the minimum enthalpy change across the test section was in effect. Increase of the inlet temperature resulted in the divergence of the inlet and outlet temperatures as the specific heat capacity of the fluid decreased. The increase in temperature difference was accelerated by the decrease in fluid flow because of the reduced driving head term, that is, the decrease in the volume coefficient of expansion.

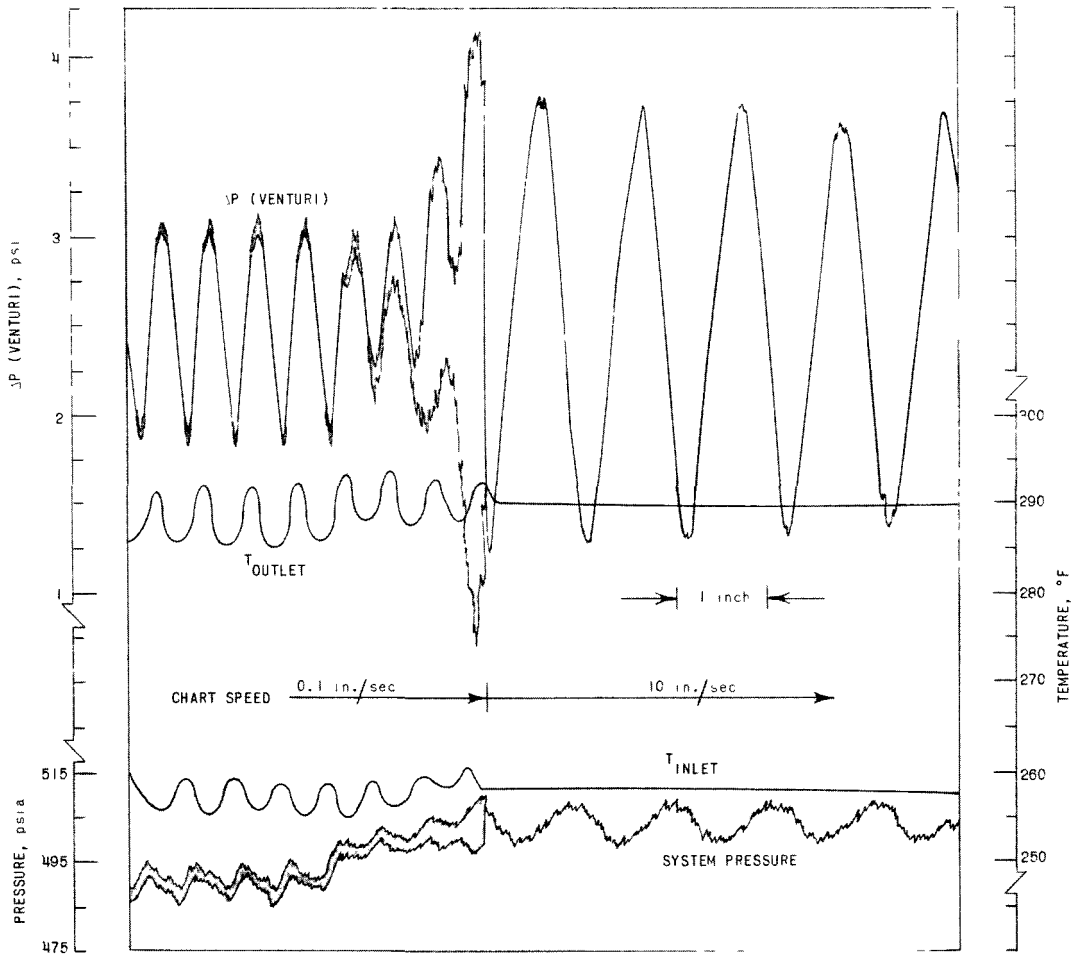

Fig. 25. Effect of Pressure Increase on Magnitude and Frequency, Loop No. 2, 14 kw, Nov. 9, 1962

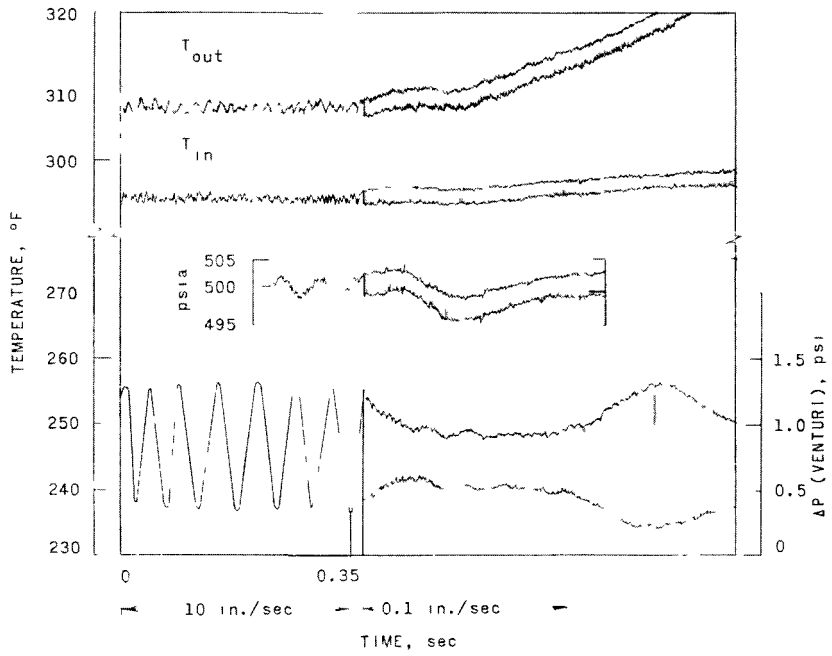

112-2199

Fig. 26. Heating through Critical Temperature at Constant Pressure, Loop No. 1

In this test program approximately 3000 ft of recordings were made over a 3-month period. The preceding figures illustrate some of the more significant events which occurred. It is also worthwhile to note that the most significant runs were made after it was realized that the maximum in the density-enthalpy product was the dividing line between the two modes of oscillation. The majority of these figures are the results of tests which were formulated to prove or disprove the significance of this maximum value. Since the loop behaved as predicted on the basis of the analytical and physical model, it is concluded that these tests were significant in determining the mechanism of sustained flow oscillations for a natural-circulation loop operating in the near-critical region.

CHAPTER VII

COMPUTER RESULTS AND DISCUSSION

The theoretical model described in this thesis was formulated to predict the transient behavior of a natural-circulation loop operating in the single-phase region near the thermodynamic critical point. To simplify the computer calculations a number of assumptions were made. The validity of these assumptions may be determined from a comparison of the predicted and the experimentally measured transients.

The first test that the computer model must satisfy is that it predict satisfactorily the measured steady-state flow rate for a given test-section power input, system pressure, and inlet enthalpy. In Fig. 27 is shown a comparison of experimental and calculated flow rates for Loop No. 1 as a function of power input. The agreement is quite good. This, however, is not surprising, since the experimental data were used to determine the correlation for the friction and momentum pressure losses used in the computer calculation of the flow rates. This procedure, rather than a conventional calculation involving the friction factor and the geometric momentum pressure loss, was used to eliminate the uncertainties in determining the form of losses due to friction and momentum. The more general procedure would be to use the standard methods of calculating these pressure losses but, since the purpose of the computer simulation was to determine the mechanism of the flow oscillations, this particular uncertainty was eliminated by using the correlation for friction and pressure losses based on this experimental data for these particular loops and operating conditions.

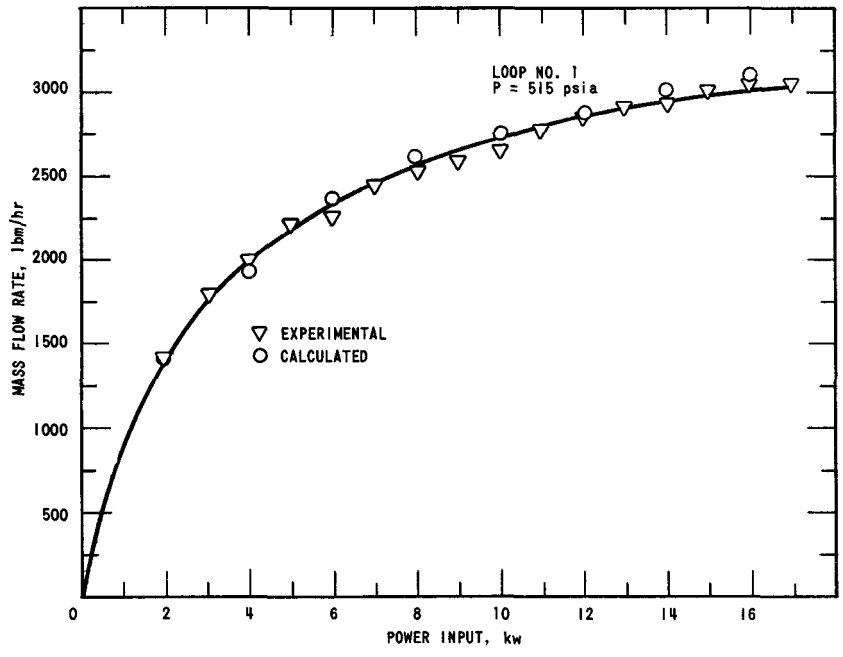

Fig. 27. Comparison of Experimental and Calculated Flow Rates

The second test of computer model is that it predict satisfactorily the measured transient flow fluctuations under all conditions. A weaker criterion is that the model predict oscillations under the same operating conditions when oscillations were encountered experimentally with the loop and predict stable flows under the same operating condition when the loop operated stably. Within this criterion the frequency and magnitude of the oscillations need not agree too closely.

To obtain a comparison of the transients, a steady-state solution based on the measured test-section power, system pressure, and inlet enthalpy was obtained. The calculated transient response in coolant flow due to a small perturbation in the power input was then obtained. Behavior at several power levels was examined by changing both power and inlet conditions to obtain the transient response of the loop.

During a transient condition, the density at any position z must vary with time, whereas under steady-state conditions the density at any position z must be constant with time. A step increase in heat input and removal will set up a new density distribution. The associated flow transient may or may not be damped. The change in the thermodynamic state of the fluid as a result of the new operating conditions may be such that density will vary with time and, hence, the flow oscillation will never be damped.

Since the transients were encountered experimentally in the thermodynamic area in which density varies the most with enthalpy and pressure, i.e., in regions in which $d\rho/dh$ changes slope, this was the region chosen for the analytical investigation. Figure 28 summarizes the results of the computer simulation of the operation of the loop in this region. Initially, the loop was taken to be in the steady-state mode. A step increase in the heat input at time zero started the transient. The frequency of the large, slow oscillation is around 0.2 cps, which is in good agreement with the experimentally measured frequency, such as is shown in Fig. 19.

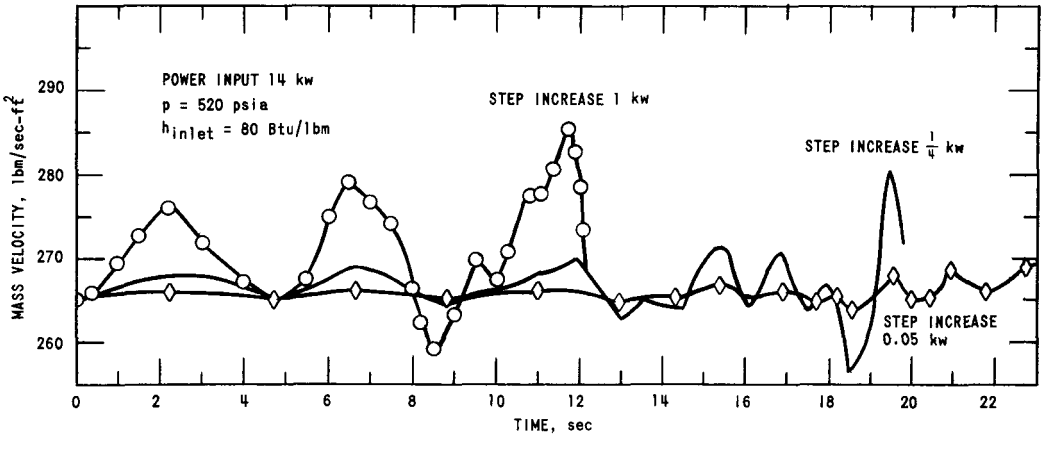

Fig. 28. Transients Encountered with Loop No. 2 for the Least Stable Case

A step increase in power input of 1 kw was sufficient to cause the numerical solution to stop at 12.5 sec because the enthalpy at some point in the loop exceeded the tabulated value. Subsequently, the step increase in power input was reduced to 0.05 kw. After about 18 sec, divergent oscillations are beginning to start up. An increase in the power input to 0.25 kw shows the divergent oscillations beginning sooner.

In Chapter III it was postulated that the position in the heater tube where the maximum in the (ρh) product versus temperature occurs will influence the frequency of the oscillation. It was reasoned that, when this maximum occurs at the upper end of the heater, smaller amounts of fluid will be involved in the expansion process and, hence, the loop would return to the normal state more quickly, resulting in transients of higher frequency. The result of the computer simulation of this occurrence is shown in Fig. 29. The pressure fluctuation is roughly 1 cps while the flow is steady. At the 8-sec point the flow is beginning to oscillate. The pressure is also beginning to fluctuate more widely. The results in this figure point out the major weakness of this model in predicing the transients of higher frequency. This will be discussed at the end of this chapter.

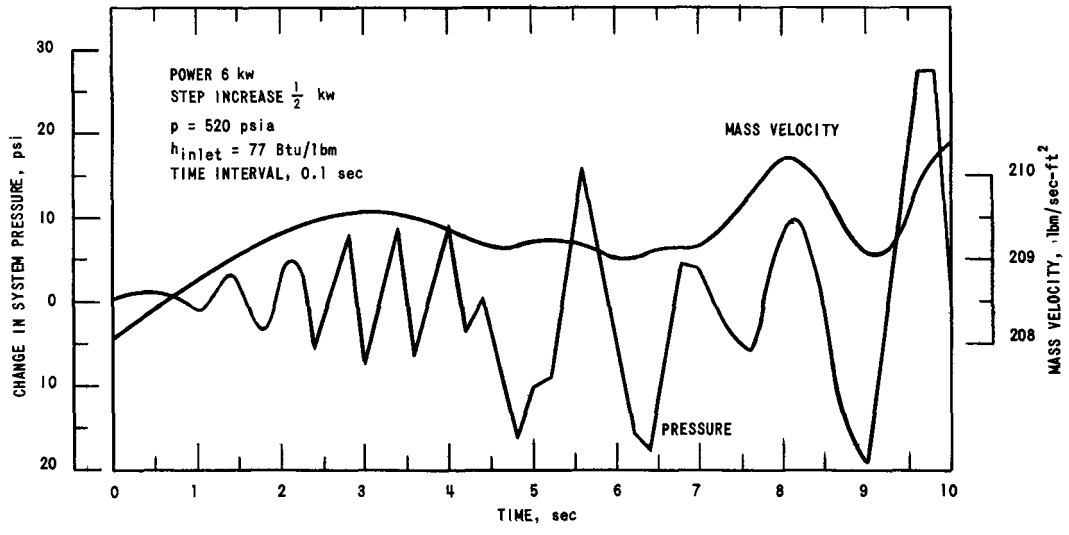

Fig. 29. Transient Behavior of Loop No. 2 Approaching the Maximum in the Density-Enthalpy Product from the Low-temperature Side

The return to stable operation after a step increase in power is shown in Figs. 30 and 31. In Fig. 30 the thermodynamic condition of the fluid is on the low-temperature side of the maximum in the density-enthalpy product, whereas in Fig. 31 the thermodynamic condition is on the high-temperature side of the maximum.

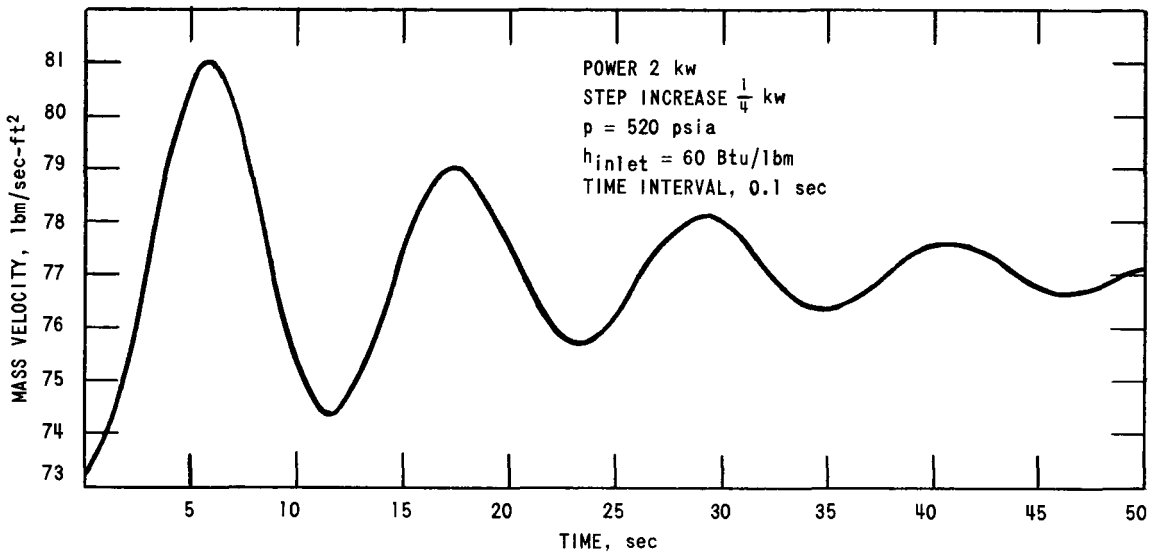

Fig. 30. Predicted Response of Loop No. 1 in a Stable Operating Region

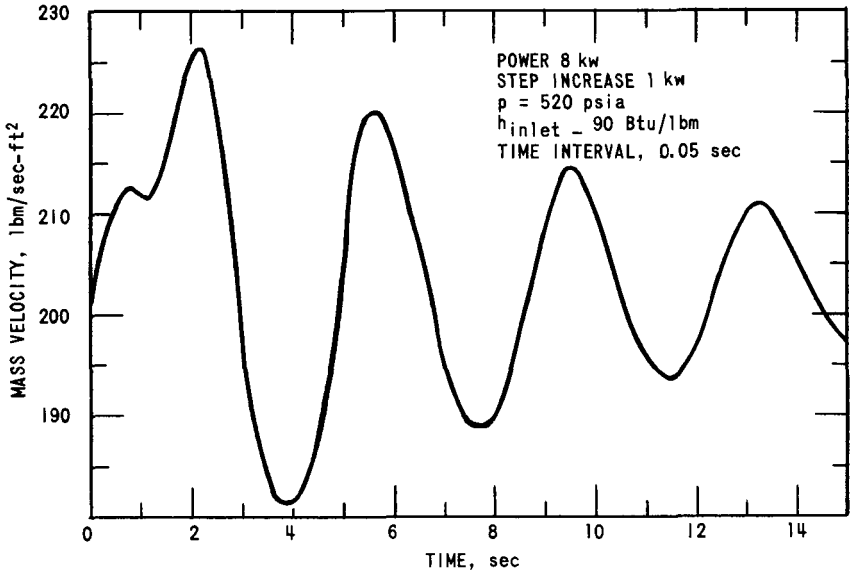

Fig. 31. Response of Loop No. 2 in a Stable Operating Region

To further illustrate the dependence of sustained flow oscillations on the thermodynamic conditions, a problem was run in which the pressure in the region of the expected unstable behavior was 600 psia. The results are shown in Fig. 32. A step increase in power input of 0.05 kw, or 0.35%, was sufficient to generate sustained oscillations.

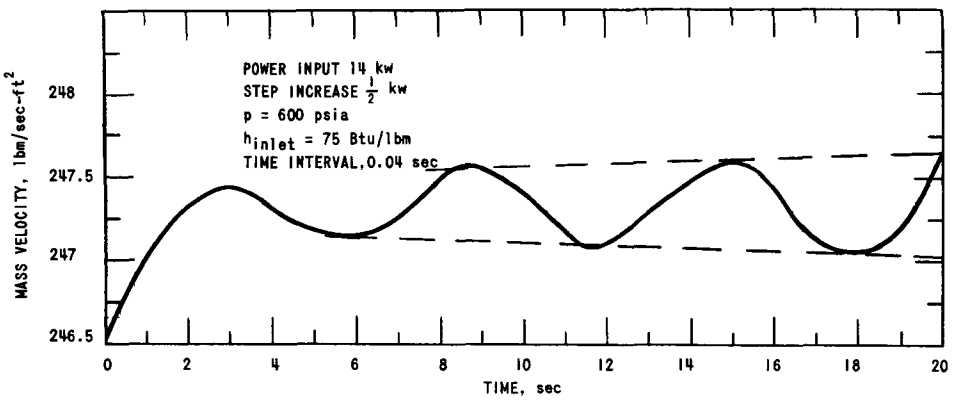

Fig. 32. Transient Behavior of Loop No. 2 Operating at 600 psia

The four major assumptions made in setting up the computer program and the implications of these assumptions are discussed below:

1. The assumption that density could be evaluated as a function of enthalpy and a reference pressure is probably the poorest assumption. Pressure variations of the magnitude found under operating conditions are sufficient to introduce flow oscillations. A rapid pressure rise throughout the entire loop results in a new density distribution not directly connected with the heat input; hence, a transient condition could develop even while holding the heat input constant.

This assumption was made for two reasons: first, an equation of state was not available, although it is presently being developed by Martin;[25] secondly, the introduction of compressibility requires a time step

$$\Delta t \leq \frac{\Delta z}{c + |u|} \quad , \quad \text{[see Ref. 34, p. 197]}$$

for numerical stability in the solution of the equations describing the system. The time step, of the order of 5×10^{-5} sec for this Freon-114 system becomes prohibitively short from a computer-time cost standpoint.

2. No local variation in the mass velocity G was allowed in the computer program. This approximation allows a much simpler program to be written. When small time steps are used, this assumption is probably not too restrictive. The approximation will not be so good when a variable cross-sectional area is introduced into the problem by the expansion and contraction of the pipe walls due to the pressure surges.

3. The system was assumed to be of constant volume. However, the volume of the system will change during the pressure surge because of the expansion and contraction of the pipe walls. To account for this effect, the equation for conservation of mass would have to be written as

$$\frac{\partial \rho}{\partial t} + \frac{\rho}{A}\frac{\partial A}{\partial t} + \frac{\partial G}{\partial z} = 0 \quad . \qquad \text{VII-1}$$

The introduction of a variable area as a function of time complicates the analysis considerably.

4. The heat input and removal was assumed to be uniform with position and time, an assumption made because as yet there is no adequate heat-transfer correlation for a fluid in the critical region. Experimental measurements by Holman and Boggs[19] for a supercritical fluid showed the heat-transfer coefficient to vary with length in an erratic and unpredictable manner. The same effect was noted in the operation of this loop. Hence, until an adequate correlation can be developed, this assumption will remain.

The validity of these assumptions as judged by the close agreement with experimental results appears to be good. The success of the analytical model in predicting the low-frequency transients suggests that the model is adequate for an analysis in which the transport of enthalpy is the major cause of the oscillations. The model was unable to predict the mass flow fluctuations at the high frequencies, although it gave some indication that transients of higher frequency would be encountered under those experimental conditions which did give the high-frequency transients. This is a direct consequence of the first assumption listed above. The inclusion of density as a function of pressure presents a large problem from an analysis viewpoint and from the computer cost standpoint.

CHAPTER VIII

DISCUSSION OF RESULTS AND CONCLUSIONS

It has been determined experimentally that operation of a single-phase, heat-transfer loop in the thermodynamic critical region of the fluid of the design studied in this experiment will produce pressure and flow fluctuations under certain conditions. The condition determined experimentally for the occurrence of sustained flow and pressure fluctuations was that the system fluid be passing through the thermodynamic region in which a maximum in the density-enthalpy product as a function of temperature, enthalpy, or density occurs. In this region it was found that as little as $1\frac{1}{4}$ kw of heating was necessary to obtain sustained flow oscillations. The loop would operate stably in the thermodynamic regions on either side of this maximum in the density-enthalpy product. It was noted experimentally that the magnitude and frequency of the pressure and flow fluctuations depended on whether the maximum in the density-enthalpy curve was being traversed from the low- or the high-temperature side. Approach from the low-temperature side resulted in a dominant frequency of 10 to 20 cps, which was 100 times the frequency found when traversing the maximum from the high-temperature side.

The pressure fluctuation encountered could be destructive to the tubing if operated continuously in this region. Therefore, if the tubing could be sized to withstand the pressure fluctuations or if the pressure fluctuations could be controlled, a system could operate in this region. It was noted that increasing the system volume in Loop No. 2 tended to reduce the severity of the pressure transients.

Physically, the pressure fluctuations are caused by a sudden decrease in the density of the fluid in the loop. This large density decrease with heat addition is the result of the particular thermodynamic state of the fluid, i.e., in the thermodynamic region in which $d\rho/dh$ undergoes changes in value. When a pressure fluctuation occurs, the associated density change sets up a new driving pressure and mass velocity. The computer model was unable to predict the mass velocity change because of the assumption of a constant reference pressure. It did give some indication that these transients could be expected.

The low-frequency transients are chiefly due to enthalpy transport, and were predicted in magnitude and frequency by this model.

The explanation for the different modes of frequencies is given in Chapter III. The high-frequency oscillation is caused by the rapid variation of density in the two vertical legs. At these frequencies, small, discrete control volumes of fluids are being emitted from the test section, and a time-varying density distribution in the riser and downcomer is established,

which gives rise to flow and pressure fluctuations. At the low frequencies, when large, discrete control volumes are being emitted from the test section, the space- and time-varying density distribution varies more slowly; hence, a more stable system or lower-frequency oscillation is encountered.

BIBLIOGRAPHY

1. Alstad, C. D., H. S. Isbin, N. R. Amundson, and J. P. Silvers, The Transient Behavior of a Single-phase Natural Circulation Water Loop System, ANL-5409 (March 1956).

2. Anderson, R. P., and P. A. Lottes, "Boiling Stability," Progress in Nuclear Energy, Series IV, Vol. 4, London: Pergamon Press (1961), Ch. 1.

3. Bonilla, Charles F. and Leon A. Sigel, "High-Intensity Natural-Convection Heat Transfer near the Critical Point," Chemical Engineering Progress Symposium Series, No. 32, Vol. 57, 1960, pp. 87-95.

4. Bringer, R. P., and J. M. Smith, Heat Transfer in the Critical Region, AIChE, 3, 49-55 (1957).

5. Chilton, H. A., A Theoretical Study of Stability in Water Flow through Heated Passages, J. of Nucl. Energy, 5, 273-284 (1957).

6. Dickenson, N. L., and C. P. Welch, Heat Transfer to Supercritical Water, Trans. Am. Soc. Mech. Engrs., 80, 746-752 (1958).

7. Dodge, B. F., Chemical Engineering Thermodynamics, First Edition, McGraw-Hill (1944).

8. Doughty, D. L., and R. M. Drake, Free Convection Heat Transfer from a Horizontal Right Cylinder to Freon-12 near the Critical State, Trans. Am. Soc. Mech. Engrs., 78, 1843-1850 (1956).

9. Fair, J. R., What You Need to Design Thermosiphon Reboilers, Petroleum Refiner, 39 (No. 2), 105-123 (1960).

10. Firstenberg, H., Boiling Songs and Associated Mechanical Vibrations, NDA-2131-12 (June 1960).

11. Foltz, H. L., and R. G. Murray, Two-phase Flow Rates and Pressure Drops in Parallel Tubes, Chem. Eng. Progr., Symposium Series, 56, 83-94 (1960).

12. Garlid, K., N. R. Amundson, and H. S. Isbin, A Theoretical Study of the Transient Operation and Stability of Two-phase Natural-circulation Loops, ANL-6381 (1961).

13. Goldman, K., "Heat Transfer to Supercritical Water and other Fluids with Temperature Dependent Properties," Chemical Engineering Progress, Symposium Series, Nuclear Engineering, Part I, Vol. 50, No. 11, 1954.

14. Goldman, K., "Heat Transfer to Supercritical Water at 5000 psi Flowing at High Mass Flow Rates through Round Tubes," Proceedings of the 1961 International Heat Transfer Conference, Part III, Aug., 1961, pp. 561-578.

15. Green, S. J., and T. W. Hunt, "Accuracy and Response of Thermocouples for Surface and Fluid Temperature Measurements," Temperature, Its Measurement and Control, Vol. 3, Part 2, p. 716 Reinhold Publishing Co. (1962).

16. Griffith, J. D., and R. H. Sabersky, Convection in a Fluid at Supercritical Pressures, ARS J., 30, 289-291 (March 1960).

17. "High Speed Aerodynamics and Jet Propulsion," Thermodynamics and Physics of Matter, Vol. 1, Princeton, N. J.: Princeton University Press (1955), pp. 419-500.

18. Hines, W. S., and H. Wolf, Pressure Oscillations Associated with Heat Transfer to Hydrocarbon Fluids at Supercritical Pressures and Temperatures, ARS J., 32, 361-366 (March 1962).

19. Holman, J. P., and J. H. Boggs, Heat Transfer to Freon-12 near the Critical State in a Natural-circulation Loop, J. Heat Transfer, 82, 221-226 (Aug 1960).

20. Hsu, Yih-Yun, and J. M. Smith, The Effect of Density Variation on Heat Transfer in the Critical Region, J. Heat Transfer, 83, 176-182 (May 1961).

21. Koppel, L. B., and J. M. Smith, "Turbulent Heat Transfer in the Critical Region," Proceedings of the 1961 International Heat Transfer Conference, Part III, Aug., 1961, pp. 585-590.

22. Lee, D. C., J. W. Dorsey, G. Z. Moore, and F. D. Mayfield, Design Data for Thermosiphon Reboilers, Chem. Eng. Progress, 52, 160-164 (April 1956).

23. Marchaterre, J. F., and M. Petrick, Review of the Status of Supercritical Water Reactor Technology, ANL-6202 (Aug 1960).

24. Martin, J. J., "Correlations and Equations Used in Calculating the Thermodynamic Properties of Freon Refrigerants," Thermodynamic and Transport Properties of Gases, Liquids, and Solids, New York: ASME and McGraw-Hill (1959), pp. 110-122.

25. Martin, J. J., Thermodynamic Properties of Dichlorotetrafluoroethane, J. Chem. Engr. Data, 5, 334-336 (1960).

26. McAdams, W. H., Eleventh Informal Monthly Report of MIT Project DIC 1-6489, NEPA-493 (Aug 18 to Sept 18, 1947).

27. Mendler, O. J., A. S. Rathbun, N. Van Huff, and A. Weiss, Natural-circulation Tests with Water at 800 to 2000 psia under Nonboiling, Local Boiling, and Bulk Boiling Conditions, J. Heat Transfer, 83, 261-271 (Aug 1961).

28. Meyer, J. E., Conservation Laws in One-dimensional Hydrodynamics, Bettis Technical Review, WAPD-BT-20 61-72 (Sept 1960).

29. Meyer, J. E., Hydrodynamic Models for the Treatment of Reactor Thermal Transients, Nuclear Science and Engineering, 10, 269-277 (1961).

30. Petukhow, B. S., E. A. Krasnoschekow, and V. S. Protopopov, "An Investigation of Heat Transfer to Fluids Flowing in Pipes under Supercritical Conditions," Proceedings of the 1961 International Heat Transfer Conference, Part III (Aug 1961), pp. 569-578.

31. Powell, W. B., Heat Transfer to Fluids in the Region of Critical Temperature, Jet Propulsion, 27 (No. 7), 776-783 (1957).

32. Quandt, E. R., "Analysis and Measurements of Flow Oscillations," Chem. Eng. Prog., Symposium Series, 57, No. 32, p. 111 (1961).

33. Rathbun, A. S., N. E. Van Huff, and A. Weiss, Natural Circulation of Water at 1200 psia under Heated, Local Boiling, and Bulk Boiling Conditions: Test Data and Analysis, WAPD-AD-TH-470 (Dec 1958).

34. Richtmyer, R. D., Difference Methods for Initial-value Problems, Interscience, New York (1957).

35. Sears, F. W., An Introduction to Thermodynamics, Second Edition, Addison Wesley (1955).

36. Schmidt, H. W., "Heat Transmission by Natural Convection at High Centrifugal Acceleration in Water-Cooled Gas-Turbine Blades," ASME General Discussion on Heat Transfer, September 11-13, 1951, pp. 361-363.

37. Schmidt, E., E. Eckert, and U. Grigull, Heat Transfer by Liquids near the Critical State, Air Material Command, AAF Translation No. 527, Wright Field, Dayton, Ohio.

38. Van Putte, D. A., and R. J. Grosh, Heat Transfer to Water in the Near-critical Region, Technical Report No. 4, Purdue University, ANL Subcontract 31-109-38-704 (Aug 1960).

39. Van Wie, N. H., and R. A. Ebel, "Machine Computation of the Thermodynamic Properties of Dichlorotetrafluoroethane," Symposium on Thermophysical Properties, McGraw-Hill (1962), pp. 246-253.

40. Van Wie, N. H., and R. A. Ebel, Some Thermodynamic Properties of Freon-114, Report No. K-1430, Vol. I and II, Chemistry-General (TID-4500, 14th Ed.) available from the Office of Technical Services, U. S. Department of Commerce, 1959.

41. Wallis, G. B., and J. H. Heasley, Oscillations in Two-phase Flow Systems, J. Heat Transfer, Trans. ASME, Series C, 83, 363-369 (1961).

42. Wissler, E. H., et al., Oscillatory Behavior of a Two-phase Natural-circulation Loop, AIChE J., 2, 157-162 (June 1956).

43. Young, V. W., Basic Engineering Thermodynamics, First Edition, McGraw-Hill (1952).

44. Zemansky, M. W., Heat and Thermodynamics, Third Edition, McGraw-Hill (1951).

45. Beckjord, E. S., Hydrodynamic Stability in Reactors, Nuclear Safety, 4, 1-10 (Sept 1962).

46. Meyer, J. E., and R. R. Rose, Application of a Momentum Integral Model to the Study of Parallel Channel Boiling Flow Oscillations, ASME Paper No. 62-HT-41.

47. Anderson, R. P., L. T. Bryant, J. C. Carter, and J. F. Marchaterre, An Analog Simulation of the Transient Behavior of Two-phase Natural-circulation Systems, AIChE Reprint 27a, Fifth National Heat Transfer Conference, Houston, Texas, Aug 1962.

48. Fluid Meters - Their Theory and Application, Report of ASME Research Committee on Fluid Meters, Fifth Edition (1959).

49. Levy, S., and E. S. Beckjord, Hydraulic Instability in a Natural Circulation Loop with Net Steam Generation at 1000 psi, ASME Publication 60-HT-27 (1960).

50. Randles, J., Kinetics of Boiling Hydraulic Loops, AEEW-R-87 (Aug 1961).

51. A. N. Nahavandi, Nucl. Sci. and Engr., 14, 272-86 (1962).

APPENDIX A

MASS FLOW RATE CALCULATIONS

The expression for calculating the mass flow rate through a venturi, assuming the flow is incompressible in the venturi and that the irreversibilities can be accounted for by using a discharge coefficient, is

$$\dot{m} = CFnA_2 \left[2 g_c \rho_1 (p_1 - p_2)\right]^{1/2} lb_m/hr \quad , \tag{1}$$

where

$\dot{m}$	flow rate, lb_m/hr
C	discharge coefficient
F	velocity of approach factor, $[1 - (A_2/A_1)^2]^{1/2}$
D	upstream tube diameter of venturi meter, 0.93 in.
d	throat diameter of venturi meter, 0.3963 in.
ρ_1	upstream fluid density, lb_m/ft^3
$p_1 - p_2$	pressure drop, psi
A_2	throat area, $in.^2$
A_1	upstream tube area, $in.^2$
n	factor to account for units
g_c	gravitational constant, 32.2 lb_m ft/lb_f-sec^2.

The throat diameter of the venturi used was 0.3963 inches. The flow discharge coefficient C was 0.98. The velocity-of-approach factor, F, was 0.983. Making these substitutions into Eq. (1) gives

$$\dot{m} = 286.2 \left[\rho_1 (p_1 - p_2)\right]^{1/2} lb_m/hr \tag{2}$$

A manometer was connected in parallel with the differential pressure transducer to provide a check on the transducer-recording system. When correcting the manometer readings, the manometer lines were assumed to be filled with Freon-114 at 80°F. The observed head was also corrected for the manometer zero. When using the manometer differential head readings, Eq. (2) becomes

$$\dot{m} = 66.7 \left(\rho_1 h_{2,95}\right)^{1/2} lb_m/hr \tag{3}$$

APPENDIX B

PROPERTIES OF FREON-114

The fluid used in this study was dichlorotetrafluoroethane ($C_2F_4Cl_2$) or Freon-114, chosen because of its low critical temperature and pressure (294.3°F and 473.2 psi), availability of thermodynamic data, and low level of toxicity. Freon is a trademark for a group of halogenated hydrocarbons, containing one or more fluorine atoms, widely used as refrigerants and propellants.

Van Wie and Ebel[39] have published tables of the thermodynamic properties of Freon-114[40] based on correlations of vapor pressure, the p-v-T relationship, saturated liquid density, and heat capacity at zero pressures published by Martin.[25] The tables were computed by means of a digital computer.

Figures 33 and 34 were prepared from data in the thermodynamic tables. It should be noted that the density and enthalpy values along an isobar in the compressed-liquid region were extrapolated from the critical temperature to the saturated liquid temperature corresponding to that pressure.

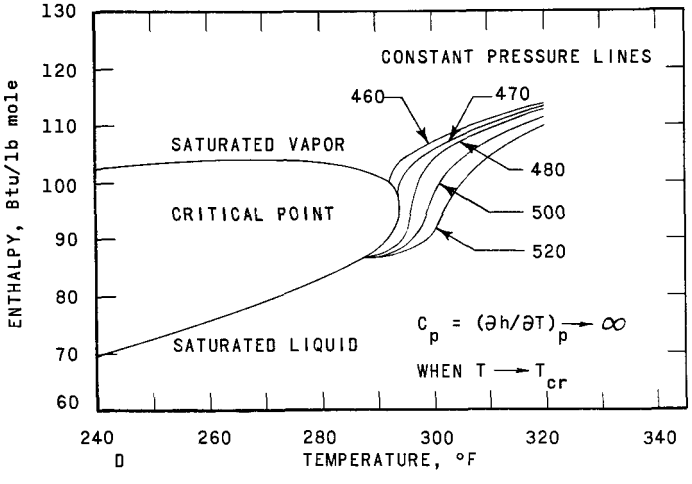

Fig. 33

Enthalpy-Temperature Relationship for Freon-114 in the Critical Region

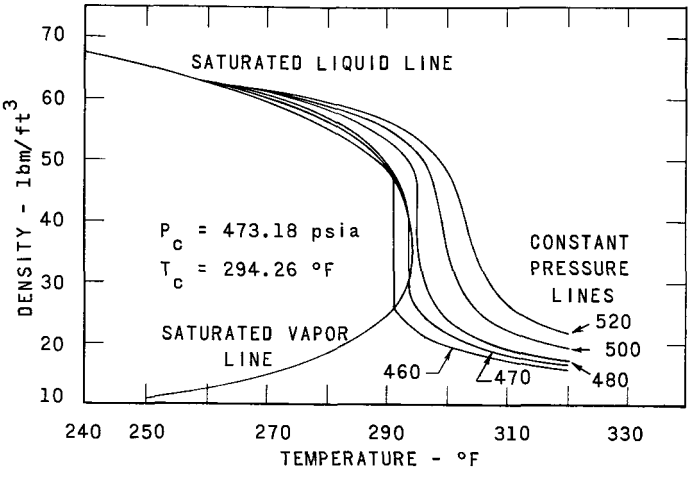

Fig. 34

Density-Temperature Relationship for Freon-114 in the Critical Region

The definition of the thermodynamic state regions as defined by several authorities is shown in Fig. 35. The definition of the critical region is not uniform with different authors. According to Ref. (17), it is not clear whether one should speak of a critical state or a critical region.

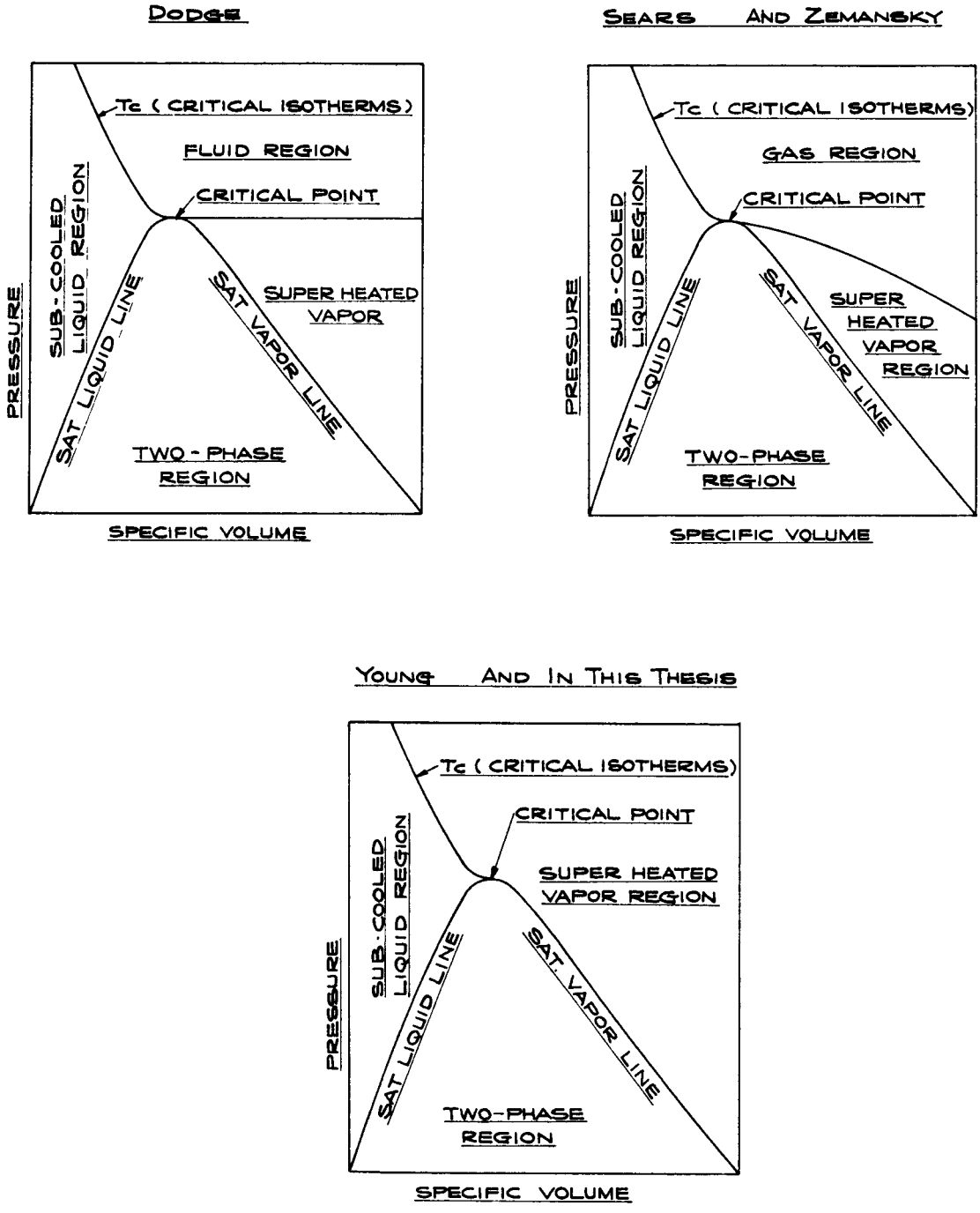

Fig. 35. Definition of State Regions Given by Various Sources Shown on the Pressure-Volume Diagram

Figure 35 shows the various regions as defined by Dodge.[7] The term fluid was given to the substance when subjected to both a pressure and temperature greater than the critical pressure and temperature. His reason for defining the fluid region as such was that a liquid at a pressure greater than the critical pressure can change to a vapor, or vice versa, without any observable phase change. He concluded that a substance in this region can be called neither a gas nor a liquid.

The various regions defined by Sears[35] and by Zemansky[44] are shown in Fig. 35 (b). Sears mentions that the boundary between the gaseous and vapor regions is unnecessary, since the properties of a vapor differ in no respect from the properties of a gas.

The regions defined by Young[43] are shown in Fig. 35 (c). He mentioned that it was difficult to classify a fluid whose temperature is very near the critical temperature and whose pressure is greater than the critical pressure. He made no attempt to define this region quantitatively.

The regions as defined by Young[43] correspond to the regions used in this thesis.

APPENDIX C

DIGITAL COMPUTER PROGRAM

In the analysis in Chapter III the finite-difference equations describing the simplified system were written and the method of solution indicated. The solution consists of two parts: (1) steady-state calculations to set up the initial conditions for the transient analysis, and (2) the transient solution. The flow diagrams for the calculations are shown in Figs. 36 and 37. The dimensions of the loops, subdivisions, and grouping are shown in Fig. 38.

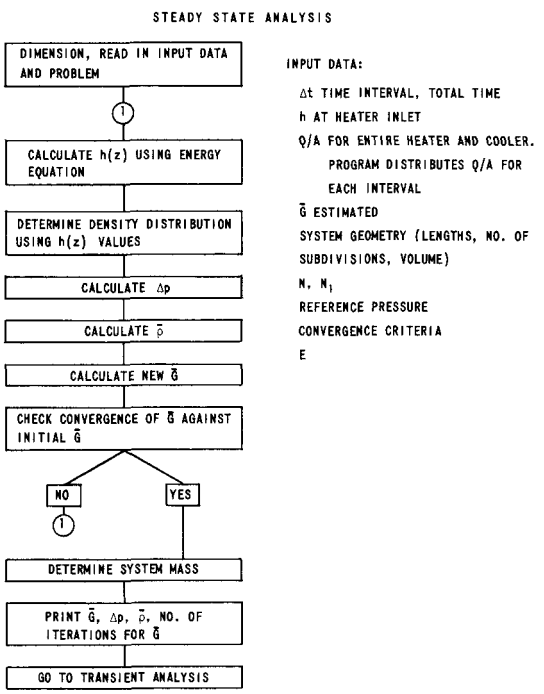

Fig. 36. Simplified Computer Flow Chart for the Steady-state Analysis

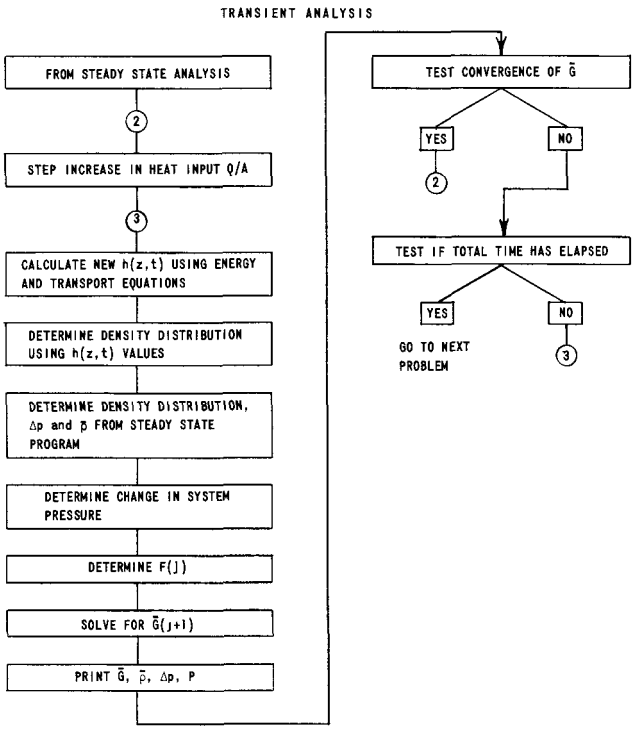

Fig. 37. Simplified Computer Flow Chart for the Transient Analysis

The computer solutions could be run for pressures of 475, 520, and 600 psia. Tabulated values of density as a function of enthalpy at these pressures were stored in the computer. Linear interpolation was used.

Because of the unknown variation of viscosity, frictional and momentum losses were obtained by correlating the driving pressure as a function of $\bar{G}^2/\bar{\rho}$. The linear equation used was of the form

$$F(j) = N_1 + N \frac{\bar{G}^2}{\bar{\rho}} \quad .$$

	Loop No. 1	Loop No. 2
N	0.1388	0.12
N_1	25.0	30.0

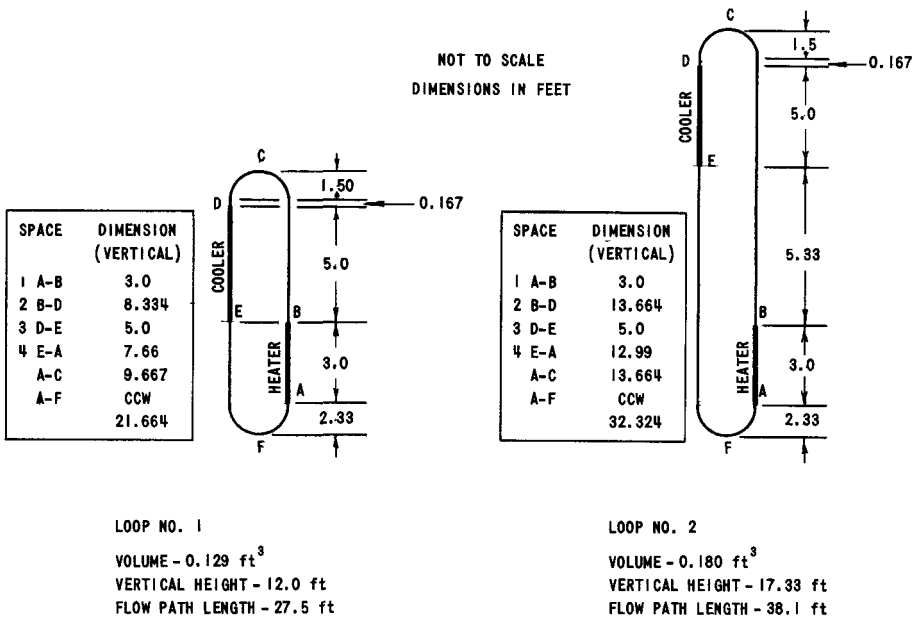

LOOP NO. 1

VOLUME - 0.129 ft^3
VERTICAL HEIGHT - 12.0 ft
FLOW PATH LENGTH - 27.5 ft

LOOP NO. 2

VOLUME - 0.180 ft^3
VERTICAL HEIGHT - 17.33 ft
FLOW PATH LENGTH - 38.1 ft

Fig. 38. Dimensions of Experimental Loops Used in Computer Program

The time increments used in the solution depended on the frequency of the transient response expected. For the higher frequency transients, a smaller time interval was used to obtain the complete transient response. For the slower transients, a larger time interval was used to reduce the solution time.

Randles[50] derived a stability criterion for the continuity equation as

$$\frac{\bar{G}}{\bar{\rho}} \frac{\Delta t}{\Delta z} < 1$$

or

$$\Delta t < \bar{\rho} \frac{\Delta z}{\bar{G}} \quad .$$

This was also the criterion used by Alstad[1] in his transient solution. For the Δz's used in this program and the mass velocities encountered, Δt was less than 0.25 sec.

The computer program written in Fortran for the IBM 704 is listed in the following pages.

```
    1644/AMU 102   TILT
    DIMENSION RHO(3,100),ENT(3,100),SPA(4),SIZE(4),ITEST(4),DEL(4),
   1DELZ(4),NSPA(4),HB(4,51),H(4,51),HBAR(4,51),HBBAR(4,51),HNU(4,51),
   2HBARNU(4,51),RBAR(4,51),DELR(51),DELRH(51),DELP(2000),
   3RHOBAR(2000),GBAR(2000),P(2000),F(2000),HOUT(2000),DELHNU(4,51),
   4GMAX(100),GMAXT(100),GMIN(100),GMINT(100),IP(3),TIME(2000)
    COMMON RHO,ENT,IP
    CALL TABLE
  1 FORMAT(4I6,1P4E12.5)
  2 FORMAT(1P6E12.5)
  3 FORMAT(2E12.5,I6)
  4 FORMAT(F16.4,1PE18.5,4E16.5)
  5 FORMAT(3E12.5,I6)
 10 READ INPUT TAPE 7,1,IPROB,IPRES,NTEST1,NTEST2,QBYA,HIN,GBAR(1),
   1EPS1
    K=1
    II=1
    IF(NTEST1)12,16,12
 12 HBLAST=0.
    READ INPUT TAPE 7,2,BR1,BR2,DN,DN1,V
    DO15I=1,4
    READ INPUT TAPE 7,3,SPA(I),SIZE(I),ITEST(I)
    DELZ(I)=SIZE(I)/SPA(I)
    NSPA(I)=SPA(I)
    HB(I,1)=HBLAST
    L=NSPA(I)
    DO 14 J=1,L
    HB(I,J+1)=HB(I,J)+DELZ(I)
 14 HBBAR(I,J)=(HB(I,J)+HB(I,J+1))/2.0
 15 HBLAST=HB(I,L+1)
 16 ITER=1
    IF(NTEST2)19,19,17
 17 READ INPUT TAPE 7,2,QCHNG,DELT,TMAX,E,HTEST
    READ INPUT TAPE 7,5,EL,TCHNG,DELTNU,ITSUP
 19 DO 50 I=1,4
    IF(ITEST(I))40,30,20
 20 DEL(I)=QBYA/SPA(I)/GBAR
    H(1,1)=HIN
    L=NSPA(I)
    DO 25 J=1,L
    H(I,J+1)=H(I,J)+DEL(I)
 25 HBAR(I,J)=(H(I,J)+H(I,J+1))/2.0
    HLAST=H(I,L+1)
    GO TO 50
 30 H(I,1)=HLAST
    L=NSPA(I)
    DO 35 J=1,L
    H(I,J+1)=HLAST
 35 HBAR(I,J)=HLAST
    GO TO 50
 40 DEL(I)=QBYA/SPA(I)/GBAR
    H(I,1)=HLAST
    L=NSPA(I)
    DO 45 J=1,L
    H(I,J+1)=H(I,J)-DEL(I)
 45 HBAR(I,J)=(H(I,J)+H(I,J+1))/2.0
    HLAST=H(I,L+1)
 50 CONTINUE
 55 DO 100 I=1,4
    L=NSPA(I)
 60 DO 65 J=1,L
    CALL INTER(HBAR(I,J),RBAR(I,J),IPRES)
```

```
      IF(RBAR(I,J))90,65,65
   65 CONTINUE
      GO TO 100
   90 WRITE OUTPUT TAPE 6,92,IPROB,I,J,HBAR(I,J)
   92 FORMAT(17H1      IN PROBLEM I6,3H H(I2,1H,I2,4H) = 1PE12.5,37H WHIC
     1H EXCEEDS THE VALUE OF THE TABLE)
      GO TO 150
  100 CONTINUE
      RHOBAR(K)=0.
      DELP(K)=0.
      DO 135 I=1,4
      L=NSPA(I)
      PSUM=0.
      RHOSUM=0.
      DO 130 J=1,L
      RHOSUM=RBAR(I,J)+RHOSUM
      IF(HBBAR(I,J)-BR1)115,120,120
  115 PSUM=PSUM-RBAR(I,J)
      GO TO 130
  120 IF(HBBAR(I,J)-BR2)125,125,115
  125 PSUM=PSUM+RBAR(I,J)
  130 CONTINUE
      RHOBAR(K)=RHOSUM/SIZE(I)*DELZ(I)+RHOBAR(K)
  135 DELP(K)=PSUM*DELZ(I)+DELP(K)
      RHOBAR(K)=RHOBAR(K)/4.
      GO TO (139,235),II
  139 GBARNU=SQRTF((DELP(K)-DN1)*RHOBAR(K)/DN)
      IF(ABSF(GBARNU-GBAR(K))-EPS1*GBAR(K))152,152,140
  140 GBAR(K)=(GBARNU+GBAR(K))/2.
      ITER=ITER+1
      IF(ITER-26)19,145,145
  145 ITER=-25
  150 NTEST2=0
  152 EM=RHOBAR(K)*V
  151 L=NSPA(1)-1
      DO 155 J=1,L
      TEMP=RBAR(1,J+1)-RBAR(1,J)
      DELR(J)=TEMP/(HBAR(1,J+1)-HBAR(1,J))
  155 DELRH(J)=(RBAR(1,J+1)*HBAR(1,J+1)-RBAR(1,J)*HBAR(1,J))/TEMP
      GO TO (156,340),II
  156 WRITE OUTPUT TAPE 6,160,IPROB,IPRES,DELT,QBYA,QCHNG,ITER,GBAR(1),
     1DELP(1),RHOBAR(1),EM,HLAST
  160 FORMAT(19H1644/AMU 102  TILT69X8HPROBLEM I6//7X11HPRESSURE = I6,
     18X10HDELTA T = F6.3,8X6HQ/A = 1PE12.5,8X10HQCHANGE = E12.5//9X9HIT
     2ERATION8X4HGBAR11X7HDELTA P9X6HRHOBAR13X1HM13X5HH OUT//I14,1PE20.5
     3,4E16.5//)
      GO TO (161,300),II
  161 WRITE OUTPUT TAPE 6,162
  162 FORMAT(19X1HJ11X17HDELTA RHO/DELTA H6X20HDELTA RHOH/DELTA RHO)
  165 L=NSPA(1)-1
      DO 170 J=1,L
  170 WRITE OUTPUT TAPE 6,175,J,DELR(J),DELRH(J)
  175 FORMAT(I21,1P2E25.5)
  180 IF(NTEST2)200,10,200
  200 K=2
      KK=2
      HOUT(1)=HLAST
      IGMAX=1
      GMAX(IGMAX)=GBAR(1)
      TIME(2)=DELT
      ACCT=DELT
  277 WRITE OUTPUT TAPE 6,278
```

```
278 FORMAT(35H0          TRANSIENT ANALYSIS RESULTS//11X4HTIME11X4HGBAR1
   11X7HDELTA P9X6HRHOBAR13X1HP14X5HH OUT/)
205 GSIGN=1.
210 QBYA=QBYA+QCHNG
211 M=NSPA(4)+1
    HNU(1,1)=H(4,M)
    DO 231 I=1,4
    IF(ITEST(I))216,215,212
212 QOVERA=QBYA
    GO TO 220
215 QOVERA=0.
    GO TO 220
216 QOVERA=-QBYA
220 DELQA=QOVERA/ SPA(I)
225 GDELZ=GBAR(K-1)/DELZ(I)
    L=NSPA(I)
    DO 229 J=1,L
1030 HBARNU(I,J)=HBAR(I,J)+DELT/(RBAR(I,J)*DELZ(I))*(DELQA-GBAR(K-1)*
   1(H(I,J+1)-HNU(I,J)))
    TAU=RBAR(I,J)/GDELZ
229 HNU(I,J+1)=H(I,J+1)+(DELT/TAU)*(2.*HBAR(I,J)-H(I,J+1)-HNU(I,J))
   1+HBARNU(I,J)-HBAR(I,J)
    IF(I-4)230,231,231
230 L=NSPA(I)
    HNU(I+1,1)=HNU(I,L+1)
231 CONTINUE
    DO 233 I=1,4
    L=NSPA(I)
    DO 232 J=1,L
    H(I,J)=HNU(I,J)
232 HBAR(I,J)=HBARNU(I,J)
    H(I,L+1)=HNU(I,L+1)
233 CONTINUE
    HOUT(K)=H(4,M)
    IF(HTEST)236,237,236
236 DO 234 I = 1,4
    L=NSPA(I)
234 WRITE OUTPUT TAPE 6,2, (H(I,J), HBAR(I,J), J = 1,L)
237 II=2
    GO TO 55
235 P(K)=(RHOBAR(K)-RHOBAR(1))/RHOBAR(1)*E
    F(K-1)=DN*GBAR(K-1)*GBAR(K-1)/RHOBAR(K-1)+DN1
    GBAR(K)=GBAR(K-1)+(32.2*DELT/EL)*(DELP(K)-F(K-1))
250 IF(GSIGN)265,255,255
255 IF(GBAR(K)-GBAR(K-1))260,300,300
260 GMAX(IGMAX )=GBAR(K-1)
    GMAXT(IGMAX)=ACCT-DELT
    GSIGN=-1.
    GO TO 300
265 IF(GBAR(K-1)-GBAR(K))270,300,300
270 GSIGN=1.
    GMIN(IGMAX)=GBAR(K-1)
    GMINT(IGMAX)=ACCT-DELT
272 IGMAX=IGMAX+1
    GO TO 300
282 LL=K-1
    DO 279 L = KK,LL,ITSUP
279 WRITE OUTPUT TAPE 6,4,TIME(L),GBAR(L),DELP(L),RHOBAR(L),P(L),
   1HOUT(L)
    WRITE OUTPUT TAPE 6,4,TIME(K),GBAR(K),DELP(K),RHOBAR(K),P(K),
   1HOUT(K)
    KK=K+1
```

```
      GO TO (304,400),JJ
  400 WRITE OUTPUT TAPE 6,401
  401 FORMAT(23H0                          TIME14X4HGMAX15X4HTIME14X4HGMIN//)
      WRITE OUTPUT TAPE 6,402,(GMAXT(J),GMAX(J),GMINT(J),GMIN(J),J=1,
     XIGMAX)
  402 FORMAT(F23.4,1PE21.6,0PF16.4,1PE21.6)
      GO TO 10
  300 IF(TMAX-ACCT)3000,3000,301
 3000 JJ=2
      GO TO 282
  301 IF(TCHNG)305,305,302
  302 IF(ACCT-TCHNG)305,303,303
  303 TCHNG=0.
      JJ=1
      GO TO 282
  304 DELT=DELTNU
  305 K=K+1
      ACCT=ACCT+DELT
      TIME(K)=TIME(K-1)+DELT
      GO TO 211
  340 JJ=2
      GO TO 282
```

```
      SUBROUTINE TABLE
      DIMENSION RHO(3,100),ENT(3,100),IP(3)
      COMMON RHO,ENT,IP
      IP(1)=475
      IP(2)=520
      IP(3)=600
      ENT(1,1)=58.178
      ENT(1,2)=60.9831
      ENT(1,3)=63.8309
      ENT(1,4)=66.7311
      ENT(1,5)=69.6994
      ENT(1,6)=70.
      ENT(1,7)=75.
      ENT(1,8)=80.
      ENT(1,9)=82.
      ENT(1,10)=84.
      ENT(1,11)=86.
      ENT(1,12)=88.
      ENT(1,13)=90.
      ENT(1,14)=92.
      ENT(1,15)=94.
      ENT(1,16)=96.
      ENT(1,17)=98.
      ENT(1,18)=100.
      ENT(1,19)=102.
      ENT(1,20)=104.
      ENT(1,21)=106.
      ENT(1,22)=108.
      ENT(1,23)=110.
      ENT(2,1)=58.178
      ENT(2,2)=60.9831
      ENT(2,3)=63.8309
      ENT(2,4)=66.7311
      ENT(2,5)=69.6994
      ENT(2,6)=70.
      ENT(2,7)=75.
      ENT(2,8)=80.
      ENT(2,9)=82.
      ENT(2,10)=84.
      ENT(2,11)=86.
      ENT(2,12)=88.
      ENT(2,13)=90.
      ENT(2,14)=92.
      ENT(2,15)=94.
      ENT(2,16)=96.
      ENT(2,17)=98.
      ENT(2,18)=100.
      ENT(2,19)=102.
      ENT(2,20)=104.
      ENT(2,21)=106.
      ENT(2,22)=108.
      ENT(2,23)=110.
      ENT(2,24)=111.5
      ENT(2,25)=113.7755
      ENT(2,26)=117.6484
      ENT(2,27)=120.0448
      ENT(3,1)=58.178
      ENT(3,2)=60.9831
      ENT(3,3)=63.8309
      ENT(3,4)=66.7311
      ENT(3,5)=69.6994
      ENT(3,6)=70.0
```

```
ENT(3,7)=75.0
ENT(3,8)=80.
ENT(3,9)=82.
ENT(3,10)=84.
ENT(3,11)=86.
ENT(3,12)=88.
ENT(3,13)=90.
ENT(3,14)=92.
ENT(3,15)=94.
ENT(3,16)=96.
ENT(3,17)=98.
ENT(3,18)=100.
ENT(3,19)=102.
ENT(3,20)=104.
ENT(3,21)=106.
ENT(3,22)=108.
ENT(3,23)=110.
ENT(3,24)=112.
ENT(3,25)=116.
RHO(1,1)=75.1446
RHO(1,2)=73.4644
RHO(1,3)=71.6714
RHO(1,4)=69.7391
RHO(1,5)=67.63
RHO(1,6)=67.5
RHO(1,7)=63.5
RHO(1,8)=58.5
RHO(1,9)=56.5
RHO(1,10)=54.2
RHO(1,11)=51.8
RHO(1,12)=49.1
RHO(1,13)=46.
RHO(1,14)=42.5
RHO(1,15)=39.
RHO(1,16)=35.
RHO(1,17)=31.
RHO(1,18)=27.5
RHO(1,19)=25.5
RHO(1,20)=23.5
RHO(1,21)=21.5
RHO(1,22)=19.8
RHO(1,23)=18.5
RHO(2,1)=75.1446
RHO(2,2)=73.4644
RHO(2,3)=71.6714
RHO(2,4)=69.7391
RHO(2,5)=67.63
RHO(2,6)=67.5
RHO(2,7)=64.8
RHO(2,8)=61.4
RHO(2,9)=59.8
RHO(2,10)=58.2
RHO(2,11)=56.
RHO(2,12)=53.6
RHO(2,13)=50.5
RHO(2,14)=47.
RHO(2,15)=43.2
RHO(2,16)=39.4
RHO(2,17)=35.8
RHO(2,18)=32.6
RHO(2,19)=30.
RHO(2,21)=25.4
```

```
RHO(2,23)=22.2
RHO(2,22)=23.8
RHO(2,20)=27.5
RHO(2,24)=21.55
RHO(2,25)=19.21
RHO(2,26)=17.7
RHO(2,27)=16.57
RHO(3,1)=75.1446
RHO(3,2)=73.4644
RHO(3,3)=71.6714
RHO(3,4)=69.7391
RHO(3,5)=67.63
RHO(3,6)=67.5
RHO(3,7)=65.
RHO(3,8)=62.
RHO(3,9)=61.5
RHO(3,10)=59.2
RHO(3,11)=57.5
RHO(3,12)=55.6
RHO(3,13)=53.5
RHO(3,14)=51.
RHO(3,15)=48.
RHO(3,16)=45.
RHO(3,17)=41.8
RHO(3,18)=38.4
RHO(3,19)=35.2
RHO(3,20)=32.5
RHO(3,21)=29.8
RHO(3,22)=27.6
RHO(3,23)=25.8
RHO(3,24)=24.6
RHO(3,25)=22.2
RETURN
```

```
      SUBROUTINE INTER(HH,R,IPRES)
      DIMENSION RHO(3,100),ENT(3,100),IP(3)
      COMMON RHO,ENT,IP
      IF(IPRES-IP(2))1000,1100,1200
1000  IF(HH-ENT(1,1))1015,1030,1005
1005  DO 1010 LL=2,100
      L=LL
      IF(HH-ENT(1,LL))1020,1030,1010
1010  CONTINUE
1015  R=-1.
      GO TO 1400
1020  II=1
      GO TO 1300
1030  R=RHO(1,L)
      GO TO 1400
1100  IF(HH-ENT(2,1))1115,1130,1105
1105  DO 1110 LL=2,100
      L=LL
      IF(HH-ENT(2,LL))1120,1130,1110
1110  CONTINUE
1115  R=-1.
      GO TO 1400
1120  II=2
      GO TO 1300
1130  R=RHO(2,L)
      GO TO 1400
1200  IF(HH-ENT(3,1))1215,1230,1205
1205  DO 1210 LL=2,100
      L=LL
      IF(HH-ENT(3,LL))1220,1230,1210
1210  CONTINUE
1215  R=-1.
      GO TO 1400
1220  II=3
      GO TO 1300
1230  R=RHO(3,L)
      GO TO 1400
1300  UP=ENT(II,L)-HH
      TOT=ENT(II,L)-ENT(II,L-1)
      DIFF=RHO(II,L)-RHO(II,L-1)
      RATIO=UP/TOT
      R=RHO(II,L)-RATIO*DIFF
1400  RETURN
```

COMPUTER PROGRAM NOMENCLATURE

ACCT	accumulated time of transient calculation, sec
BR 1	space boundary for top of loop
BR 2	space boundary for bottom of loop
CALL INTER	calling for interpolation subroutine
DEL	$(Q/A)_n/\bar{G}$
DELP	gravitational driving head, Δp,
DELR	change in average density between two successive increments
DELRH	$d(\rho h)/d\rho$
DELT	time interval by which solution is advanced, Δt
DELZ	size of increment in each space
DN	constant multiplier of $\bar{G}^2/\bar{\rho}$
DN_1	additive constant in equation calculating F
E	modulus of compressibility, psi
EK	momentum loss factor
EL	flow path length of loop, L, ft
EM	mass of fluid in loop, lb_m
ENT	enthalpy in table
EPS 1	mass velocity convergence criterion for steady state, usually 1%
EPS 2	convergence criterion for G in transient analysis, usually 1%
F	friction pressure loss
GC	gravitational constant, g_c, 32.2 lb_m-ft/lb_f-sec^2
GMAX	maximum mass velocity, $lb_m/sec\text{-}ft^2$
H	enthalpy at boundary points
HB	enthalpy at boundary of each space
HBAR	average enthalpy in a space increment
HBARNU	new average enthalpy in a space increment at the advanced time $\bar{h}$ (j + 1)
HBBAR	enthalpy at boundary points
HBLAST	inlet enthalpy to heater

HIN	inlet enthalpy to heater
HNU	new enthalpy at end points of space increment at time $t + \Delta t$, $h_{n,e}(j+1)$
HOUT	outlet enthalpy from heater
IGMAX	first maximum in the mass velocity
ITER	number of times G is recalculated in steady state for convergence
ITEST	test to determine which space problem solution is in
ITSUP	specifies which interations in transient solution are printed
NSPA	number of increments each space is divided into
NTEST1	test to determine in which loop geometry problem is to be run
NTEST2	test to allow problem solution to advance to the transient solution
P(K)	change in system pressure
PRES	system pressure
PROB	problem number
PSUM	summation of average densities in each increment
QBYA	Q/A
QCHNG	step increase in Q/A for transient case
RBAR	average density in increment
RHO	density
RHOBAR	average density of fluid in loop, lb_m/ft^3
RHOSUM	summation of average densities in each increment
SIZE	specifies length of each space
SPA(I)	designates number of spaces in loop I = 1 heater I = 2 riser I = 3 cooler I = 4 lower portion of cold leg
SQRTF	square-root subroutine
TMAX	maximum time problem is allowed to run
V	volume of loop, ft^3

APPENDIX D

ALTERNATE DERIVATION AND ANALYSIS

As indicated in the text, the density-enthalpy product was an important thermodynamic variable. The maximum in this product represented a region of unstable operation. The cause of the maximum was analyzed in terms of a change in the rate of change in density with respect to enthalpy. This was shown to result in nonuniform acceleration of a fluid control volume as it passes through the heater or cooler; therefore, a transient condition develops.

Since the density-enthalpy product appears in the energy equation and density appears in the continuity equation, it is instructive to make an analysis considering the density-enthalpy product as a function of density, which enables the energy and continuity equations to be combined directly. The continuity equation is

$$(G)_{inlet} - (G)_{exit} = \Delta z \frac{\partial \rho}{\partial t} \quad . \qquad \text{D-1}$$

The energy equation is

$$(Gh)_{inlet} - (Gh)_{exit} + (Q/A) = \Delta z \frac{d}{dt} (\rho h) \quad . \qquad \text{D-2}$$

An alternate way of writing the energy equation is

$$[(Gh)_{inlet} + (Q/A)] - (Gh)_{exit} = \Delta z \frac{d(\rho h)}{d\rho} \frac{\partial \rho}{\partial t} \quad . \qquad \text{D-3}$$

Introduction of the continuity equation, D-1, into Eq. D-3 gives

$$[(Gh)_{inlet} + (Q/A)] - (Gh)_{exit} = \frac{d(\rho h)}{d\rho} [(G)_{inlet} - (G)_{exit}] \quad . \qquad \text{D-4}$$

In a transient developed by heat addition, the left-hand side of Eq. D-4 is always positive; therefore, so should be the right-hand side. Three cases need to be considered: (1) $d(\rho h)/d\rho$ negative throughout the control volume; (2) $d(\rho h)/d\rho$ positive; and (3) $d(\rho h)/d\rho$ negative at the inlet, positive at the outlet. A plot of ρh as a function of ρ is shown in Fig. 39 for Freon-114.

When $d(\rho h)/d\rho$ is negative, $(G)_{exit}$ must be greater than $(G)_{inlet}$ to make the right-hand side of Eq. D-4 positive, that is, the fluid in the control volume is accelerated. When $d(\rho h)/d\rho$ is positive, $(G)_{exit}$ must be less than $(G)_{inlet}$ to satisfy Eq. D-4, that is, the fluid is decelerated.

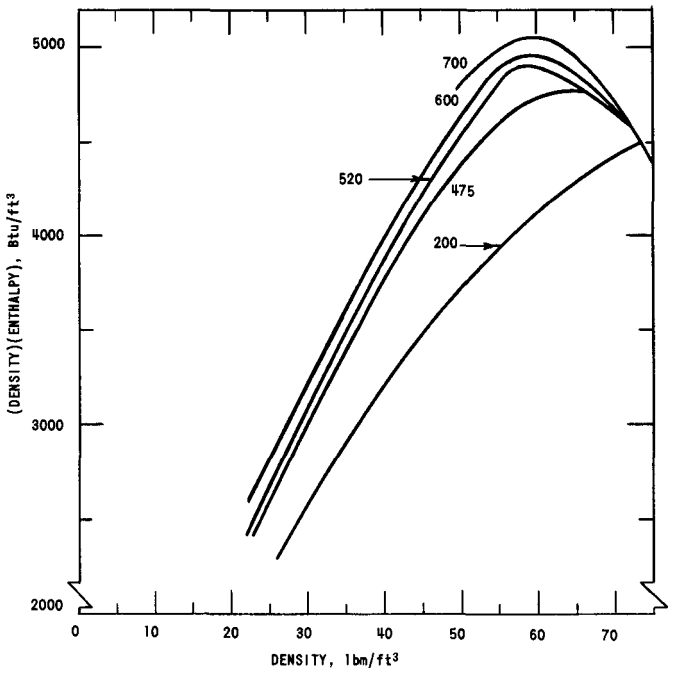

Fig. 39

Density-Enthalpy Product for Freon-114 along an Isobar as a Function of Density

When the control volume corresponding to the two cases are chosen so that the slope is negative in one and positive in the other, i.e., one on each side of the maximum, an interesting conclusion can be drawn. The fluid is first accelerated and then decelerated; consequently, a transient develops. The magnitude of the transient depends on the interaction of the mass velocity with the momentum equation, written as

$$(L/g_c)\frac{d\bar{G}}{dt} = \Delta p - F \quad . \qquad \text{D-5}$$

The equations as developed and conclusions drawn are applicable to both single- and two-phase fluids. The primary difference between the single- and the two-phase case is that the latter is more difficult to handle because of the increased complexity in specifying the control-volume density and enthalpy and in determining the driving head, friction losses, and acceleration losses of the system. To illustrate this point, a plot of ρh versus ρ for 600 psia water in thermodynamic equilibrium with the vapor and the same plot for a supercritical pressure are shown in Fig. 40. It can be seen that the slope of the 600 psi curve corresponds to that of supercritical water at 4000 psi.

Since the ρh product is a double-valued function of ρ, the fraction $\Delta(\rho h)/\Delta\rho$ can be positive, zero, or negative. Consider the case when $\Delta(\rho h)$ is zero and $\Delta\rho$ has a finite value. This corresponds to the fluid entering the control volume in the subcooled state at the thermodynamic condition defined by $[\rho h, p]$ and leaving in the two-phase region at the state defined

by the same two coordinates [ρh, p]. If Δ(ρh) equals zero, the right-hand side of Eq. D-4 is zero; hence, the equation cannot be satisfied by this condition. Thus, a transient must develop to satisfy the basic energy and continuity equations.

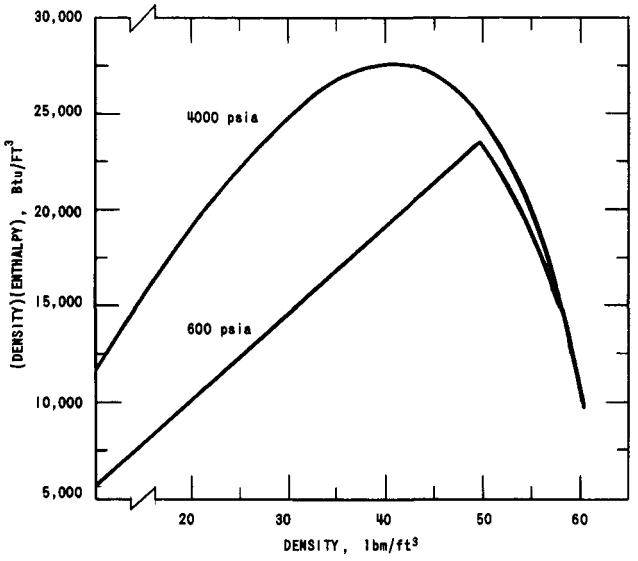

Fig. 40. The Variation of the Density-Enthalpy Product with Density along Isobars for Water

Experimental and analytical verification of this approach for a single-phase system is presented in this thesis. Experimental work by Levy and Beckjord[49] and verification by the analytical analysis of Randles[50] extends the approach to two-phase systems.

Randles found, through use of a digital computer to obtain simultaneous solutions of the conservation and state equations, that, at the values of water subcooling studied in the Levy and Beckjord experiment, the outlet velocity always increased when the inlet velocity decreased, and vice versa; that is, the outlet acceleration is always opposite in sign to the inlet acceleration. This is also the conclusion drawn from this analysis.

Randles also found that at 50°F subcooling and 127 kw/liter of power, the computer gave solutions for the flow which first exhibited strongly divergent oscillations and then, at t = 3.4 sec, underwent an extremely rapid fluctuation. This fluctuation resulted in a flow reversal with which the computer could not cope; hence, the calculations ceased. This condition corresponds to the approach of $\Delta(\rho h)/\Delta\rho$ to zero.

The basic analysis and the experimental results in the literature point to the fact that there are no simple or absolute criteria for predicting the transients in diabatic systems. This analysis points toward the thermodynamic condition of the fluid as being the most important factor in the initiation of sustained transients. Once the transient is initiated, the interaction of the mass velocity with the momentum equation determines whether or not the transient will be damped strongly enough to prevent further oscillations. If the damping is insufficient to damp the thermal driving force, sustained oscillations will occur.

APPENDIX E

Table I

SELECTED DATA

Run Identity	System Pressure, psig	Pressure Fluctuation, psig	Power Input, kw	Inlet Temp of Heater, °F	Outlet Temp of Heater, °F	Δp of Venturi, psi	Change in Venturi Δp, psi	Frequency, cps	Remarks
Loop No. 1									
16 Oct. 62 1	505	± 18	4	257	278	0.75	±3.5	15	Reduced pressure to 475 psig.
Roll No. 1									Loop became stable.
2	505	± 4	6	195	231			24	Initial transient, 4 to 6 kw, Δp_V off.
3	505	± 10	6	247	276	1	±3.0	17	Reduced pressure to 473 psig. Loop became stable.
16 Oct. 62 1	503	± 5	8	232	268	1.1	±0.1	18	Initial transient
Roll No. 2 2	505	± 5	8	233	270			15	A periodic heating type transient
3	505	± 18	8	239	275	1.1	±3.5	17	Reduced pressure to 490. Loop became stable.
5	505	± 20	8	251	284	1.25	±3.5	15	
6	505	± 20	10	248	285	1.5	±3.5	15	
17 Oct. 62 1	505	± 8	10	198	242	1.0	±0.3	21	Initial transient
2	507	± 10	10	221	262	1.15	±0.2	20	
3	505	± 30	10	248	283	1.35	±3.5	14	
4	505	± 20	12	238	281	1.5	±2.5	16	
5	525	± 20	6	247	275	1.3	±3.5	9	
6	525	± 15	4	261	282	0.75	±3.0	16	
7	525	± 11	8	245	278	1.0	±2.5	17	
8	525	± 22	10	248	283	1.35	±3.5	15	
9	525	± 25	12	243	280	1.35	±4.0	15	
18 Oct. 62 1	520	± 20	14	225	265	1.35	±4	14	
Roll No. 1 2	505	± 27	6	251	281	1.30	±3.5	15	
3	505	± 20	6	245	272	1.30	±2.0	16	
4	505	± 17	6	245	273	1.35	±2.0	16	
5	505	± 10	5	246	271	0.80	±0.7	16	
6	505	± 15	5	253	276	0.80	±0.7	16	
7	505	± 12	5	250	274	0.80	±1.5	16	
8	505	± 10	4	253	274	0.75	±1	16	
9	505	± 5	4	254	274	0.70	±1	15	
10	505	± 12	3	260	277	0.60	±1.5	14	
11	505	± 9	3	261	277	0.60	±2.0	14	
12	505	± 5	2	266	279	0.45	±2.0	14	
Roll No. 2 1	505	± 7	2	265	278	0.45	±2	14	
2	525	± 16	6	249	276	0.85	±2	15	
3	525	± 16	6	247	274	0.85	±2	15	
4	525	± 12	4	261	281	0.80	±3	14	
5	525	± 5	2	274	285	0.45	±1	12	
6	525	± 5	2	279	289	0.45	±1	11	
7	525	± 5	2	279	290	0.45	±1	11	
8	485	± 17	6	245	271	0.80	±3	15	
9	485	± 12	5	247	276	0.75	±2	15	
10	485	± 12	4	251	275	0.80	±2	14	
11	485	± 15	3	259	276	0.65	±1	14	
23 Oct. 62 1	406	± 2	6	262	277			0.16	Transition to two phases
Roll No. 1 2	505	± 4	10	274	296			8	
3	505	± 11	10	270	290			10	
4	505	± 17	10	263	293			10	
5	505	± 25	10	254	289			12	
6	335	± 7	9		220			1.5	Subcooled
7	335	± 6	6	228	255			0.15	Subcooled
Roll No. 2 1	505	± 50	6	246	279			15	Cooling down
2	507	± 2	18	277	302			7.5	Cooling down
3	507	± 3	18	278	302			7	Cooling down
4	460	± 10	12	243	281			1.6	Heating
5	60	± 2	4					0.2	
6	555	± 25	8	246	281			16	
7 Nov. 62 1	605	± 7	4	268	290	0.85	±2	14	
8 Nov. 62 1	485	± 2	4	274	290	0.80	±0.5	10	
2	494	± 1	1½	277	285	0.45	±0.25	10	
3	600	± 4	3	291	304	0.70	±1	10	
4	465	± 5	6	274	248	1.1	±0.10	1.5	Cooling down
9 Nov. 62 1	496	± 2	14	276	295	2.5	±0.5	8	
Roll No. 1 2	510	± 2	8	285	299	2.4	±0.1	6.6	
Loop No. 2									
1 Oct. 62 1	515	± 10	3	275	292	0.40	±3	13	
Roll No. 2 2	500	± 1	3	302	315	0.35	±0.25	9	
3	500	± 11	4	266	290	0.55	±2	16	
4	500	± 25	5	269	292	0.75	±3	14	
3 Oct. 62 1	500	± 2	8	282	301	1.30	±0.5	9	
Roll No. 1									

NOMENCLATURE

A	Cross-sectional area, ft^2
A_H	Heat-transfer area, ft^2
c	Velocity of sound, ft/sec
d	Diameter, ft
D_l	Lumped internal drag forces, lb_f
E	Voltage across test section, v
f	Single-phase friction factor
F	Total frictional losses, lb_f/ft^2
F'	Frictional loss per unit length, $lb_f/(ft^2)(ft)$
g	Local acceleration of gravity, ft/sec^2
g_c	Constant of proportionality, 32.2 lb_m-ft/lb_f-sec^2
G	Mass velocity, $lb_m/(sec)(ft^2)$
h	Specific enthalpy, Btu/lb_m
j	Integer denoting time position
L	Length, ft
n	Integer denoting space position
N	Variable constant defined by Eq. III-9
$\dot{m}$	Mass flow rate, lb_m/hr
p	Pressure, lb_f/ft^2
p*	Reference pressure, psi
Q	Linear rate of heat input to fluid, Btu/(sec)(ft)
t	Time, sec
T	Fluid temperature, °F
V	Total volume of loop, ft^3
V_n	Volume of subdivision, $(A_n \Delta z_n)$ ft^3
z	Elevation, ft
z_n	Length of subdivision, ft

Greek Letters

ρ	Density, lb_m/ft^3
ρ	Electrical resistivity, μohm-in.
T	Time interval, defined by Eq. III-16

Superscripts

$(\bar{})$	Bar over symbol denotes average value

Subscripts

n	Denotes space position
i	Inlet condition
e	Exit condition

ACKNOWLEDGMENT

I wish to acknowledge the contributions of the many people who have aided and encouraged my academic career, but more particularly the following: The Associated Midwest Universities for the financial support of this work; Dr. J. H. Boggs, who traveled a good many miles in directing this thesis; Dr. Michael Petrick, Argonne National Laboratory, sponsor of this thesis; Leonard Indykiewicz, for the fine job of constructing the apparatus and aiding in the test program; and Judith A. Koerner, for the excellent job of preparing the computer program.